Thiago Ouriques Machado

SYNTHESIS OF POLY (THIOETHER-ESTER) NANOPARTICLES DERIVED FROM RENEWABLE RESOURCES VIA THIOL-ENE POLYMERIZATION IN MINIEMULSION

Dissertação submetida ao Programa de Programa de Pós-Graduação em Engenharia Química da Universidade Federal de Santa Catarina para a obtenção do Grau de Mestre em Engenharia Química

Orientador: Prof. Dr. Pedro Henrique Hermes de Araújo

Coorientadora: Profª. Drª. Claudia Sayer

Florianópolis
2015

Ficha de identificação da obra elaborada pelo autor
através do Programa de Geração Automática da Biblioteca Universitária
da UFSC.

Machado, Thiago Ouriques
SYNTHESIS OF POLY (THIOETHER-ESTER) NANOPARTICLES DERIVED FROM RENEWABLE RESOURCES VIA THIOL-ENE POLYMERIZATION IN MINIEMULSION / Thiago Ouriques Machado ; orientador, Pedro Henrique Hermes de Araújo ; coorientadora, Claudia Sayer – Florianópolis, SC, 2015

121 p.

Dissertação (mestrado) – Universidade Federal de Santa Catarina, Centro Tecnológico. Programa de Pós-Graduação em Engenharia Química.

Inclui referência

1. Engenharia Química. 2. Polimerização tiol-eno em miniemulsão. 3. Monômero renovável. 4. Nanopartícula. I. De Araújo, Pedro Henrique Hermes. II. Universidade Federal de Santa Catarina. Programa de Pós-Graduação em Engenharia Química. III. Título.

Thiago Ouriques Machado

SYNTHESIS OF POLY (THIOETHER-ESTER) NANOPARTICLES DERIVED FROM RENEWABLE RESOURCES VIA THIOL-ENE POLYMERIZATION IN MINIEMULSION

Esta Dissertação foi julgada adequada para obtenção do Título de Mestre, e aprovada em sua forma final pelo Programa de Pós-Graduação em Engenharia Química da Universidade Federal de Santa Catarina.

Florianópolis, 09 de Setembro de 2015.

_____
Prof.ª Cíntia Soares, Dr.ª
Coordenadora do Curso

_____
Prof. Pedro Henrique Hermes de Araújo, Dr.
Orientador
Universidade Federal de Santa Catarina

_____
Prof.ª Claudia Sayer, Dr.ª
Coorientadora
Universidade Federal de Santa Catarina

Banca Examinadora:

_____
Prof. Marcelo Kaminski Lenzi, Dr.
Universidade Federal do Paraná

_____
Prof.ª Cristiane da Costa Bresolin, Dr.ª
Universidade Federal de Santa Caratina

_____
Prof. Sérgio Henrique Pezzin, Dr.
Universidade do Estado de Santa Catarina

AKNOWLEDGEMENT

Eu agradeço aos meus pais por terem sido meus primeiros professores. À minha família por todo o amor e por sempre me apoiarem e me motivarem a seguir meus sonhos mesmo quando isso quis dizer ir morar do outro lado do planeta.

Agradeço aos meu orientadores Dr. Pedro e Dr.ª Claudia por me darem o privilégio de trabalhar com eles desde a graduação. Eu aprendi muito com vocês dois. Obrigado pela confiança que foi em mim depositada.

Aos meus amigos e colegas do LCP pela amizade e pelo apoio.

Gostaria de agradecer especialmente àqueles que me ajudaram nos momentos difíceis dos últimos dois anos.

Aos meus amigos desde a época da graduação, Felipe (Phelps), Leonardo e Orlando.

Aos meus amigos da adolescência. Bianca, Camila, Felipe (Pato), Guilherme e Mariana, obrigado pelo amor incondicional e por fazerem parte da minha vida todos esses anos.

Ao Conselho Nacional de Desenvolvimento Científico e Tecnológico (CNPq) e à Coordenação de Aperfeiçoamento de Pessoal de Nível Superior (CAPES) pelo suporte financeiro.

Ao Laboratório Central de Microscopia Eletrônica, Universidade Federal de Santa Catarina (LCME-UFSC) pelas imagens de TEM.

Ao Laboratório de Propriedades Físicas de Alimentos (PROFI), Departamento de Engenharia Química e Engenharia de Alimentos – UFSC, pelas análises de DSC.

Ao Laboratório de Ressonância Magnética Nuclear, Universidade de Brasília, (LRMN – UnB) pelas análises de NMR.

Ao Laboratório de Difração de Raios X (LDRX - UFSC) pelas análises de XRD.

“One, remember to look up at the stars and not down at your feet. Two, never give up work. Work gives you meaning and purpose and life is empty without it. Three, if you are lucky enough to find love, remember it is there and don't throw it away.”

(Stephen Hawking, 2010)

ABSTRACT

Green chemistry has drawn attention from researchers and even some industries due to concerns about the depletion of fossil oil reserves and aggravation in the global warming and other environmental issues. Polymeric materials from biofeedstocks-derived monomers are a promising environmentally friendly alternative to petrol-derived polymers, especially for high value added applications. In this context, vegetable oils and saccharides are interesting raw materials that can be applied as chemical platforms in the synthesis of novel fully renewable monomers through chemical modification. In addition, thiol-ene polymerization has been shown as a versatile tool to produce polymers from fully renewable α,ω-diene monomers bearing, for example ester, ether, or amide functional groups in the backbone chain. However, works portraying the polymerization of renewable monomers through thiol-ene polymerization in dispersed medium are still uncommon. Herein, it is presented the synthesis and characterisation of poly(thioether-ester) nanoparticles via thiol-ene polymerization in miniemulsion using a monomer derived from renewable resources. The synthesis of a renewable α,ω-diene diester monomer, dianhydro-D-glucityl diundec-10-enoate (DGU), produced from 10-undecenoic acid (derived from castor oil) and isosorbide (derived from starch) was performed. DGU was copolymerized with 1,4-butanedithiol ($Bu(SH)_2$) through thiol-ene polymerization both in bulk and miniemulsion to yield linear semi-crystalline poly(thioether-ester)s. Different parameters were evaluated such as reaction temperature, initiator concentration, surfactant type and surfactant concentration. Particle size distribution and morphology was observed by DLS and TEM respectively resulting in spherical particles with an intensity average particle diameter around 200 nm. Polymer with higher molecular weight was obtained by miniemulsion polymerization when compared to bulk polymerization. Number average molecular weight of 11 kDa was obtained through miniemulsion polymerization at 80°C for 4h using AIBN at 1 mol% (in relation to $Bu(SH)_2$). Furthermore, DSC and XRD analyses have shown that the synthesized polymer was semi-crystalline with a degree of crystallinity above 20% and T_m around 60°C. Finally, depending on the co-stabilizer type, hexadecane or Crodamol, and amount, phase segregation within polymer particles was observed through DSC.

Keywords: Thiol-ene polymerization in miniemulsion. Renewable monomer. Nanoparticle.

RESUMO

A química verde tem chamado a atenção de pesquisadores e até mesmo de algumas indústrias devido à preocupação com o esgotamento das reservas fósseis e o agravamento de problemas ambientais. Materiais poliméricos obtidos de monômeros derivados de fontes renováveis são uma alternativa ambientalmente correta aos polímeros derivados do petróleo, especialmente para aplicações de alto valor agregado. Neste contexto, óleos vegetais e sacarídeos são matérias-primas interessantes que podem ser utilizadas como plataformas químicas para a síntese de novos monômeros, completamente renováveis, através da modificação química. Além disso, polimerização tiol-eno mostrou-se uma versátil ferramenta para a produção de polímeros a partir de monômeros verdes (α,ω-dienos) providos de grupos funcionais como éster, éter ou amida na cadeia principal. Entretanto, trabalhos sobre a polimerização de monômeros renováveis através da polimerização tiol-eno em meios dispersos ainda são escassos. Neste trabalho, a síntese e a caracterização de nanopartículas de poli(tioéter-éster) via polimerização tiol-eno em miniemulsão usando um monômero proveniente de fontes renováveis são apresentadas. O monômero verde utilizado é um α,ω-dieno diéster, diundec-10-enoato de dianidro-D-glucitila (DGU), produzido a partir de ácido 10-undecenóico (derivado do óleo de mamona) e isosorbídeo (derivado do amido). DGU foi copolimerizado com 1,4-butanoditiol ($Bu(SH)_2$) através polimerização tiol-eno em massa e em miniemulsão para produzir poli(tioéter-éster) linear e semicristalino. Diferentes parâmetros foram avaliados, como por exemplo temperatura, concentração de iniciador, tipo e concentração do surfactante. A distribuição de tamanho e a morfologia das partículas foram observadas por DLS e TEM respectivamente, revelando partículas esféricas com diâmetro de 200 nm. O polímero obtido pela polimerização em miniemulsão, 11 kDa onde as condições reacionais foram 80°C por 4h usando 1 mol% de AIBN (em relação ao $Bu(SH)_2$), mostrou-se com maior massa molar em comparação àquele obtido em polimerização em massa. Análises de DSC e DRX mostraram que o polímero sintetizado é semicristalino com grau de cristalinidade de pelo menos 20% e T_m em torno de 60°C. Dependendo do tipo de co-estabilizador utilizado, hexadecano ou Crodamol, e da quantidade, pode-se observar por DSC segregação de fases nas partículas poliméricas.

Palavras-chave: Polimerização tiol-eno em miniemulsão. Monômero renovável. Nanopartícula.

LIST OF FIGURES

LIST OF TABLES

LIST OF ABBREVIATIONS AND ACRONYMS

AIBN – Azobisisobutyronitrile
$Bu(SH)_2$ – 1,4-Butanedithiol
$CDCl_3$ – Deuterated chloroform
Crod. – Crodamol GTCC
DGU – Dianhydro-D-glucityl diundec-10-enoate
DLS –Dynamic light scattering
DSC – Differential Scanning Calorimetry
Eq. – Equation
FTIR - Fourier Transform Infrared Spectroscopy
GPC – Gel permeation chromatography
HATR - Horizontal Attenuated Total Reflectance
HD – Hexadecane
KPS – Potassium persulphate
Lut. – Lutensol
MMA – Methyl methacrylate
(^{1}H)NMR – (Proton) Nuclear Magnetic Resonance
PDI – Polydispersion index
SDS – Sodium dodecyl sulphate
Surf. – Surfactant
TEM – Transmission electron microscopy
TG – Triglyceride
THF – Tetrahydrofuran
USDA – United States Department of Agriculture
XRD – X-ray diffraction

LIST OF SYMBOLS

ΔH_m – Enthalpy of melting
°C – Degree Celsius
% – Percentage
Dp – Particle diameter [nm]
Dp_0 – Droplet diameter [nm]
H_2O – Water
M_N – Number average molecular weight [kDa]
mol% – Mol percentage
M_W – Weight average molecular weight [kDa]
nm – Nanometer
T_g – Glass transition temperature [K]
T_m – Melting temperature [K]
w.% – Weight percentage
w./w. – Weight-to-weight ratio

TABLE OF CONTENTS

CHAPTER I

1 INTRODUCTION

Green chemistry has drawn attention from researchers and even some industries due to concerns about the depletion of fossil oil reserves and aggravation in the global warming and other environmental issues (CLARK, 2009). Therefore, in the past few decades, sustainable efforts have been extensively devoted to prepare new polymers from renewable environmentally friendly raw materials. In this context, fatty acids from vegetable oils and saccharides, or sugars, stand out as highly convenient raw materials because they are both abundant worldwide, inexpensive, provide stereochemical diversity and can potentially yield biocompatible and biodegradable materials (MEIER; METZGER; SCHUBERT, 2007; BELGACEM; GANDINI, 2008).

However, polymerization attempts of vegetable oils, which are multifunctional monomers, usually ended up with the synthesis of cross-linked polymers. Vegetable oils are usually copolymerized to non-renewable monomers such as styrene (LU; LAROCK, 2010; MEIORIN; ARANGUREN; MOSIEWICKI, 2012), divinylbenzene, norbonadiene, and acrylates (LU; LAROCK, 2009, 2010) to achieve the required thermal and mechanical properties. On the other hand, they are promising platforms for the synthesis of novel monomers by chemical modification. Vegetable oils are mainly composed by triglycerides, which in its turn possess several reaction sites within the molecule such as the acyl group, double bonds and even hydroxyls that can undergo chemical modifications to yield a vast variety of monomeric molecules (MUTLU, 2012; VILELA; SILVESTRE; MEIER, 2012). By designing the monomer using vegetable oils, or other biofeedstocks such as sugars, as chemical platform, it is possible to include in the polymer molecule functional groups or even chemical bonds that facilitate biodegradation. For example, the inclusion of strategically positioned grafts in the polymeric back-bone that could enable the enzymes to attach more easily to the substrate binding site or the inclusion of disulphide bonds in the polymer's main chain.

Thiol-ene reactions are often considered as either click or green chemistry reactions because they can be carried out at mild conditions, normally achieve high conversion and do not generate any environmentally hazardous by-products (HOYLE; LEE; ROPER, 2004; HOYLE; BOWMAN, 2010; CLAUDINO, 2011). Thiol-ene reactions have been extensively utilized for surface and molecules

functionalization (FEIDENHANS'L *et al.*, 2014; CHEN *et al.*, 2015; IONESCU *et al.*, 2015; KUHLMANN *et al.*, 2015), molecules conjugation (STENZEL, 2013; KUHLMANN *et al.*, 2015), crosslinking (ACOSTA ORTIZ *et al.*, 2010; WANG *et al.*, 2013), grafting (KOLB; MEIER, 2013), UV-curable coatings (BLACK; RAWLINS, 2009; SANGERMANO *et al.*, 2009; ÇAKMAKÇI *et al.*, 2012) and polymerization of renewable monomers (KREYE; TÓTH; MEIER, 2011; TÜRÜNÇ *et al.*, 2012; KOLB; MEIER, 2013; TÜRÜNÇ; MEIER, 2013; YOSHIMURA *et al.*, 2015).

Thiol-ene polymerization possess a step-growth mechanism through free-radical reactions. A reaction between monofunctional ene and thiol molecules leads to adducts. Difunctional monomers polymerize to yield linear polymers, whilst multifunctional monomers form a polymeric network (CRAMER *et al.*, 2003). Most of the work found in the literature portrays cross-linked thiol-ene polymers, such as hydrogels and resins, to use in diverse applications that range from photocurable coatings (BLACK; RAWLINS, 2009; CARLBORG *et al.*, 2014) to biomedical (KI *et al.*, 2014; LIN; KI; SHIH, 2015). Recently, linear thiol-ene polymers have been utilized to synthesize nano- and microparticles through heterogeneous phase polymerization techniques (DURHAM; SHIPP, 2014; JASINSKI *et al.*, 2014a; LOBRY *et al.*, 2014; AMATO *et al.*, 2015).

Moreover, thiol-ene polymerization has been shown as a versatile tool to produce polymers from fully renewable α,ω-diene monomers bearing, for example ester, ether, or amide functional groups in the main chain (TÜRÜNÇ; MEIER, 2013). Some of these moieties, such as ester functionality, are interesting because they can be readily hydrolysed and therefore are potentially (bio) degradable. Moreover, sulphide bonds were found to tune degradability of acrylates (RYDHOLM; BOWMAN; ANSETH, 2005; RYDHOLM *et al.*, 2006b; RYDHOLM; ANSETH; BOWMAN, 2007).

Based on the above facts and considerations, polymeric materials from biofeedstocks-derived monomers are a promising environmentally friendly alternative to petrol-derived polymers, especially for purposes as biomedical applications when either biocompatibility or biodegradability (or even both) become highly relevant. Nanoparticles from renewable monomers are only recently being studied, in addition there are only 4 papers, so far, published in the literature concerning thiol-ene polymerization in heterogeneous systems. Thiol-ene polymerization in miniemulsion is a promising technique to synthesize nanoparticles, or even nanocapsules and hybrid particles, from

renewable monomers. Besides, thiol-ene polymerization kinetics in miniemulsion is expected to greatly differ from both traditional free-radical and step-growth miniemulsion polymerizations and it certainly needs to be evaluated.

1.1 OBJECTIVES

1.1.1 General Objectives

This work aims to investigate the synthesis of a novel monomer derived from renewable raw materials, such as vegetable oil and saccharide, and subsequently to use the produced green monomer to perform thiol-ene polymerization in miniemulsion to yield polymer nanoparticles and in bulk for comparison.

1.1.2 Specific Objectives

1 – Synthesis and characterisation of a renewable α,ω-diene diester monomer using castor oil and isosorbide as chemical platforms.
2 – Synthesis and characterisation of polymeric sub-micrometric particles through thiol-ene polymerization in miniemulsion using the synthesized α,ω-diene diester monomer.
3 – Evaluate the influence of the type and amount of surfactant in thiol-ene miniemulsion polymerization.
4 – Evaluate the effect of temperature, initiator type and concentration on molecular weight in thiol-ene polymerization in miniemulsion.
5 – Compare molecular weight results from bulk polymerization and miniemulsion polymerization to evaluate the existence of radical compartmentalization in thiol-ene polymerization
6 – Characterise the obtained polymeric material regarding its crystallinity and thermal properties.
7 – Investigate the effect of type and amount co-stabilizer to either produce polymeric particles with internal phase segregation or incorporate the co-stabilizer in the polymeric matrix.
8 – Evaluate molecular weight kinetics of thiol-ene polymerization in miniemulsion and possibly functional group conversion.

CHAPTER II

2 SYNTHESIS OF MONOMERS FROM RENEWABLE RESOURCES

In the past few decades, efforts to achieve sustainability in diverse scientific and technologic fields have been done. Concerns about the depletion of fossil oil reserves and an aggravation in the global warming are driving a pursuit for renewable raw materials substituents(MEIER; METZGER; SCHUBERT, 2007). The utilization of renewable resources should be a compromise assumed in the development of new technologies. The replacement of the traditional non-renewable raw materials of existent technologies should also be stimulated.

Renewable raw materials commonly utilized in the chemical industry are plant oils, polysaccharides from vegetal or animal fonts (starch, cellulose, chitosan and chitin), mono- and disaccharides, and wood (cellulose, lignin, hemicellulose and natural rubber) (MEIER; METZGER; SCHUBERT, 2007; BELGACEM; GANDINI, 2008; MUTLU, 2012).

The modification of natural polymers is a longstanding approach, which has been exhaustively investigated since the nineteenth century. There are several techniques developed to chemically modify natural polymers in order to achieve the desired characteristic for the material, e.g. inserting functional groups, cross-liking, blending or copolymerizing to a different class of polymer (SHALABY; SHAH, 1991; GÜNAY; THEATO; KLOK, 2011, 2013). However, modifying naturally-obtained materials can be complicated due to its structural complexity. On the other hand, the synthesis of novel classes of monomers is a very interesting manner of designing the polymeric macromolecule and overcome some issues such as (bio) degradability and physical properties.

By designing the monomer, it is possible to include in the polymeric molecule functional groups or even chemical bonds that facilitate biodegradation, e.g. the inclusion of strategically positioned grafts in the polymeric backbone that could enable the enzymes to attach more easily to the substrate binding site or the inclusion of disulphide bonds in the polymer's main chain.

Modification of natural polymers is also restrained to the physical properties of the material to be modified. Desired features for specific applications could be more easily reached by polymerization of

monomeric species rather than modification of an already existing macromolecule.

2.1 VEGETABLE OILS AS RENEWABLE RESOURCES IN POLYMER CHEMISTRY

Vegetable oils are one of the most widely used renewable resources in the chemical industries owing to their excellent environmental credentials, including their biodegradability, low toxicity, avoidance of volatile organic chemicals, easy availability and relatively low price (VERHÉ, 2004; BELGACEM; GANDINI, 2008). According to a report from USDA (2015), the global production of the major vegetable oils in the period 2013/14 summed 170.87 million metric tons (Table 1), comparing it to annual production from 2012/13 there was an increase of roughly 10 million metric tons. The prospective is that the worldwide production continues to rise based on the data from Table 1.

Table 1 Annual production of the main vegetable oils.

Vegetable Oil	Annual Production (million metric tons)				
	2010/11	2011/12	2012/13	2013/14	Feb 2014/15
Coconut	3.71	3.41	3.66	3.46	3.43
Cottonseed	4.96	5.22	5.21	5.13	5.12
Olive	3.27	3.45	2.44	3.15	2.34
Palm	49.14	52.44	56.49	59.42	62.44
Palm Kernel	5.75	6.16	6.57	6.99	7.29
Peanut	5.31	5.29	5.49	5.58	5.52
Rapeseed	23.03	24.10	24.92	26.43	26.95
Soybean	41.40	42.73	43.10	44.96	47.44
Sunflowerseed	12.21	14.73	13.27	15.75	15.18
Total	148.76	157.53	161.13	170.87	175.69

Source: USDA (2015).

Vegetable oil's average price is higher when compared to petrol, for instance palm, canola and coconut oils have average prices (Oct-Sept 2013/14) of respectively USD 803; 954; 1278 per metric ton according to USDA. Crude oil's price for the same period was USD 93.26 and 98.52 per barrel from WTI (EUA) and Brent (Europe), respectively (EIA, 2015), which is approximately USD 684 and 722 per metric ton depending on the oil density. The price of vegetable oil is expected to decrease in the future with the increase of its utilization in sustainable industries. In fact, vegetable oils are used in chemical industries as ingredients or components in many manufactured products, such as soaps, drying agents, paints, coatings, insulators, hydraulic fluids, lubricants, monomers (e.g. dimer acids and polyols) and polymers (TURLEY, 2008).

Vegetable oils consist mainly of triglycerides (TG), about 93–98 wt.%, together with di- and monoglycerides and phosphoglycerides as minor components (SENIHA GÜNER; YAĞCI; TUNCER ERCIYES, 2006; LU; LAROCK, 2009). Triglycerides consist of three fatty acid chains esterified to a glycerol molecule (Figure 1). TG differ dramatically in the ratio and the type of fatty acids, which depends on their origins (Table 1). Table 2 shows the fatty acid content and double bond per TG of commodity vegetable oils from different origins.

Figure 1. General chemical structure of triglycerides. R_1, R_2, and R_3 correspond to fatty acid chains.

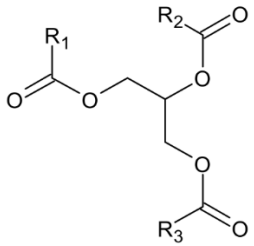

Source: Author.

Table 2 Fatty acid content (%) and double bond per TG in commodity vegetable oils.

Vegetable Oil	Fatty acids content (%)					= / TG[b]
	Palmitic	Stearic	Oleic	Linoleic	Linolenic	
Castor[a]	0.9	0.8	2.9	4.5	0.6	-
Corn	10.9	2.0	25.4	59.6	1.2	4.5
Linseed	5.5	3.5	19.1	15.3	56.6	6.6
Palm	44.4	4.1	39.3	10.0	0.4	1.8
Soybean	11.0	4.0	23.4	53.2	7.8	4.6

Obs.: (a) castor oil contains ricinoleic acid in the range of 87.7-90.4%. (b) Double bond per triglyceride.
Source: (LU; LAROCK, 2009).

Some important structural features make the fatty acids an interesting platform for polymer chemistry such as straight carbon chain, unsaturation, also some special fatty acids contain other functional groups such as hydroxy or epoxy groups in the vicinity of the double bonds (VERHÉ, 2004). Figure 2 shows the chemical structures of the fatty acids most commonly used in polymer chemistry: oleic, linoleic, linolenic, ricinoleic, and erucic acids (ESPINOSA; MEIER, 2011).

Figure 2. Fatty acids most commonly used in polymer chemistry: (a) oleic, (b) linoleic, (c) linolenic, (d) ricinoleic, and (e) erucic acids.

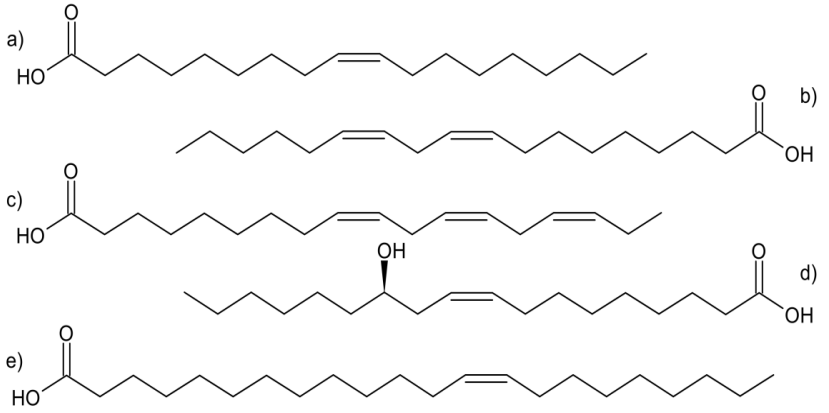

Source: Adapted from (ESPINOSA; MEIER, 2011).

2.1.1 Polymerization of Vegetable Oils

The polymerization of plant oil has been vastly studied, however it is still a challenge to obtain polymers suitable for applications in which petrol derived polymers are already well-established (LU; LAROCK, 2009, 2010). Triglycerides can undergo cationic polymerization (LI; LAROCK, 2005), free radical polymerization (ESEN; KÜSEFOĞLU; WOOL, 2007), or olefin metathesis polymerization (RYBAK; FOKOU; MEIER, 2008; ROMERA *et al.*, 2015), due to the presence of double bonds in their chain.

2.1.1.1 Free Radical Polymerization of Vegetable Oil

Carbon-carbon double bonds contained in plant oils are likely to be polymerized via free radical mechanism. Even so, radical polymerization of fatty acids and triglycerides has not been given plenty attention due to the presence of chain transfer processes which occur in the allylic positions of fatty acids chains (LU; LAROCK, 2009). Chain transfer processes reduce the average molecular weight of the final polymer; therefore, there is a high chance of obtaining low molecular weight polymers through free radical method.

Conjugated carbon–carbon double bonds in vegetable oils are usually used for free radical polymerization because their double bonds are relatively easily attacked by free radicals (LI; LAROCK, 2001, 2002a; LI; HANSON; LAROCK, 2001).

2.1.1.2 Cationic Polymerization of Plant Oil

Carbon-carbon double bonds in fatty acids are slightly more nucleophilic than those in ethylene and propylene; therefore, vegetable oils are also capable of being polymerized through cationic route. The conjugated double bonds from drying oils – oils that undergo crosslinking by the action of oxygen – are even more reactive for cationic polymerization. Plant oils can be thermodynamically considered as cationic monomers (LU; LAROCK, 2009)

2.1.1.3 Olefin Metathesis Polymerization of Plant Oils

Olefin metathesis is a metal-catalysed reaction where the alkylidene groups are exchanged. The most common metal-complexes, utilized for this process, are those containing W, Mo, Re or Ru.

Several techniques have been developed for olefin metathesis to be employed in polymer synthesis such as acyclic diene metathesis (ADMET) polymerization (RYBAK; FOKOU; MEIER, 2008), acyclic triene metathesis (ATMET) polymerization (RYBAK; FOKOU; MEIER, 2008; ROMERA *et al.*, 2015) and ring-opening metathesis polymerization (ROMP) (XIA; LAROCK, 2010).

Meier's group (2008) has performed ADMET and ATMET polymerizations of soybean oil and glyceryl triundec-10-enoate respectively, resulting in a range of materials from sticky oils to rubber. Romera and colleagues (2015) studied the ATMET polymerization of linseed oil both in bulk and in miniemulsion. The authors reported low molecular weight (M_N = 6 kDa) and justified that the presence of oleic acid moieties and saturated fatty acids limited both molecular weight increase and cross-linking because they acted as chain-stoppers.

2.3 MONOMERS FROM PLANT OILS

Despite all the attempts to synthesize green polymers capable of replacing commercial polymers, the polymerization of raw vegetable oils has not quite shown itself as a suitable alternative to achieve physical and chemical properties similar to petrol-derived polymers. The polymerization attempts of triglycerides, which are multifunctional monomers, usually ended up with the synthesis of cross-linked polymers. Vegetable oils are usually copolymerized to non-renewable monomers such as styrene, divinylbenzene, norbonadiene and acrylates to achieve the required physical-chemical properties (LI; LAROCK, 2001, 2002b; LI; HANSON; LAROCK, 2001; LU; LAROCK, 2009, 2010; MEIORIN; ARANGUREN; MOSIEWICKI, 2012).

Novel monomers derived from plant oils have been investigated due to the possibility of designing the monomeric molecules. Many types of polymers can be synthesized from fatty acids-derived monomers; for instance polyesters and polyamides (MEIER; METZGER; SCHUBERT, 2007; KREYE *et al.*, 2012; VILELA; SILVESTRE; MEIER, 2012).

Fatty acids are very interesting platforms for novel monomers syntheses because they provide a vast stereochemical diversity and a variety of chemical modifications are possible. There are typically 5 chemically reactive sites, shown in Figure 3, where a triglyceride can be chemically modified to synthesize different kinds of monomers (MUTLU, 2012).

Figure 3. Structure of a generic triglyceride displaying its chemically reactive sites.

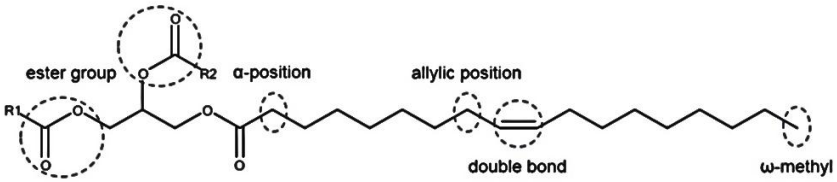

Source: Adapted from Mutlu (2012).

Many are the chemical reactions that triglycerides can be submitted to, e.g. hydrolysis, transesterification, halogenation, saponification, reduction, amination, ozonolysis, epoxidation, metathesis, thiol-ene coupling, carbonylation, addition reaction, Fiedel-Krafts alkylation, Claisen condensation, ω-oxidation and numerous more. Traditionally most of the reactions utilized to modify the chemical structure of fatty acids focus on the ester group to synthesize fatty alcohols, soaps, esters, thioesters, hydrazides, amides or amines. However, in the past two decades the attention has turned to functionalize the alkyl chain of the fatty acid, especially through reactions involving the double bond present in some fatty acids chains (MUTLU, 2012).

Many sorts of monomers can be synthesized starting from vegetable oil platforms, such as hydrocarboxylic acids, hydroxyesters, diesters, dicarboxylic acids, polyols and α,ω dienes containing several functionalities (OVETKOVIĆ *et al.*, 2008; RYBAK; MEIER, 2008; QUINZLER; MECKING, 2009, 2010; KREYE; TÓTH; MEIER, 2011; TRZASKOWSKI *et al.*, 2011; KREYE *et al.*, 2012; CARDOSO *et al.*, 2014)

Ovetković *et al.* (2008), synthesized 9-hydroxynonanoic acid methyl ester from castor oil through ozonation followed by reductive ozonolysis. The monomer was prepared in two steps and then polycondensed to yield polyhydroxy alcanoate. Quinzler and Mercking (2010) used catalysed methoxycarbonylation reactions (PUGH; PRINGLE; DRENT, 2001; JIMÉNEZ-RODRIGUEZ; EASTHAM; COLE-HAMILTON, 2005) to produce α,ω-diesters monomers from unsaturated fatty acid esters and subsequently longer-chain aliphatic polyesters (M_w up to $2 \cdot 10^4$ g·mol$^{-1)}$. Interestingly, the complete incorporation of the carbon-backbone in the polymeric chain provided sufficient melt and crystallization temperatures for thermoplastic

processing and applications similar to conventional non-renewable polymers.

Yang and co-workers (2010) described a biochemical route to produce ω-carboxy fatty acid monomers from oleic, erucic and epoxy stearic acids through whole-cell biotransformations catalysed by C. tropicalis ATCC20962. After the biochemical oxidation of terminal methyl groups into carboxylic acids moieties, the monomers underwent enzymatically catalysed polycondensation with diols yielding polyesters formed by unsaturated and epoxidized repeating units, i.e. a good retention of functionality of the fatty acid was observed.

Trzaskowski and co-workers (2011) synthesized poly (1,20-eicosadiyl-1,20-eicosanedioate) (Mn = 10^4 g mol^{-1}) through polycondensation of stoichiometric amounts of 1,20-eicosanedioc acid and eicosane-1,20-diol catalyzed by titanium alkoxides. The C_{20} diacid and C_{20} diol used as co-monomers were synthesized by self-metathesis of undec-10-enoic acid followed by hydrogenation. The corresponding α,ω-diene undec-10-enyl undec-10-enoate was prepared by esterification of undecenoic acid with undec-10-en-1-ol catalysed by titanium isopropoxide as previously reported in the literature by Rybak and Meier (2008). ADMET polymerization of the corresponding α,ω-diene yielded a molecular weight 2.8 times higher.

Kreye *et al.* (2011) synthesized through Ugi reaction (UGI; FETZER; STEINBRÜCKNER, 1959; DÖMLING, 2006) α,ω-diene amide monomers . Kreye and colleagues produced successfully different varieties of poly-1-(alkylcarbamoyl) carboxamides via ADMET and thiol-ene polymerization. Thus, Ugi reaction is a powerful tool to synthesize highly substituted α,ω-diene amide monomers from renewable resources, in this case, castor oil derivatives.

Vilela and co-workers (2012) reported the utilization of a fatty acid from rapeseed oil, erucic acid, as platform to produce monomers by self-metathesis followed by hydrogenation of the 9-ω unsaturation, yielding 1,26-hexacosanedioic acid. This long-chain α,ω-dicarboxylic acid was then polycondensed to hexacosane-1,26-diol, generated from the former by reduction, which yielded an aliphatic long-chain polyester 26,26. The research group also successfully polymerized the 1,26-hexacosanedioic acid with short-chain alkanediols, dodecane-1,12-diol and butane-1,4-diol, generating polyesters 12,26 and 4,26, respectively.

Cardoso *et al.* (2014) synthesized an α,ω-diene diester, namely 1,3-propylene diundec-10-enoate, from undec-10-oic acid and 1,3-propanediol derived from castor oil and glycerol, respectively. α,ω-Diene diester monomer underwent homopolymerization through

ADMET both in bulk and in miniemulsion. Polymer particles obtained from miniemulsion presented sizes from 150 to 350 nm, depending on the type and concentration of the surfactants utilized. ADMET polymerization in miniemulsion yielded polymers with higher molecular weight (M_n up to 15 kDa) than ADMET polymerization in bulk (M_n up to 7 kDa).

2.4 SUGARS AS RENEWABLE RESOURCES IN POLYMER CHEMISTRY

Sugars or carbohydrates, as vegetable oils, are renewable resources that have been explored in polymer chemistry. Carbohydrates are essential building blocks in nature, therefore are widely available at inexpensive prices. The total global supply of carbohydrates in 2012 was 2.4 billion tons; in addition, cellulosic material and others wastes can be processed into sugar, e.g. by hydrolysis with acids, and other organic raw materials for chemical industries (DELOITTE, 2014). Consequently, the inevitable changeover of the chemical industry to biofeedstocks as its raw materials, due to fossil resources depletion, might certainly embrace carbohydrates and its derivatives. In polymer chemistry, carbohydrates are important building blocks to produce biodegradable and biocompatible materials. There is a rich variety of sugar-based monomers that can be obtained, e.g. alditols; lactones, aldonic and aldaric acids; and aminosugars (GALBIS; GARCÍA-MARTÍN, 2008).

2.4.1 Polymerization of sugar-based monomers

Carbohydrates are multifunctional monomers; therefore, its polymerization is not straightforward. Their functionality usually needs to be reduced in order to prevent side reactions, for instance overly crosslinked polymers. (GALBIS & GARCÍA-MARTIN, 2008). The most representative sugar-derived polymers that have been synthesized are polyesters, polycarbonates, polyethers, and polyurethanes, usually synthesized from dianhydroalditols (OKADA; TACHIKAWA; AOI, 1997, 2000; YOKOE; KEIGO; OKADA, 2003; GALBIS; GARCÍA-MARTÍN, 2008; FENOUILLOT *et al.*, 2010; BESSE *et al.*, 2013; YOON *et al.*, 2013; POLLONI, 2014; SADLER *et al.*, 2014).

Alditols are polyols and they occur extensively in nature. In addition, aldoses and ketoses can be reduced to alditols with the

generation of new hydroxyl groups from the carbonyl functions; for instante, D-glucose (aldose) is reduced into D-glucitol (polyol), trivially referred to as ‘sorbitol’. The reduction of ketoses generates a new stereogenic centre, and gives two epimeric alditols; for example, D-fructose produces D-mannitol and D-glucitol. Acyclic alditols are multifunctional molecules; therefore, in order to avoid undesirable side-reactions, their cyclic forms, dianhydroalditols, are usually used in polymer chemistry. Furthermore, the thermostability of these dianhydroalditol monomers may be higher than that of other aliphatic diols, which raises the glass transition temperature of the corresponding polymers (GALBIS; GARCÍA-MARTÍN, 2008).

2.4.2 Isosorbide

Isosorbide (dianhydro-D-glucitol) is a polyol indirectly derived from glucose. It is produced by dehydration from sorbitol and, therefore, it is a renewable raw material from biomass. Dianhydro D-glucitol has been produced in industrial scale by several years due to the commercial importance of its nitro and methyl derivatives. The production is a multi-step process where isosorbide is the very last product, starting from starch and going on with D-glucose and sorbitol. Isosorbide has been already remarkably commented and discussed in the literature as an important chemical platform for the future replacement of petroleum-based materials (FLÈCHE; HUCHETTE, 1986; ROSE; PALKOVITS, 2012).

Figure 4. Isosorbide chemical structure.

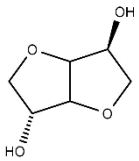

Source: Author.

Isosorbide is a secondary cyclic alcohol made of two cis fused tetrahydrofuran rings. The angle between the rings is 120°, with two secondary alcohol groups in position 2 and 5. The hydroxyl in position 2 is in *exo* conformation while the one in 5 has an *endo* conformation, what promotes an *intra*-molecular hydrogen bond that can be detected through IR spectroscopy (FLÈCHE; HUCHETTE, 1986). Some physical-chemical properties of crystallized isosorbide are shown in Table 3.

Table 3. Physical-chemical properties of isosorbide.

Melting temperature	61 – 64°C
Boiling temperature	140°C (10 mmHg)
Flash point	$>$ 150°C
Optical rotation ($[a_D]$)	+43.9
Soluble in	Water, alcohol, dioxane, ketones
Almost insoluble in	Hydrocarbons, ethers, esters

Source: (FLÈCHE; HUCHETTE, 1986)

Isosorbide possesses a unique chemical structure and it is worth to comment some details on its reactivity. Hydroxyl groups' reactivity in position 2 and 5 depends on the reagent and the solvent used and on the steric hindrance, especially in the case of substitution reactions that could be either inside or outside the V-rings. For example, the endo-group 5 presents higher reactivity toward esterification with acyl halides due to intra-molecular hydrogen bonding of this group with the adjacent ring-oxygen atom, whereas it has been demonstrated that esterification with acetic anhydride in pyridine takes place favourably in position 2 (FLÈCHE; HUCHETTE, 1986).

Isosorbide has been widely used in the pharmaceutical industry for several years. Its nitro and dinitro derivatives are known since 1939 as vaso-dilators and there is a great interest in using dinitrate isosorbide for infarct treatment (FLÈCHE; HUCHETTE, 1986)

In the field of polymeric materials, isosorbide, as a diol, is firstly employed to synthesize or modify polycondensates, such as polyurethanes and polyesters (FENOUILLOT *et al.*, 2010). Nonetheless, due to its physical-chemical properties, isosorbide has also been applied in the synthesis of novel monomers to be polymerized via metathesis (FOKOU; MEIER, 2009).

Fokou and Meier (2009) described the synthesis of a novel monomer using isosorbide and 10-undecenoic acid as 100% renewable building blocks. The resulting molecule is an α,ω- diene diester and it was polymerized by ADMET polymerization. They obtained polyesters with molecular weight (M_n) up to 8400 Da depending on the reaction conditions; also they reported the physical-chemical characteristics of the polymer such as melting temperature and degree of isomerization.

Yoon and co-workers (2013) produced high-molecular-weight polyester, up to 71100 Da weight-average molecular weight, and with a high T_g of 131°C. Isosorbide was esterified to cis/trans-1,4-cyclohexanedicarboxylic acid to yield homopolyesters. Isosorbide is a diol with considerably low reactivity which normally results in a long polymerization time. However, the authors utilized acetic anhydride to perform an *in situ* acetylation of isosorbide, they found out that this method accelerates the chain growth of the polymer.

Besse and colleagues (2013) synthesized isocyanate-free polyurethanes from isorsorbide derived dicyclocarbonate and four different diamines. Dicyclocarbonate was obtained from epoxidized isosorbide by carbonatation. Synthesized linear and branched polyhydroxyurethanes presented T_g from -8 to 59°C and degradation temperatures from 234 to 255°C depending on the diamine utilized.

Sadler *et al.* (2014) utilized isosorbide as one of the diol structural constituents to produce unsaturated polyesters (UPE) to be used as thermosetting resins. Isosorbide was found to increase mechanical properties and T_g according to its concentration. However, the increase in the isosorbide content reduced the solubility of the resin in styrene, which was used as reactive diluent for blending the resins. Authors stated that although current formulations are inadequate for high-performance thermosetting applications, these resins do have viscosities that fall within the necessary ranges for composite application and adequately compare to some commercial UPE resins. Furthermore, it may be possible to use isosorbide in the future to improve current aromatic-based UPE resins.

Azizi and co-workers (2014) synthesized isosorbide-based polyurethane microcapsules for cosmeto-textile applications. Microcapsules were prepared by interfacial polycondensation method in an o/w emulsion system. SEM images have clearly shown spherical core-shell morphology of the particles, where the shell was constituted of PU and the core was constituted of neroline perfume. Particles presented unimodal size distribution in volume, with an average particle

size of 27 μm. Encapsulation efficiency of perfume was determined through ^{1}H NMR and accounted for 30%.

Finally, isosorbide is an attractive renewable resource derived compound to be used in the polymeric materials field due to its unique bi-ring structure, physical-chemical properties and the fact that it is derived from starch, not from petroleum. Isosorbide polymers have superior thermal and optical properties due to its molecular rigidity and the chirality of its asymmetrical hydroxyl groups (YOON *et al.*, 2013). In addition, several works can be found in the literature reporting biodegradable polymers obtained from isosorbide which widens its application scope (OKADA; TACHIKAWA; AOI, 1997, 2000; OKADA *et al.*, 2000; OKADA, 2002; YOKOE; KEIGO; OKADA, 2003; YOKOE; AOI; OKADA, 2005).

2.5 FINAL CONSIDERATIONS

An extensive number of papers have been published in the past two decades regarding the use of biofeedstocks in polymer chemistry. Herein, two promising platforms for novel renewable polymeric materials were presented: vegetable oils and carbohydrates. Both renewable raw materials are inexpensive and worldwide available.

Natural polymers can be modified to yield different materials, for instance, natural rubber undergoes vulcanization and has its individual polymer chains cross-linked, improving mechanical properties. That being said, modifying naturally-obtained materials can be complicated due to its structural complexity, for example many natural polymers are multifunctional such as starch, a polymeric carbohydrate. On the other hand, the synthesis of novel classes of monomers is a very interesting manner of designing the polymeric macromolecule.

Vegetable oils can undergo polymerization by different mechanisms, however, the straightforward polymerization of raw vegetable oils has not quite shown itself as a suitable alternative to achieve physical and chemical properties similar to petrol-derived polymers. Carbohydrates have been used to synthesize polyesters, polycarbonates, polyethers and polyurethanes. The most utilized carbohydrate monomers are dianhydroalditols, such as isosorbide, because they possess only two hydroxyl groups.

Rather than being polymerized directly, triglycerides and carbohydrates can be used as chemical platforms for new monomers syntheses. Triglycerides and fatty acids by extension, and carbohydrates feature a vast stereochemical diversity and many reactive sites that can

be chemically modified. One of the purposes of the present study is, therefore, to combine both fatty acid and carbohydrate into an environmentally friendly monomer. 10-Undecenoic acid, obtained bt pyrolysis of castor oil, and isosorbide, derived from starch, were utilized to synthesize a α,ω-diene diester monomer.

CHAPTER III

This Chapter is part of a publication entitled "**Thiol-Ene Polymerisation: A Promising Technique to Obtain Novel Biomaterials**" submitted to the European Polymer Journal.

3 THIOL-ENE REACTIONS

Thiol-ene reactions are often considered as click-chemistry reactions because they can be carried out under mild conditions and normally provide a high yielding and generation of inoffensive by-products (HOYLE; LEE; ROPER, 2004; HOYLE; BOWMAN, 2010). Novel materials are arising from thiol-ene reactions due to the interest on the unique crosslinking structure, improved mechanical properties, clean and environmentally harmless reaction, fast and regioselective polymerization, and degradability improvement that sulphide moieties can provide (REDDY; ANSETH; BOWMAN, 2005; RYDHOLM *et al.*, 2007; RYDHOLM; ANSETH; BOWMAN, 2007). In this context, thiol-ene polymers containing hydrolysable functional groups (RYDHOLM; BOWMAN; ANSETH, 2005; RYDHOLM *et al.*, 2006a, 2006b, 2007; RYDHOLM; ANSETH; BOWMAN, 2007; AIMETTI; MACHEN; ANSETH, 2009; WANG *et al.*, 2013), e.g. ester groups, are especially interesting in order to obtain (bio) degradable materials. In addition, many of the diene monomers used in thiol-ene polymerization are derived from renewable raw materials (TÜRÜNÇ; MEIER, 2010, 2013; FIRDAUS; MONTERO DE ESPINOSA; MEIER, 2011; WU *et al.*, 2011; TÜRÜNÇ *et al.*, 2012; VAN DEN BERG *et al.*, 2013).

Thiol-ene reactions have been extensively utilized for surface and molecules functionalization (FEIDENHANS'L *et al.*, 2014; CHEN *et al.*, 2015; IONESCU *et al.*, 2015; KUHLMANN *et al.*, 2015), molecules conjugation (STENZEL, 2013; KUHLMANN *et al.*, 2015), crosslinking (ACOSTA ORTIZ *et al.*, 2010; WANG *et al.*, 2013), grafting (KOLB; MEIER, 2013), UV-curable coatings (BLACK; RAWLINS, 2009; SANGERMANO *et al.*, 2009; ÇAKMAKÇI *et al.*, 2012) and polymerization of renewable monomers (KREYE; TÓTH; MEIER, 2011; TÜRÜNÇ *et al.*, 2012; KOLB; MEIER, 2013; TÜRÜNÇ; MEIER, 2013; YOSHIMURA *et al.*, 2015). In addition, some studies reported a set of biomedical applications for thiol-ene polymers such as preparation of nanoparticles and hydrogels suitable for drug-delivery systems, biomimetic hydrogels, dental restorative resins and hydrogels for tissue regeneration (CARIOSCIA *et al.*, 2005; LU *et*

al., 2005; AIMETTI; MACHEN; ANSETH, 2009; ZOU *et al.*, 2011; ROBERTS; BRYANT, 2013; ŠTORHA; MUN; KHUTORYANSKIY, 2013; HACHET *et al.*, 2014; KI *et al.*, 2014; VANDENBERGH *et al.*, 2014; YANG *et al.*, 2014). Thiol-ene polymers as biomaterials is, however, an underexplored field.

3.1 HISTORY AND CONTEXT

Thiol chemistry is a versatile tool and its use has been reported over several years comprising several fields. Posner (1905) first described, in 1905, the addition of mercaptans to olefins, the author reports the thiol coupling to different types of mono and bi-unsaturated compounds such as aliphatics, aromatics, terpenes, and hydroaromatics. Posner noticed that the structure of the olefin exercises strong influence on the fate of the reaction and that mercaptans are added to double bonds in an anti-Markovnikov arrangement. Furthermore, two of the 15 studied diolefins, namely limonene and cyclo-pentadiene, yielded only monoaddition products, probably in reason of the different reactivity of the double bonds present in the molecules.

Amongst a set of thiol group reactions, thiol-ene free radical addition drags special interest due to its application range and simplicity. Early work on this field has appeared in late 1930s to early 1950s (KHARASCH; READ; MAYO, 1938; MEISSNER; THOMPSON, 1938; HOYLE; LEE; ROPER, 2004). For over 70 years the photochemistry of thiols has been investigated from several points of view e.g. thiol decomposition, as a source of hydrogen atoms in the gas phase and in solution, as a source of thiyl radicals ($R\dot{S}$) (CARLSON; KNIGHT, 1973). Marvel and Chambers (1948) developed the first method to synthesize solid polymeric alkylene sulphides with molecular weight up to 14 kDa based on papers published then that reported non-distillable residues upon allyl mercaptan synthesis and afterward the utilization of dithiols and diolefins to synthesize liquid polymeric alkylene sulphides with molecular weight up to 1.3 kDa.

Marvel and Chambers (1948) utilized a set of different dithiols and diolefins but the UV-initiated polymerization between hexamethylenedithiol and 1,5-hexadiene portrayed the best result. Infrared absorption analysis revealed that the synthesized linear polymers had a structure resulted from an anti-Markovnikov addition, which agrees with Posner's work. X-ray diffraction showed that the solid polymers obtained presented crystalline structure.

There were several efforts, from late 1970s to early 1990s, to solidly introduce thiol-ene photopolymerization in industrial scale (HOYLE; LEE; ROPER, 2004). By the early 2000's many of the basics of thiol–ene chemistry were well defined, thiol-ene free-radical photoinitiated polymerization became significant due to several advantages over conventional free radical-polymerization such as fast reaction rates and reduced influence of oxygen inhibition. Their use for relatively simple materials applications, such as protective coatings and film were amply touted (HOYLE; LEE; ROPER, 2004; HOYLE; BOWMAN, 2010).

In the past few years the growing interest in green chemistry has drawn attention to thiol-ene polymerization as a technique to synthesize polymers from non-depleting sources and in several others emerging technologies. Moreover, thiol-ene reactions are regioselective, most require mild conditions, and are insensitive to ambient conditions such as oxygen and humidity (HOYLE; BOWMAN, 2010); this versatility makes thiol-ene chemistry a promising tool that can be applied in a set of applications e.g. resins (AUVERGNE *et al.*, 2012), protective polymers (BERGER; DELHALLE; MEKHALIF, 2009; SANGERMANO *et al.*, 2009; ÇAKMAKÇI *et al.*, 2012; CHEN *et al.*, 2015), polymers with optical properties (LI; ZHOU; HOYLE, 2009; FEIDENHANS'L *et al.*, 2014), biomedical and bioconjugated molecules (ROBERTS; BRYANT, 2013).

Thiol-ene reaction relies on the liability of thiol hydrogen. Thermochemical characteristics of thiols are an important factor influencing mechanistic elucidations of thiol-ene kinetics. Initial work on thiol group free-radical reactions had been done through a photochemical approach (KNIGHT, 1974), however the cleavage of sulphur-hydrogen bond can be promoted indirectly by heat- or light-generated nucleophilic radicals obtained from the cleavage of initiators, as in conventional free-radical polymerization (HOYLE; LEE; ROPER, 2004; CLAUDINO, 2011).

The $C-S$ bond is the weakest one in the molecule, about 73 kcal·mol^{-1}, while the $S-H$ bond is 88 ± 5 kcal·mol^{-1}. Regardless of this energy difference, the main decomposition is the $S-H$ cleavage due to liability of the sulphydryl hydrogen, which is the essentially exclusive site of abstractive attack on thiol molecule. In a system where there are others molecules susceptible to radical attack, e.g. olefins, the considerably lower activation energy for hydrogen removal from thiol group as compared to other hydrogen donor groups results in a high reactivity (KNIGHT, 1974)

The hydrogen abstraction from the thiol group generates highly reactive thiyl radicals ($R\dot{S}$) that add to a wide range of unsaturated compounds, virtually, any non-sterically hindered ene is capable of participating the reaction; though, for a given thiol, electron-rich enes polymerize much more rapidly than electron-poor enes (HOYLE; BOWMAN, 2010). The addition of a thiol across the olefin double bond is an exothermic reaction and the enthalpy depends mainly on the sort of the double bond, *i.e.* electron-poor double bonds give off more energy than electron-rich double bonds (HOYLE; BOWMAN, 2010).

3.1.1 Thiol-ene reaction mechanism

Primary studies regarding thiol-ene kinetics took place through the prism of photochemistry. The first investigations of the photochemical decomposition of thiols date back to 1938 (KHARASCH; READ; MAYO, 1938; MEISSNER; THOMPSON, 1938). Steer and Knight (1969) wrote a very elucidating paper on reactions of thiyl radicals; the authors studied the photolysis of methanethiol as a pure substrate and with added NO, as radical scavenger, C_2H_4, and inert gases. The mechanism proposed by the authors presented qualitative agreement to the observed kinetics data, thus several rate-constant ratios had been determined.

Knight (1974) provided a detailed description of the kinetic steps of the photoinitiated addition of methanethiol to ethylene in gas phase:

$$CH_3SH + h\upsilon \rightarrow CH_3\dot{S} + \dot{H} \quad (1)$$

$$\dot{H} + CH_3SH \rightarrow CH_3\dot{S} + H_2 \quad (2)$$

$$\dot{H} + C_2H_4 \rightarrow \dot{C}_2H_5 \quad (3)$$

$$\dot{C}_2H_5 + CH_3SH \rightarrow C_2H_6 + CH_3\dot{S} \quad (4)$$

$$C_2H_6 + xC_2H_4 + CH_3SH \rightarrow \text{higher alkenes} + CH_3\dot{S} \quad (5)$$

$$2CH_3\dot{S} \rightleftarrows CH_3SSCH_3{}^* \xrightarrow{M} CH_3SSCH_3 \quad (6)$$

$$CH_3\dot{S} + C_2H_4 \rightleftarrows CH_3S\dot{C}_2H_4 \quad (7)$$

$$CH_3S\dot{C}_2H_4 + CH_3SH \rightarrow CH_3\dot{S} + CH_3SC_2H_5 \quad (8)$$

The previous mechanism presents the existing reactions involved in a thiol-ene addition elucidated by analysing the products formed in the overall reaction, in this instance: methyl ethyl sulphide (8), hydrogen (2), and ethane (4). Methyl ethyl sulphide ($CH_3SC_2H_5$) is the major product observed in the process. Hydrogen and methyl ethyl disulphide, the main chain termination products, decrease with increasing ethylene pressure (STEER; KNIGHT, 1969).

Knight's group (1969, 1973) studied the photolysis of mercaptans, namely ethanethiol, in condensed phase. Hydrogen and diethyl disulphide were the only products detected; in addition, hydrogen and disulphide yields were the same. Due to the equivalence between the reaction products, the authors ruled out termination through thyil radical disproportionation, therefore termination occurs by combination of two radicals.

Martin, Jourdain and Le Bras (1988) wrote a clarifying paper portraying the fate of the hydrogen atom in reactions with methanethiol and ethanethiol; rather than participating in molecular hydrogen production or triggering the formation of a carbon-centred radical in the alkene, Ḣ can take part in hydrogen sulphide production among other possible reaction paths. The authors estimated kinetic constants and elucidated the reaction mechanisms.

3.2 THIOL-ENE POLYMERIZATION

Thiol-ene polymerization proceeds as the traditional free-radical polymerization, featuring three steps: initiation, propagation, and termination, plus a chain transfer step. In the mechanistically fundamental chain-transfer pace a carbon-centred radical transfers its electron to a thiol group. Generally, it is used a thiol:ene ratio of 1:1 in order to avoid side-reactions, such as reaction 6 where disulphide is formed. It is important to notice that a proper copolymerization between olefin and thiol molecules will only take place if the first is a diene and the latter a dithiol.

Figure 5 shows a simplified scheme of thiol-ene copolymerization. Firstly, a thiol is decomposed into thiyl radicals through hydrogen abstraction, which can be by photo- or thermoinitiation with the aid or not of initiators. Secondly, the thiyl radical attacks the double bond and add to the olefin. Finally, chain transfer occurs and the unpaired electron from a carbon-centred radical is transferred to another thiol group and another thiyl radical is generated, re-initialising the cycle. Thus, thiol-ene polymerization

revolves around the alternation between thiyl radical propagation across ene functional groups and chain-transfer reactions (HOYLE; BOWMAN, 2010). Termination, Figure 6, occurs through radical combination rather than disproportionation, as discussed by Carlson and Knight (1973), thiyl/thiyl coupling yielding a disulphide specie, thiyl/carbon-centred radical coupling and carbon-centred/carbon-centred radicals coupling. Cramer and co-workers (2003) elucidated that chain transfer is the rate-limiting step by performing studies on thiol-ene photo-polymerization modelling through the polymerization kinetics behaviour.

Figure 5. I. Step-growth polymerization: addition of a thiyl radical across the double bond. II. Chain-transfer from a carbon-centred radical to a thiol group.

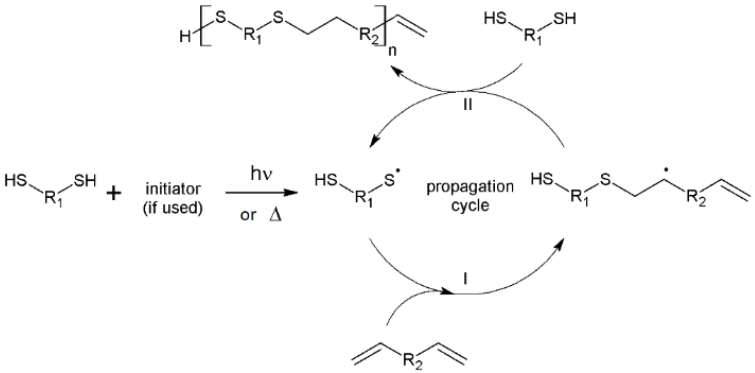

Source: Adapted from (CLAUDINO, 2011).

Figure 6. Termination mechanisms present in thiol-ene polymerization.

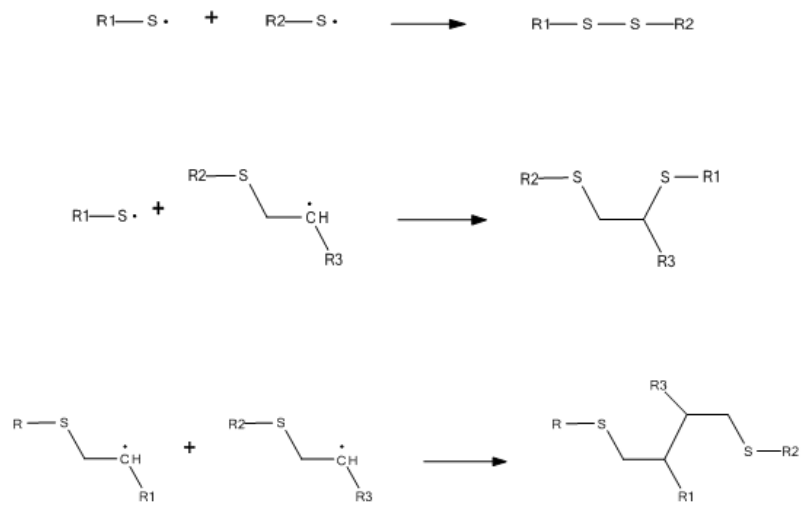

Source: Author.

In the ideal step-growth thiol–ene reaction, there is no propagation of the carbon-centred radical through the ene moiety (homopolymerization), the carbon-centred radical is always transferred to a thiol moiety. Normally, conversions approach 100 % unless mass-transfer limitations prevent such from being achieved. The net reaction, therefore, is simply the combination of the thiol and ene functional groups, which causes the molecular weight and network structure to evolve in a manner that is identical to any other step-growth polymerization reactions at the same time as empowering all of the benefits of a rapid, photo- or thermoinitiated radical mediated process (HOYLE; BOWMAN, 2010). The diene may undergo homopolymerization in a non-ideal system. It depends on the relative reactivity of both monomers, i.e., the propagation rate constant (k_P) is significantly higher than chain transfer rate constant (k_{ct}).

Differently from traditional free-radical polymerization, the presence of oxygen does not inhibit thiol-ene polymerization. In the presence of oxygen, additional chain-transfer reactions occur, the oxygen is incorporated into the growing polymer chains as a peroxy radical that undergoes chain transfer with a thiol to generate a thyil radical (CRAMER; BOWMAN, 2001). For a detailed discussion on the role of the oxygen in the thiol-ene reaction, the reader is referred to the

work by O'Brien, Cramer and Bowman (2006) approaching the overall effect of oxygen in thiol-acrylate photopolymerization.

3.2.1 Reactivity of thiol and ene compounds

Morgan, Magnota and Ketley (1977) evaluated the effect of both thiol and olefin structures on the overall rate towards thiol-ene addition reaction. Their work stated two fundamental rules. First, the overall conversion of thiol-ene reaction is directly related to the electron density on the ene, with electron-rich enes reacting faster than electron-poor enes in reason of the electrophilic nature of thiyl radicals. Electron-donating substituents attached or close to the double bond accelerate thiol addition while electron-withdrawing groups decrease the addition rate. The most common exception to this rule is when the carbon-centred allyl radical is resonance-stabilized, e.g. conjugated dienes. Second, mercaptopropionate esters copolymerize more rapidly than mercaptoacetate esters, which in turn react more rapidly than alkyl mercaptans, because of the intramolecular interaction between the sulphydryl hydrogen and the carbonyl that weakens $S-H$ bond enhancing hydrogen liability.

Roper and co-workers (2004) also investigated the influence of chemical structure in the reactivity of alkenes towards thiol-ene photopolymerization and their results corroborate Morgan *et al.*'s observations. Primarily, any non-hindered terminal ene group reacts rapidly and its aliphatic hydrocarbon substituent chain length has no effect on the reaction; accordingly, its reactivity is higher than internal alkenes. The authors observed that chain transfer to the thiol is the rate-limiting step corroborating Cramer *et al.*'s (2003) results. Therefore, any change in the alkene structure that disrupts chain transfer from the carbon-centred radical to the thiol, e.g. steric hindrance, causes a reduction in k_{ct}, and therefore decreases the overall reaction rate (ROPER *et al.*, 2004).

Hoyle; Lee & Roper (2004) classify the reactivity of the enes towards thiol-ene reaction through the ratio k_p/k_{ct}; even though not all the olefins cited are dienes, the following sequence also can be considered regarding thiol-ene polymerization:

Norborene > Vinyl ether > Propenyl > Alkene ≈ Vinyl ester > N-Vinyl amides > Allyl ether > N-Vinyl amides > Acrylate > Acrylonitrile ~ Methacrylate > Styrene > Conjugated dienes.

Norborene presents a remarkably fast polymerization rate because of the significant energy liberation after the thiyl radical addition across

the π-bond, which reliefs the ring strain, and the succeeding quick H-abstraction rate of the sulphydryl hydrogen by the carbon-centred radical. Methacrylate, styrene, and conjugated dienes possess low reaction rates owing to the high stability of their respective carbon-centred radicals that have intrinsically low H-abstraction rate constants (HOYLE; LEE; ROPER, 2004).

3.2.2 Thiol-ene polymers degradation

Bowman's group performed primary works on the subject of thiol-ene polymers degradation. Initial studies in the literature presented results on thiol-acrylate polymers degradation and others containing the ester group in the main chain (poly (thioether-ester)) probably due to the ease hydrolysis of ester groups, already demonstrated elsewhere (MÜLLER; KLEEBERG; DECKWER, 2001; WITT *et al.*, 2001; MUELLER, 2006; NAIR; LAURENCIN, 2007; LEJA; LEWANDOWICZ, 2010).

Reddy, Anseth and Bowman (2005) investigated the degradability of thiol-acrylate hydrogels. The authors have shown it is possible to synthesize polymeric networks with specific degradation profiles. Hydrogels were obtained through copolymerizing multifunctional thiol monomers with PLA-b-PEG-b-PLA based diacrylate monomers. Due to the nature of the acrylate double bonds, two different polymerization mechanisms are observed: chain growth polymerization, i.e. acrylate homopolymerization, and step growth polymerization, addition of thiol across the ene double bond. The balance between these two mechanisms, which is controlled through stoichiometry, dictates the network structure and, ultimately, the degradation behaviour. In addition, the number of crosslinks per kinetic chain was shown to decrease with increasing thiol concentration or decreasing thiol functionality, thus providing a facile means to control the network evolution and hence the degradation behaviour.

A paper recently published (WU *et al.*, 2015) evaluated the acidic degradation of linear poly(ß-thioether ester) and poly(ß-thioether ester-co-lactone) copolymers. Although Wu *et al.* chose an enzymatic polymerization route; ß-thioether ester moieties are achievable also through thiol-ene click chemistry. Wu *et al.* (2015) analyzed molecular weight loss and polydispersity variation according to the pH under which the degradation was carried out and to the duration of the degradation essay. The authors stated that the thioether-ester polymers are stable under physiological pH conditions but can be easily

hydrolyzed under acidic conditions, and therefore these polymers are potential acid-degradable polymers for biomedical applications.

Bowman's group obtained further results on biodegradability of thioether-ester polymers regarding the influence of the position of the sulphide groups in the degradation rate. Rydholm, Anseth & Bowman (2007) observed that the distance between the sulphide and the ester groups affects directly the degradation. The closer the sulphide group is to the ester group the faster hydrolysis is; e.g. when the number of carbons between these two groups are increased from 1 to 2 hydrolysis rate constant became about 4 times lower. For further information regarding thioether-ester/acrylate polymers degradation, the reader is referred to the works of Bowman's group (REDDY; ANSETH; BOWMAN, 2005; RYDHOLM; BOWMAN; ANSETH, 2005; RYDHOLM *et al.*, 2006b; RYDHOLM; ANSETH; BOWMAN, 2007).

Natural and synthetic biodegradable polymers have prospective applications in drug and protein delivery, tissue engineering, and environmental issues. These polymers breakdown into smaller molecules under specific biological stimuli. Novel biomaterials are arising from thiol-ene polymerization due to the interest on the unique crosslinking structure, improved mechanical properties, clean and environmentally harmless reaction, fast and regioselective polymerization, and degradability improvement that thiol-ene moieties can provide (REDDY, ANSETH & BOWMAN, 2005; RYDHOLM, ANSETH & BOWMAN, 2007). Thiol-ene polymers are thereby good candidates for biomedical applications and some of these applications have already been reported in the literature (AIMETTI, MACHEN & ANSETH, 2009; WANG *et al.*, 2013; VANDENBERGH *et al.*, 2014).

Bowman's group performed primary works on the subject of thiol-ene degradation. Initial studies in the literature presented results on degradation of thiol-acrylate hydrogels; probably due to the ease hydrolysis of ester groups already discussed elsewhere (MÜLLER; KLEEBERG; DECKWER, 2001; LUCAS *et al.*, 2008; TIAN *et al.*, 2012).

3.3 THIOL-ENE REATIONS: APPLICATIONS

Thiol-ene reactions have been extensively utilized for surface and molecules functionalization (FEIDENHANS'L *et al.*, 2014; CHEN *et al.*, 2015; IONESCU *et al.*, 2015; KUHLMANN *et al.*, 2015), molecules conjugation (STENZEL, 2013; KUHLMANN *et al.*, 2015), crosslinking (ACOSTA ORTIZ *et al.*, 2010; WANG *et al.*, 2013), grafting (KOLB;

MEIER, 2013), UV-curable coatings(BLACK; RAWLINS, 2009; SANGERMANO *et al.*, 2009; ÇAKMAKÇI *et al.*, 2012), and polymerization of renewable monomers. (KREYE; TÓTH; MEIER, 2011; TÜRÜNÇ *et al.*, 2012; KOLB; MEIER, 2013; TÜRÜNÇ; MEIER, 2013; YOSHIMURA *et al.*, 2015). However, little attention has been paid to the potential to synthesize biocompatible and biodegradable polymers for biomedical application through thiol-ene polymerization. Natural and synthetic biodegradable polymers have prospective applications in drug and protein delivery, tissue engineering, and environmental issues. These polymers breakdown into smaller molecules under specific biological stimuli. Innovative biomaterials are arising from thiol-ene polymerization due to the interest on the unique crosslinking structure, improved mechanical properties, clean and environmentally harmless reaction, fast and regioselective polymerization, and degradability improvement that thiol-ene moieties can provide (REDDY; ANSETH; BOWMAN, 2005; RYDHOLM *et al.*, 2006b, 2007). Thiol-ene polymers are thereby good candidates for various biomedical applications, and some of these applications have already been reported in the literature (AIMETTI; MACHEN; ANSETH, 2009; WANG *et al.*, 2013; VANDENBERGH *et al.*, 2014; AMATO *et al.*, 2015).

3.4 FINAL CONSIDERATIONS

Herein, the basics of thiol-ene polymerization and its applications were discussed. Thiol-ene polymerization is very often considered as a click-chemistry reaction for it can be carried out under mild conditions and normally provides a high yielding and generation of inoffensive byproducts. Thiol-ene polymerization is a versatile method that can be carried out by thermal or photoinitiation and normally yields high conversion (>99%) and possess a rapid kinetics. In addition, by using monomers with different functionalities, it is possible to tune some polymers properties such as degree of crosslinking, degradability, shrinkage stress and other physical features. Depending on the application, different physical and chemical characteristics are desired; e.g. for drug release within the human body it is very important for polymeric vectors to be (bio) degradable, on the other hand it is essential for dental restorative composites or coatings to be non-degradable and possess hydrolytic stability.

Applications for thiol-ene polymers in the past few years are mostly as hydrogels and cross-linked polymers. These polymers have been successfully synthesized comprising different kinds of multifunctional enes and thiols. Studies reported that thiol-ene polymers are suitable for preparation of nanoparticles, and hydrogels for drug-delivery systems, biomimetic hydrogels, and dental restorative resins. Furthermore, many authors reported the possibility of tuning the surface chemistry of hydrogels and nanoparticles by using non-stoichiometric thiol-ene ratios, which could lead to free thiol groups on the surface, which in turn are capable of binding to other molecules such as proteins. This is a very good prospective to further study enzyme-responsive nanoparticles by anchoring a substrate on the nanoparticle surface. As a dental restorative resin, thiol-ene polymers displayed superior mechanical characteristics when compared to the currently utilized methacrylate resins. Thiol-ene polymers as biomedical materials is a field still underexplored; not many papers have been published under this subject even though there are many advantages in using these materials. For instance, it could be studied the accelerated ester group degradation due to the presence of sulphide moieties in the polymeric backbone towards drug release, the possibility to create bioconjugates on nanoparticles surface using non-reacted thiol groups on its surface to create stimuli-responsive nanocarriers and nanodevices for clinical exams and imaging.

CHAPTER IV

4. MINIEMULSION POLYMERIZATION

Miniemulsions are heterophase systems in which sub-micrometric droplets of one phase, typically ranging from 50 to 500 nm (ANTONIETTI; LANDFESTER, 2002), are dispersed in a second continuous phase. When the miniemulsion consists in an oil-in-water dispersion it is called direct miniemulsion; the contrary system, i.e. water-in-oil dispersion, is named inverse miniemulsion.

In contrast to conventional emulsion polymerization, that features micelar nucleation, miniemulsion polymerization presents droplet nucleation, as shown in the pioneering work of Ugeldtad *et al.* (1973), i.e. there is no need for mass transfer of monomer through the continuous phase, and therefore the droplets are the polymerization loci. Ideally, this means that every droplet formed through (mini) emulsification process may become a particle after polymerization. Consequently, it is often considered that every droplet acts like a bulk polymerization nanoreactor (BECHTHOLD *et al.*, 2000; ANTONIETTI; LANDFESTER, 2002).

Miniemulsion is formed prior to polymerization by high shear energy (e.g. by ultrasonication or high-pressure homogenization) which breaks down the disperse phase into sub-micrometric droplets, typically droplet size range from 50 to 500 nm (BECHTHOLD *et al.*, 2000; ANTONIETTI; LANDFESTER, 2002). Although miniemulsion droplets are thermodynamically unstable, they are kinetically metastable and therefore preserve their colloidal property for a few hours up until a few months. Figure 7 shows a scheme to produce a direct miniemulsion. Two immiscible phases are subjected to high shear, resulting in small, homogeneous, and narrowly distributed nanodroplets. Inside the droplet phase, an osmotic pressure agent (co-stabilizer) and possible agents for further encapsulation are included. In a subsequent reaction process, ideally no change of the droplets is observed (LANDFESTER, 2009).

Figure 7. Miniemulsion polymerization process scheme.

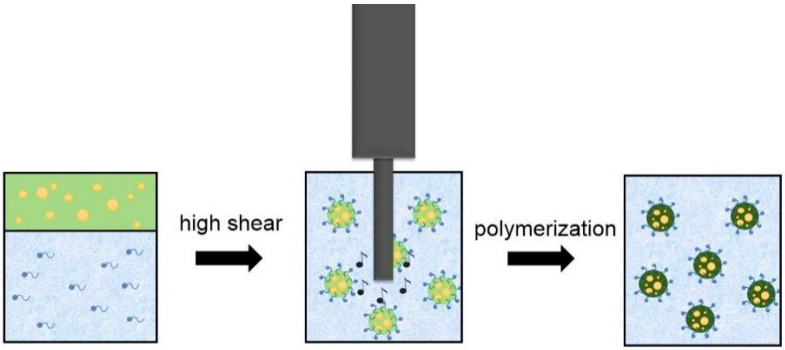

Source: Adapted from (LANDFESTER, 2009).

The organic phase contains traditionally monomer, a co-stabilizer, and initiator. Aqueous phase contains water and surfactant. Organic and aqueous phases undergo either a mechanical or a magnetic stirring to form a macroemulsion. Miniemulsion is then obtained when the macroemulsion is submitted to high shear energy by means of, usually, an ultrasonic probe. Once droplets are formed they may be polymerized into particles. Droplets are stabilized by two main mechanisms. First, surfactant minimizes droplets coalescence (see Figure 8) and stabilizes the particles electrostatically or sterically and hence impedes droplets, as well as particles, to come in close contact and aggregate.

Figure 8. Coalescence scheme.

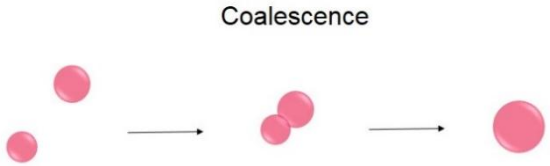

Source: Author

Second, miniemulsion always features a distribution in droplet size even when surfactant provides sufficient colloidal stability. Droplets with different sizes present different interfacial energies or Laplace pressures, which is inversely proportional to size, and this determines droplet size distribution; in addition, it is a driving force for

diffusion between the droplets. Diffusion leads to the growth of the bigger droplets in detriment of the smaller ones, a process known as diffusional degradation or Ostwald ripening. Figure 9 shows a scheme of diffusional degradation. The addition of co-stabilizer in the dispersed phase, substance with the least water solubility of all components in the system, retards the diffusional degradation.

Figure 9. Diffusional degradation scheme.

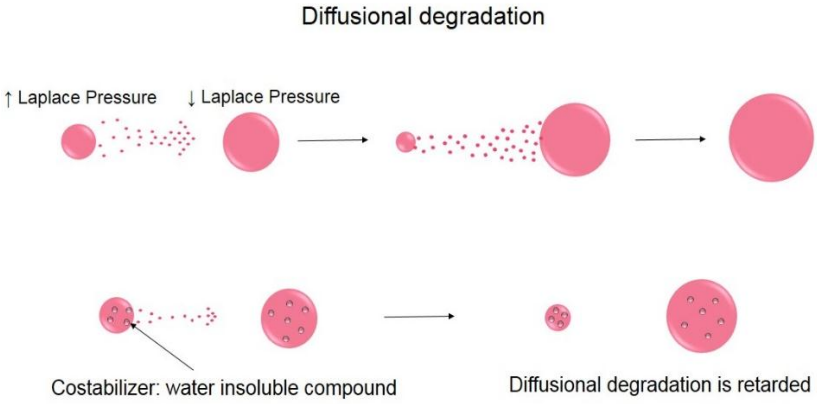

Source: Author.

Co-stabilizers cannot be able to diffuse through the aqueous phase from one droplet to another; therefore, a difference in concentration of the co-stabilizer inside the droplets, which increases with decreasing droplet size, creates a counterforce upon monomer diffusion. Consequently, due to the presence of co-stabilizer an osmotic pressure builds up that counteracts the Laplace pressure responsible for diffusional degradation. (ANTONIETTI; LANDFESTER, 2002; ASUA, 2002; LANDFESTER, 2003; SCHORK *et al.*, 2005; STAUDT *et al.*, 2013).

Many types of polymerization reactions can be adapted to be carried out using a miniemulsion system, e.g. polycondensation (ANTONIETTI; LANDFESTER, 2002; BARRÈRE; LANDFESTER, 2003; LANDFESTER, 2003; VALÉRIO; ARAÚJO; SAYER, 2013; VALÉRIO *et al.*, 2014), radical polymerization (ANTONIETTI; LANDFESTER, 2002; ASUA, 2002;

LANDFESTER, 2003), enzymatic polymerization (QI; JONES; SCHORK, 2006; KOHRI *et al.*, 2012), ATMET (DE O. ROMERA *et al.*, 2015) and ADMET (CARDOSO *et al.*, 2014) polymerization, and thiol-ene polymerization (JASINSKI *et al.*, 2014b; LOBRY *et al.*, 2014).

In addition, miniemulsion polymerization is a versatile technique to synthesize sub-micrometric particles or capsules that suit for a wide range of applications that can hardly be achieved through other heterophase processes, e.g. in situ encapsulation (ROMIO *et al.*, 2009a, 2009b; BERNARDY *et al.*, 2010; CARDOSO; ARAÚJO; SAYER, 2013), hybrid particles (ROMIO *et al.*, 2013; STAUDT *et al.*, 2013; CHIARADIA *et al.*, 2015; MERKEL *et al.*, 2015), drug delivery systems (MESSERSCHMIDT *et al.*, 2009; BEHZADI *et al.*, 2014; BAIER *et al.*, 2015; FEUSER *et al.*, 2015).

4.1 THIOL-ENE POLYMERIZATION IN MINIEMULSION

Thiol-ene polymerization in miniemulsion is a fresh field, many characteristics are still to be studied, such as kinetics and mechanism (JASINSKI *et al.*, 2014b; LOBRY *et al.*, 2014; AMATO *et al.*, 2015). Some studies have been performed on the production of cross-linked polymer through thiol-ene polymerization in miniemulsion. Only in 2014, the first papers portraying the synthesis of linear polymers through thiol-ene polymerization were published.

Lobry *et al.* (2014) published a short communication reporting the synthesis of linear poly(thioether) nanoparticles via thiol-ene photopolymerization in miniemulsion in a continuous-flow microreactor. Co-monomers used were ethylene glycol dithiol and diallyl adipate. Hexadecane was used as co-estabilizer against diffusional degradation and sodium dodecyl sulphate was used as surfactant. A thermal analysis of the produced polymer through DSC revealed a glass transition temperature (T_g) of – 63 °C and a melting temperature (T_m) of 18 °C. The polymer was insoluble in most organic solvents due to its high crystallinity (55%) and therefore the authors characterised the molecular weight only for the soluble part (M_n = 30 kDa).

Jasinski *et al.* (2014) presented a complete work regarding the synthesis of linear poly(thioether) nanoparticles in miniemulsion using ethylene glycol dithiol and diallyl adipate as co-monomers. Thiol-ene photopolymerization in miniemulsion yielded a poly(thioesther-ester)

latex with average particle size of 130 nm. Calorimetric analyses showed a T_g of – 63 °C and a semicrystalline behaviour (degree of crystallinity = 55%) indicated by an endothermic melting peak at 18 °C and an exothermic recrystallization peak at 6 °C.

Amato *et al.* (2015) synthesized cross-linked polythioether nanoparticles through thiol-ene photopolymerization in miniemulsion. Amato *et al.* investigated the effects of surfactant concentration, organic phase weight percentage and the influence of the co-stabilizer in thiol-ene miniemulsions. In addition, by performing non-stoichiometric thiol-ene polymerizations nanoparticles containing either thiol or ene functional groups on the surface, depending on which monomer was in excess, were obtained. These surface functional groups were utilized for post-polymerization modifications; fluorescent markers were attached to the surface. Polythioether nanoparticles with ene surface groups underwent radical-mediated thiol-ene addition with 7-mercapto-4-methylcoumarin (blue marker), and nanoparticles with thiol surface groups underwent thiol-ene Michael addition with Texas Red maleimide (red marker). Post-polymerization modified nanoparticles were analysed via fluorescence microscopy.

At first glance, thiol-ene polymerization in miniemulsion, as free-radical reactions that follows through step-growth mechanism, might present kinetic characteristics very different from traditional free-radical miniemulsion polymerization. Few works have been published regarding thiol-ene bulk polymerization (CRAMER; BOWMAN, 2001; CRAMER *et al.*, 2003; COLE; JANKOUSKY; BOWMAN, 2013). Cramer *et al.* (2003) stated that in thiol-ene polymerization complicating kinetic factors from diffusion controlled reactions or early gelation are not as significant as in traditional chain growth systems because thiol-ene systems do not exhibit conventional auto-acceleration behaviour and do not gel until high conversions are obtained due to their step-growth nature. However, many other important factors, such as the average number of radicals per particle, nucleation mechanism and solubility of the monomer(s) in the aqueous phase are relevant to miniemulsion polymerization kinetics (SCHORK *et al.*, 2005).

Furthermore, in thiol-ene co-polymerizations in miniemulsion where thiol and ene monomers possibly will present different solubility towards water, co-monomer composition in the polymerization locus, i.e. inside the droplets, might be quite different from the overall co-monomer composition; and since thiol-ene reactions are very sensible to functional group ratio (thiol:ene) this could be a serious hindrance to overcome.

4.2 FINAL CONSIDERATIONS

Miniemulsion polymerization has become an important technique in the past decades due to its versatility. Many types of materials can be synthesized through miniemulsion polymerization and the application range is vast.

Historically, the synthesis of aqueous polymer dispersions has focused on radical chain-growth polymerization of low-cost acrylate or styrene emulsions. In addition, step-growth polymerization to produce polyesters and polyurethanes were also performed in miniemulsion.

Thiol-ene step-growth polymerization in miniemulsion is being currently investigated and only a handful of articles have been published in the literature. Thiol-ene polymerization is a click reaction that has been utilized for many applications from UV-curable coatings to biomedicine. In addition, thiol-ene polymerization has been remarkably utilized to produce polymers from fully renewable diene monomers that are usually derived from fatty acids and therefore provide potential degradability properties to the polymer. The prospective of obtaining high molecular weight polyesters in aqueous dispersed medium is, *per se*, a great advantage in performing thiol-ene polymerization in miniemulsion. In addition, henceforth many other types of interesting materials could be obtained, e.g. nanocomposites, nanocapsules, hybrid particles and so on.

“Complications arose, ensued, were overcome.”
(Jack Sparrow, 2006)

CHAPTER V

5 RENEWABLE RESOURCES DERIVED POLY (ESTER-THIOETHER) NANOPARTICLES AND CAPSULES VIA THIOL-ENE POLYMERIZATION IN MINIEMULSION

5.1 INTRODUCTION

This chapter presents the experimental procedure and the results and discussion of the synthesis of a fully renewable diene diester monomer (derived from castor oil and isosorbide) and its copolymerization with butanedithiol via thiol-ene polymerization in miniemulsion to yield poly(thioether-ester) nanoparticles. Step-growth polymerization normally comprises water-sensitive precursors (polyurethane) or water byproduct (polyester) leading to equilibrium processes. Polyurethanes are produced based on water-sensitive precursors (isocyanates), their reaction with water generates polyurea, and in aqueous dispersed medium this leads to the formation of polyurea-urethane; urea moieties possess lower molecular weight than urethane moieties causing an overall decrease in the molecular weight. In addition, synthesis of polyester involves the formation of water as byproduct and thus synthesis of polyester in aqueous dispersed medium leads to low yield and low molecular weight due to chemical equilibrium. Although their implementation in aqueous dispersed medium has proven to be feasible, peculiar conditions are required to avoid poor yields and low molecular weights (BARRÈRE; LANDFESTER, 2003; VALÉRIO; ARAÚJO; SAYER, 2013; VALÉRIO *et al.*, 2014).

In this work, the synthesis of poly(thioether-ester) nanoparticles via thiol-ene step-growth polymerization in miniemulsion is presented. Thiol-ene polymerization in miniemulsion is a field still underexplored and poly(thioether-ester) nanoparticles have prospective applications as biodegradable biomaterial.

5.2 EXPERIMENTAL PROCEDURE

5.2.1 Materials

10-Undecenoic acid (Sigma-Aldrich, 98%, CAS: 112-38-9), dianhydro-D-glucitol (Aldrich, 98%, CAS: 652-67-5), p-toluenesulfonic

acid monohydrate (Sigma-Aldrich, 98.5%, CAS: 6192-52-5), sodium dodecyl sulfate (SDS, Vetec, CAS: 151-21-3), potassium persulphate (KPS, Vetec, 99%, CAS: 7727-21-1), azobisisobutyronitrile (AIBN, Vetec, 98%, CAS: 78-67-1), Lutensol AT80 (Lut. AT80, BASF), which is a C16C18 fatty alcohol ethoxylate with 80 ethylene oxide units, Lutensol AT50 (Lut. AT50, BASF) poly(ethylene oxide) hexadecyl ether with 50 ethylene oxide units, hexadecane (HD, Vetec, 99%, CAS: 544-76-3), and Crodamol GTCC (Crod.), a fully saturated triglyceride consisted mainly of esters of caprylic acid (C8) and capric acid (C10) extracted from coconut oil purchased from Alfa Aesar. All materials were used as received except for AIBN that was recrystallized. Distilled water was used in all experiments.

5.2.2 Dianhydro-D-glucityl diundec-10-enoate (DGU) Synthesis

60 g of 10-undecenoic acid (purity: 98%, 318.9 mmol), 16.08 g of 1,4 dianhydro-D-glucitol (purity: 98%, 107.8 mmol) and 3 g (15.7 mmol) of p-toluensulfonic acid were placed in a round-bottomed flask with magnetic stirrer and a Dean-Stark apparatus. Then, 200 mL of toluene were added and the resulting reaction mixture was heated to reflux, up to 135°C. Water was collected as the reaction proceeded and once the reaction was completed, the reaction mixture was allowed to cool down. Figure 10 shows a scheme of the esterification reaction. Toluene was removed under reduced pressure and the residue was filtered through a short pad of basic aluminium oxide followed by a short pad of silica gel 60 using hexane as eluent. After removing the hexane, the crude product was dissolved in diethyl ether (200 mL), washed twice with 1N $NaHCO_3$ solution (200 mL) and once with water (200 mL) from reverse osmosis. The organic fraction was dried with anhydrous $MgSO_4$ and the solvent was removed under reduced pressure. The resulting product was subjected to thin-layer chromatography over silica gel and eluted with mixtures of hexane/diethyl ether (7:1) and hexane/diethyl ether (8:2).

Figure 10. Esterification reaction of 10-undecenoic acid and dianhydro-D-glucitol to yield dianhydro-D-glucityl diundec-10-enoate.

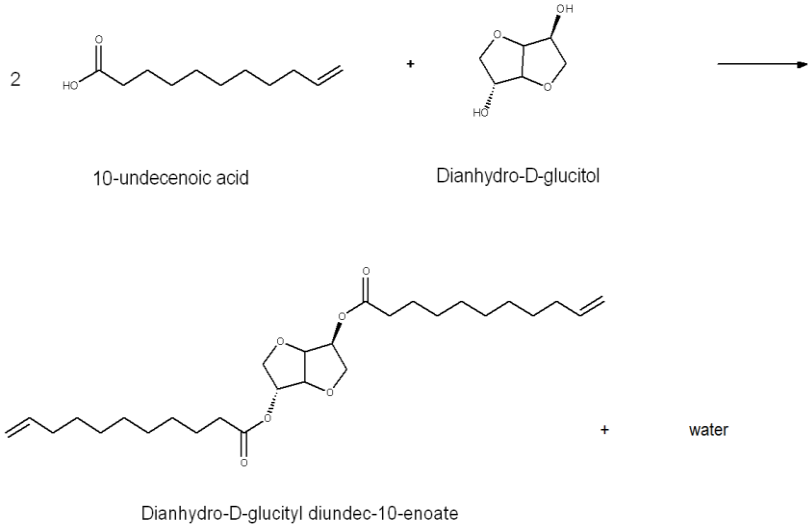

Source: Author.

5.2.3 Bulk Polymerization

DGU was placed in a conical vial and organic-soluble initiator was added, then the mixture was let under magnetic stirring until complete initiator solubilisation. After initiator solubilisation, $BuSH_2$ was added to the system (typically, 1:1 $BuSH_2$-to-DGU molar ratio). The polymerization was carried out at determined temperature (60, 70, 80 or 90 °C) for 4 to 8 h in a dry block heater.

Table 4 shows a typical bulk polymerization formulation which contains 2.1 mmols of both DGU and $Bu(SH)_2$, initiators at 1 mol% in relation to $Bu(SH)_2$. Formulations were eventually modified to test different conditions but every modification or condition tested is specified in the discussion.

Table 4. Typical bulk polymerization formulation used as basis to test different conditions. DGU-to- $Bu(SH)_2$ molar ratio is 1:1 and AIBN is added at 1 mol% in relation to dithiol.

Entry	DGU (g)	$Bu(SH)_2$ (mL)	AIBN (g)
B1	1.00	0.24	0.0034

5.2.4 Miniemulsion Polymerization

The aqueous phase was prepared using water and surfactant at determined concentration in relation to distilled water and, if used, water-soluble initiator (KPS); the mixture was let under magnetic stirring until complete surfactant (and initiator, if used) solubilisation. The organic phase was prepared using dianhydro-D-glucityl diundec-10-enoate (DGU) and, if used, organic-soluble initiator (AIBN); the mixture was let under magnetic stirring until complete initiator solubilisation. The aqueous phase was added to the organic phase in a 20 mL vial and an emulsion was formed under vigorous magnetic stirring (500 rpm) for 10 minutes. Then 1,4-butanedithiol ($BuSH_2$) was added (typically, 1:1 $BuSH_2$-to-DGU molar ratio) to the system with a micropipette and it was let under mild magnetic stirring (250 rpm) for 5 minutes. The final emulsion underwent sonication for 2 minutes, at 70 % of amplitude in a pulse regimen (10 s sonication, 5 s pause) using a Fisher Scientific Sonic Dismembrator model 500 and a 1/2" tip in ice bath. After miniemulsion preparation, the system was placed in a silicone oil bath at determined temperature (60, 70, 80 or 90 °C) and polymerization was carried out for 4 to 8 h.

Figure 11 shows a scheme of miniemulsion preparation. Table 5 displays standard formulations for miniemulsion polymerizations, typically 2.1 mmol of both DGU and $Bu(SH)_2$, initiators at 1 mol% in relation to $Bu(SH)_2$ and 8 $mmol \cdot cm^{-3}$ of surfactant were used. HD and Crod. were used as co-stabilizers at 10 wt.% in relation to monomers combined weight. Water amount in miniemulsions containing co-stabilizers was increased in order to maintain the same organic phase/aqueous phase weight ratio. Formulations were eventually modified to test different conditions but every modification or condition tested is specified in the discussion.

Figure 11. Miniemulsion preparation procedure.

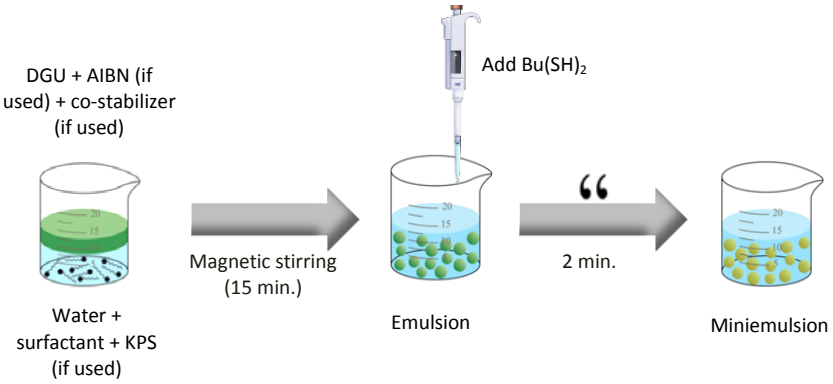

Source: Author.

Table 5. Typical miniemulsion polymerization formulations used as basis to test different conditions. DGU-to- $Bu(SH)_2$ molar ratio is 1:1 and AIBN or KPS is added at 1 mol% in relation to dithiol. Surfactants at 8 mmol·cm^{-3}. HD and Crod. at 10 wt.% in relation to monomers combined weight.

Reactants	Entry					
	M1	M2	M3	M4	M5	M6
DGU (g)	1.00	1.00	1.00	1.00	1.00	1.00
$Bu(SH)_2$ (mL)	0.24	0.24	0.24	0.24	0.24	0.24
AIBN (g)	0.0034	0.0034	0.0034	-	0.0034	0.0034
HD (g)	-	-	-	-	0.123	-
Crod. (g)	-	-	-	-	-	0.123
H_2O (g)	5.00	5.00	5.00	5.00	5.50	5.50
KPS (g)	-	-	-	0.0056	-	-
Lut. AT80 (g)	0.15	-	-	0.15	-	-
Lut. AT50 (g)	-	0.10	-	-	0.15	0.15
SDS (g)	-	-	0.0122	-	-	-

5.2.4.1 Thiol-ene polymerization kinetics in miniemulsion

Thiol-ene polymerization in miniemulsion kinetics experiments were carried out in sealed ampoules in order to evaluate the dithiol conversion, functional group conversion, and molecular weight. The ampoules were immersed in a thermal bath at 80 °C at the beginning of the reaction and were withdrawn at fixed times and quickly quenched in

an ice bath to stop the reaction. Miniemulsion was prepared as described in the section 5.2.4. Kinetics experiments were performed using 3 g of DGU (6.3 mmol), 0.735 mL of $Bu(SH)_2$ (6.3 mmol), 0.0368 g of SDS, 15 g of distilled H_2O, and either 10.3 mg of AIBN (63 µmol) or 17.0 mg of KPS (63 µmol).

Dithiol monomer conversions were calculated from the ratio of polymer weight and initial monomer weight. The polymer weight of each sample was determined gravimetrically.

5.2.5 Proton Nuclear Magnetic Resonance (^{1}H NMR)

^{1}H NMR analyses were recorded in deuterated chloroform, $CDCl_3$, using a Bruker Ascend 600 spectrometer at 600 MHz. Chemical shifts (δ) are reported in part per million (ppm) relative to tetramethylsilane (TMS) intern standard used for calibrating chemical shift (TMS, δ = 0,00 ppm). Analyses were performed it the Laboratório de Ressonância Magnética Nuclear – LRMN, University of Brasília – UnB, Brazil.

5.2.6 Fourier Transform Infrared Spectroscopy (FTIR)

FTIR for liquid samples (DGU) was performed on an IR Prestige-21 spectrophotometer from Shimadzu with Horizontal Attenuated Total Reflectance (HATR) accessory (ZnSe plate) from Pike, in the range of wavenumbers 4000–600 cm^{-1}. A single drop of the liquid sample was placed on the ZnSe plate and analysed in order to investigate the functional group peaks and the presence of water.

For solid polymer samples, Attenuated-total-reflectance Fourier-transform-infrared (ATR-FTIR) spectroscopy was performed on a Bruker spectrometer, model TENSOR 27, in the range of wavenumbers 4000–600 cm^{-1} by accumulating 32 scans at a resolution of 4 cm^{-1}. Solid polymer samples ATR-FTIR analyses were performed in the Laboratório de Materiais (LABMAT) at the Mechanical Engineering Department of the Federal University of Santa Catarina. Samples were analysed as powder.

5.2.7 Particle Size Measurements

Particle size distribution was measured by dynamic light scattering (DLS) using a Zetasizer Nano S equipment from Malvern Instruments. A drop from either the miniemulsion or the latex was

placed in a glass cuvette and diluted in distilled water prior to the measurement. Analyses were performed in the Laboratório de Controle e Processos de Polimerização (LCP) at the Department of Chemical and Food Engineering of the Federal University of Santa Catarina.

5.2.8 Gel Permeation Chromatography (GPC)

The polymer was precipitated from the latex by adding the latter in cold methanol under vigorous stirring, then the mixture was filtered and 0.05 g of the polymer retained was diluted in 4 mL of tetrahydrofuran (THF). The obtained solution was filtered through a nylon syringe filter, pore: 0.45 µm, diameter: 33 mm. The molecular weight distributions were obtained through gel permeation chromatography using a high-performance liquid chromatography equipment (HPLC, model LC 20-A, Shimadzu) and Shim Pack GPC800 Series columns (GPC 801, GPC 804 e GPC 807), also from Shimadzu. THF was used as eluent with volumetric flow rate of 1 $mL \cdot min^{-1}$ at 40 °C. The GPC system was calibrated using polystyrene standards with molecular weight ranging from 580 to $9.225 \cdot 10^6$ $g \cdot mol^{-1}$. Analyses were performed in the Laboratório de Controle e Processos de Polimerização (LCP) at the Department of Chemical and Food Engineering of the Federal University of Santa Catarina.

5.2.9 Differential Scanning Calorimetry (DSC)

Samples of dried polymer with more than 5 mg were analysed using a DSC 4000 Perkin Elmer, under inert atmosphere (20 $mL \cdot min^{-1}$), from - 60 to 150 °C at a heating rate of 10 °C/min. The thermal history was removed prior to the analyses at a heating rate of 20 °C/min and cooling rate of -20 °C/min. The melting temperatures were thus obtained from the second heating run. Analyses were performed in the Laboratório de Propriedades Físicas de Alimentos (PROFI) at the Department of Chemical and Food Engineering of the Federal University of Santa Catarina.

5.2.10 X-ray Diffraction (XRD)

Crystallinity characterisation was performed by X-ray diffraction (XRD) using a PANalytical X'PERT X-ray system λ= 1.5406 Å Cu $K\alpha_1$ radiation and $2\theta = 10 - 70°$ range, employing a scanning rate of 2.5º/min.

The crystallinity of the synthesized thioether-ester polymers was analysed through X-ray diffraction. The degree of crystallinity was estimated using Eq. 9 (CHALMERS; MEIER, 2008):

$$X_C(\%) = \frac{I_C}{I_C + K \cdot I_A} \cdot 100 \quad (9)$$

where I_C is the sum of the area of all crystalline reflections, I_A is the area of the amorphous halo, and K is a proportionality constant to account for the relative scattering of the amorphous and crystalline phases which is close to 1 in many cases (CHALMERS; MEIER, 2008).

Analyses were performed in the Laboratório de Difração de Raios X (LDRX), Federal University of Santa Catarina.

5.2.11 Transmission Electron Microscopy

Particle morphology characterisation was performed by Transmission Electron Microscopy (TEM) using a JEM-1011 TEM (100 kV).The as-synthesized latex was diluted, in distilled water, down to 0.01% of solids content. One single drop of the diluted latex (0.5% of solid content) was placed on an either carbon-coated or parlodium-coated copper grid and it was dried under room conditions overnight. Analyses were performed in the Laboratório Central de Microscopia Eletrônica (LCME), Federal University of Santa Catarina.

5.3 RESULTS AND DISCUSSION

5.3.1 Synthesis and characterisation of a fully renewable monomer derived from castor oil and isosorbide

A fully renewable diene diester monomer, Dianhydro-D-glucityl diundec-10-enoate (DGU), was produced through esterification in organic solvent (toluene) of 10-undecenoic acid (derived from castor oil) and isosorbide (derived from starch). Fokou and Meier (2009) reported the synthesis of this same diene monomer structure through a different, more complex, synthetic route. Fokou and Meier utilized DGU for metathesis polymerization and obtained number average molecular weight up to 8400 with experiments carried out at 80°C for 5 h using second generation Grubbs metathesis catalyst; herein, the diene monomer is used for thiol-ene polymerization in miniemulsion.

Figure 12 shows the characteristic ^{1}H NMR spectrum of DGU, characterised as follows:

^{1}H-NMR (600 MHz, $CDCl_3$, δ): 5.81-5.74 (m, 2H, 2x-CH=CH_2), 5.16 (d, 1H, -COO-CH-), 5.11 (q, 1H, -COO-CH-), 4.98-4.89 (m, 4H, 2x-CH=CH_2), 4.79 (t, 1H, -CH_2 -O-CH-), 4.43 (d, 1H, -CH_2-O-CH-), 3.97-3.94 (dd, 1H, -CH_2-O-CH-), 3.93-3.89 (m, 2H, -CH_2-O- CH-), 3.76 (dd, 1H, -CH_2-O-CH-), 2.33 (t, 2H, CH_2COO-), 2.27 (t, 2H, CH_2COO-), 2.00 (q, 4H, 2xCH_2-CH=CH_2), 1.63- 1.53 (m, 4H, 2xCH_2CH_2COO-), 1.36-1.31 (m, 4H, 2xCH_2) 1.29-1.23 (br.s, 16H, 2x[4CH_2]) ppm.

In addition, FTIR spectrum from DGU in Figure 13 is in agreement with the anticipated structure. Peaks in 3076 cm^{-1}, 1640 cm^{-1} and 910 cm^{-1} correspond respectively to =C–H stretch in the unsaturated hydrocarbon chain, C=C stretch and CH_2 out-of-plane wag from CH=CH_2 in vinyl compounds. A shoulder at 2977 cm^{-1} corresponding to ene groups can also be observed. At 2930 cm^{1} one can observe a peak correspondent to CH antisymmetric and symmetric stretching from –CH_3 and –CH_2– in aliphatic moieties. At 2850 cm^{-1}, it is presented CH stretching modes from –CH_3 attached to oxygen. The very strong peak at 1740 cm^{-1} indicates C=O stretch in esters. Peaks at 1162 cm^{-1} and 1095 cm^{-1} stand for respectively C-O-C antisymmetric stretch in esters and C-O-C stretch in ethers. CH_2 out-of-plane wag from HC=CH_2 in vinyl compounds shows up at 910 cm^{-1}. Moreover, it was not detected any –OH peak referent to water or 10-undecoic acid.

Figure 12. Characteristic ^{1}H NMR spectrum of DGU and peaks labelled and match to the hydrogen atoms in the molecule.

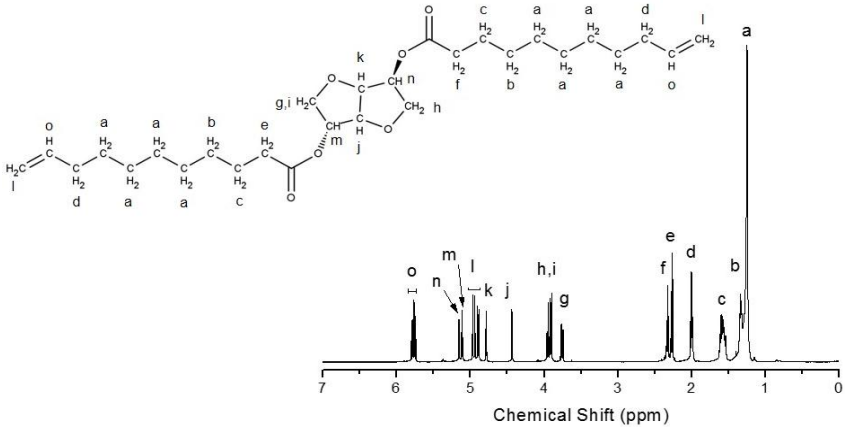

Source: Author.

Figure 13. Characteristic FTIR-HATR spectrum of purified DGU.

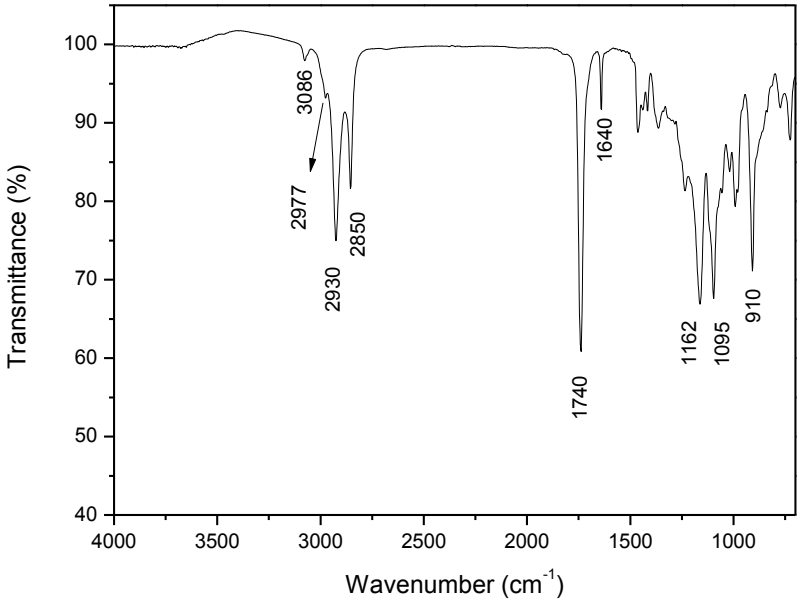

DGU was copolymerized with $Bu(SH)_2$ both in bulk and in miniemulsion. All miniemulsion and latex samples presented fair stability. DGU-to-$Bu(SH)_2$ ratio was kept 1:1 for most polymerization experiments. In addition, miniemulsions were prepared to obtain lattices with high solid content of 20 to 25%.

5.3.2 Development of poly (thioether-ester) via thiol-ene miniemulsion polymerization

Poly (thioether-ester) nanoparticles were prepared via miniemulsion polymerization using a diene monomer (DGU) derived from renewable resources. Table 6 shows the intensity average droplet size and dispersion of DLS, and ultimately particle size and dispersion of DLS, from three miniemulsion polymerization experiments carried out at 80°C for 4h using 1 mol% of AIBN as initiator, i.e. identical reactions except for the type of surfactant utilized. All surfactants were tested in the same concentration, 8 $mmol \cdot cm^{-3}$.

Table 6. Average droplet size (Dp_0) and dispersion (PDI_0) of DLS, and ultimately particle size (Dp) and dispersion (PDI) of DLS for miniemulsions with different surfactants tested at 8 mmol·cm^{-3}. Reactions carried out at 80°C for 4h using 1 mol% of AIBN.

Entry	Surfactant	Dp_0 (nm)	PDI_0	Dp (nm)	PDI
M1	Lut. AT 80	246 ± 11	0.29 ± 0.04	196 ± 1	0.18 ± 0.01
M2	Lut. AT 50	260 ± 14	0.38 ± 0.04	221 ± 3	0.30 ± 0.04
M3	SDS	197 ± 3	0.20 ± 0.02	188 ± 3	0.24 ± 0.01

Figure 14 displays the particle size distribution (PSD) for miniemulsions from Table 6. It shows a very small population of macrodroplets, which is attributed to issues in sonication step during the miniemulsion preparation. It is important to consider that part of the 1,4-butanedithiol generates thiyl species during the sonication, once a radical is formed it triggers the polymerization before the miniemulsification step is concluded. Premature polymerization may ultimately affect sonication efficiency due to the viscosity increase. In addition, DGU is a very hydrophobic compound and therefore no co-stabilizer was necessary in order to avoid diffusional degradation.

Figure 14. Particle size distribution (PSD) for miniemulsion polymerizations with different surfactants (Lut. AT80 – M1; Lut. AT50 – M2; and SDS – M3) tested at 8 mmol·cm^{-3}. Reactions carried out at 80°C for 4h using 1 mol% of AIBN.

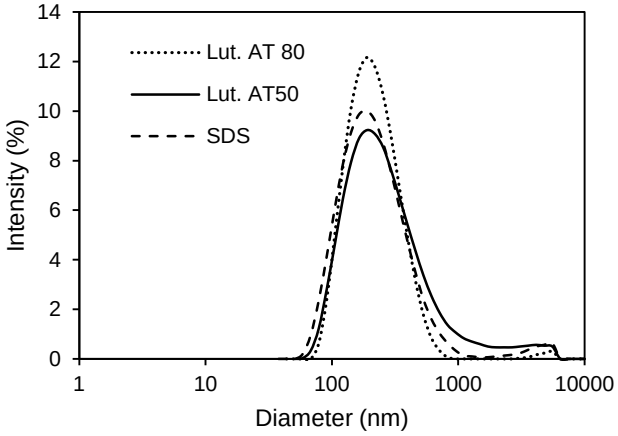

In fact, some authors (AMATO *et al.*, 2015) have experienced this phenomenon and reported in their published work. Amato *et*

al. (2015) have included inhibitor in the miniemulsion formulation to avoid polymerization during sonication step. This attempt was not adopted in this work in order to achieve a fair comparison between different types of initiator (AIBN and KPS). However, gravimetric analyses revealed a $Bu(SH)_2$ conversion of at least 35 % and 10 % after sonication when, respectively, AIBN and KPS were utilized; plus an initiatorless attempt evidenced a 10% conversion owe to polymerization during sonication.

Samples using non-ionic surfactants M1 and M2 showed considerable difference between droplet and particle sizes. For sample M3 with the anionic surfactant SDS the difference between droplet and particle size as well as dispersion before and after polymerization is less than 10% and therefore can be neglected. Lut. AT50 yielded higher droplet and particles sizes than Lut AT80. SDS provided the lowest particle size and the narrowest PSD. There are two explanations for the observed results. Firstly, Lut. AT80 possesses a higher molecular weight and a higher surface coverage per mole unit – as it normally happens for non-ionic surfactants when their chain/molecular weight is increased – than Lut AT50 (HOLMBERG *et al.*, 2002). Thus a higher quantity of Lut. AT 50 – which possesses molecular weight 1.5 times lower (see Table 7) – is needed for a similar system to be obtained in order to balance number of moles of surfactant and surface coverage. Secondly, even though SDS provides lower surface coverage, differently from non-ionic surfactants, it provides electrostatic stabilisation to the droplets/nanoparticles, a powerful mechanism to avoid loss of colloidal stability.

Table 7. Molecular weight and surface coverage of the surfactants tested in mimiemulsion polymerization.

Surfactant	M.W. ($g \cdot mol^{-1}$)	CMC ($mmol \cdot L^{-1}$)	Surface coverage ($m^2 \cdot mol^{-1}$) (water/MMA interface)
Lut. AT 80	3780	$1.1 \cdot 10^{-3}$(LERCH, 2012)	-
Lut. AT 50	2460	$2 \cdot 10^{-3}$ (MERKEL *et al.*, 2015)	$7.41 \cdot 10^{5}$ (MERKEL *et al.*, 2015)
SDS	288.68	5.5 (MERKEL *et al.*, 2015)	$6.17 \cdot 10^{5}$ (MERKEL *et al.*, 2015)

Higher Lut AT50 and SDS concentrations, 16 $mmol \cdot cm^{-3}$, were tested. As expected, lower average particle sizes and narrower particle size distributions were obtained with the increase of the surfactant

concentration. At 16 mmol·cm^{-3} the final lattices presented particle diameter of 175 ± 1 and 138.5 ± 0.4 for miniemulsions containing, respectively, Lut. AT50 and SDS; plus low PDI (<0.2) was obtained. Note that doubling up Lut AT50 molar concentration its weight percentage becomes higher than the weight percentage in which Lut AT80 was added to the miniemulsions.

Figures 15 and 16 exhibit some TEM images of the synthesized lattices. Figures 15a and 15b show poly (thioether-ester) nanoparticles stabilised with Lut. AT80 and Lut. AT50 respectively – some particles in Figure 14b are indicated by black arrows. Figure16a shows poly DGU-Bu(SH)$_2$ nanoparticles stabilised with SDS. It is important to mention that, herein, it is presented the first TEM images of thiol-ene linear polymers sub-micrometric particles, specifically poly (ester-thioether).

Figure 15. Poly (thioether-ester) nanoparticles stabilised with: (a) Lut. AT80 (M1) and (b) Lut. AT50 (16 mmol·cm^{-3}). In (b) black arrows indicate particles.

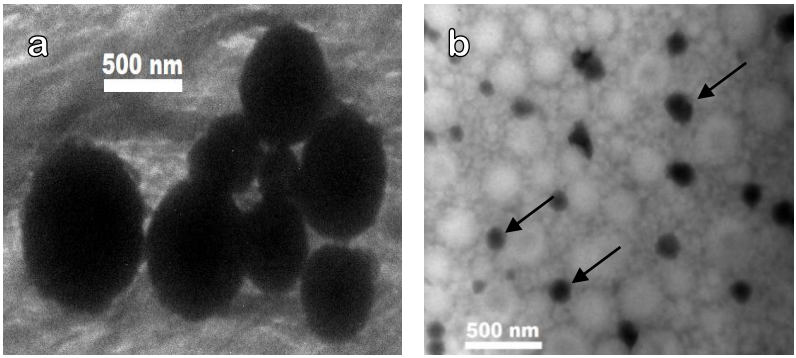

The morphology of non-cross-linked polymer particles with low glass transition temperature and low melting point (<100°C) are not very often successfully analysed by TEM, except in cases when cryo-TEM is available. Nonetheless, the morphology of poly (DGU-Bu(SH)$_2$) particles was effectively visualized when TEM equipment was operated at the lowest current possible, which in its turn provides low image resolution. Polymeric particles melted during the microscopy session when the current was increased in order to obtain better images; Figure 16 compares the same particles before (a) and after melting (b).

Figure 16. Poly (thioether-ester) nanoparticles stabilised with SDS (M3). Polymer particles before (a) and after (b) melting under electron beam.

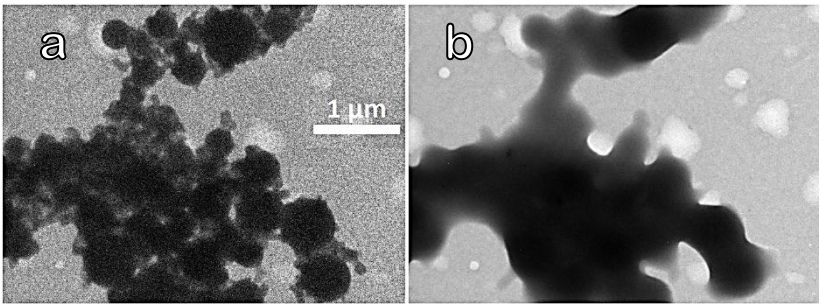

Obs.: Both (a) and (b) images have the same scale.

Poly(thioether-ester) particles produced by thiol-ene copolymerization of DGU with $Bu(SH_2)$ in miniemulsion presented spherical morphology. Furthermore, TEM analyses corroborate DLS results, that even though there is a majority of small particles, a population of macroparticles is also existent and draws more attention in TEM images due to their bigger size and easier visualization.

Polymerization reactions were carried out under different conditions, such as reaction time, temperature, and amount of initiator, to evaluate the effect on molecular weight distribution. Thiol-ene polymerization is an unique reaction that combines both step-growth and free-radical mechanisms (HOYLE; LEE; ROPER, 2004; HOYLE; BOWMAN, 2010), therefore it was expected to obtain higher average molecular weights for higher functional groups conversion, which increases with the time of the reaction. Table 8 shows the average molecular weight and the molecular weight dispersion (M_W/M_N) for 4, 6 and 8 h of polymer samples synthesized via bulk polymerization (B samples) at 70°C and using 1 mol% of AIBN in relation to $Bu(SH)_2$.

Table 8. Mean average and weight average molecular weight and molecular weight disperion of polymer samples polymerized for 4, 6 and 8 h via bulk polymerization (1 mol% of AIBN).

Entry	Time (h)	M_N (kDa)	M_W (kDa)	M_W/M_N
B1	4	6.68	13.99	2.10
	6	7.08	15.00	2.12
	8	6.88	14.16	2.05

Bulk polymerization results (B1) from Table 8 suggest that molecular weight does not change from 4 to 8 hours, which might indicate that functional group conversion may have already reached a maximum value. Ideally, functional group conversion should increase with time and by consequence the degree of polymerization; however, many are the issues such as the increase in viscosity that causes low mobility of growing polymer chains that affect directly functional group conversion and restrict the degree of polymerization.

A set of polymerization experiments were carried out at different temperatures (see Table 9), ranging from 60 to 90°C, for 4 h. Both bulk and miniemulsion polymerizations used 1 mol% of AIBN in relation to $Bu(SH)_2$. Figure 17 and Figure 18 display miniemulsion polymerizations and bulk polymerizations obtained molecular weight distribution in terms of the normalized signal vs. retention time from GPC. In Figure 17, correspondent to miniemulsion polymerization, molecular weight distribution curves are closer than in Figure 18, correspondent to bulk polymerization, and therefore apparently molecular weight distribution is less sensitive to temperature in miniemulsion than in bulk polymerization.

Table 9. Number average and weight average molecular weight of polymer samples polymerized at 60, 70, 80 and 90°C for 4 h via miniemulsion (M samples) and bulk (B samples) using 1 mol% of AIBN. Lut. AT80 at 8 mmol•cm-3 was used as surfactant.

Entry	T (°C)	Dp (nm)	M_N (kDa)	M_W (kDa)
M7	60	218 ± 2	2.18	4.64
M8	70	194 ± 2	10.87	34.54
M1	80	196 ± 1	11.13	38.26
M9	90	213 ± 3	9.72	26.79
B2	60	-	2.98	5.82
B1	70	-	6.68	14.00
B3	80	-	8.26	21.42
B4	90	-	4.27	11.45

Figure 17. Molecular weight distribution, in terms of the normalized signal vs. retention time, of miniemulsion polymerization experiments carried out at 60 (M7), 70 (M8), 80 (M1), and 90°C (M9) for 4h using 1 mol% of AIBN.

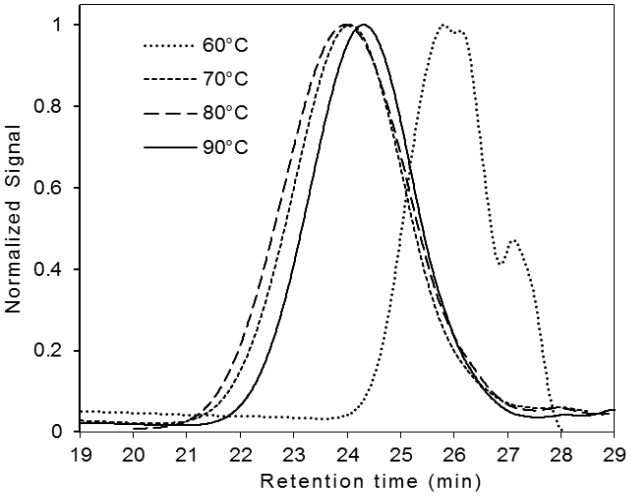

Table 9 shows that comparing the molecular weight of polymer samples synthesized at the same conditions except for the polymerization technique, either miniemulsion or bulk; samples synthesized via thiol-ene polymerization in miniemulsion resulted in higher molecular weight than in bulk polymerization for all the temperatures tested, except for 60°C. This indicates that at some extent there is an effect of radical compartmentalization, which in its turn occurs when a single radical is confined to the droplet and thus bimolecular termination (Figure 6) is supressed (LANDFESTER, 2003). At 60°C, the initiator half-life is about 20h (Eq. 11) and, therefore, polymerization reaction occurs virtually with no initiator decomposition; thus there is no difference in molecular weight of the samples from both bulk and miniemulsion polymerizations.

Figure 18. . Molecular weight distribution, in terms of the normalized signal vs. retention time, of bulk polymerization experiments carried out at 60 (B1), 70 (B2), 80 (B3), and 90°C (B4) for 4h using 1 mol% of AIBN.

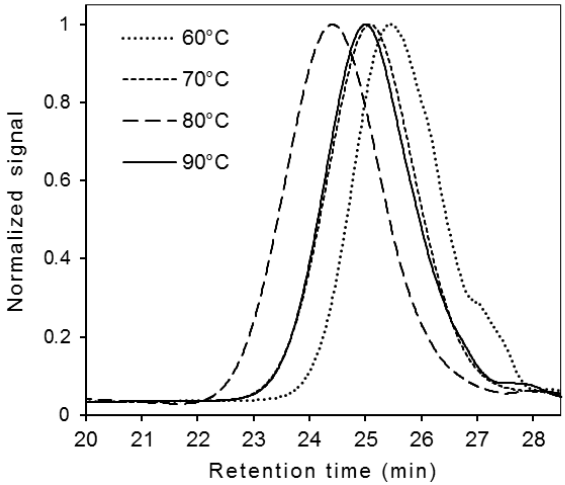

Results in Table 9 and Figures 17 and 18 show that, in general, increasing the temperature of the polymerization there is an increase in molecular weight. Nevertheless, at 90 °C a decrease in M_N was observed. Firstly, rate constants – from initiator decomposition (k_d), propagation (k_p), chain-transfer (k_{ct}), and termination (k_t) – are temperature-dependent. Constant rates dependence from different polymerization steps behave differently towards temperature. It could mean that, for example, at 90 °C k_t becomes much higher than k_{ct}. In addition, thiol-ene polymerization is a step-growth polymerization that proceeds as free radical reactions and therefore it needs to undergo initiation (Figure 5). In step-growth polymerizations, molecular weight depends on functional group conversion, which in its turn depends on temperature. As thiol-ene polymerization combines both step-growth and free radical mechanisms; it is reasonable to consider that with the increase in temperature the initiator decomposes at a faster rate and thus functional groups are allowed to react faster and the degree of polymerization is enhanced because more thiyl radicals are being generated.

Thus, based on the displayed results, 80°C is the temperature condition that provided the highest molecular weight results for both miniemulsion and bulk polymerization.

Reaction conditions were fixed at 4 h and 80°C also because of the half-life of AIBN in order to test the effects of other parameters. In free-radical polymerization, various initiators are used depending on their rates of decomposition. The decomposition of initiators can be conveniently expressed in terms of the initiator half-life ($t_{1/2}$), which is defined as the time for the concentration of initiator to decrease to one half of its original value (ODIAN, 2009). The decomposition constant of AIBN in toluene is given by the Eq. (10) (BRANDRUP *et al*., 1999):

$$k_d(s^{-1}) = 1.58 \cdot 10^{15} \times exp\left(\frac{-128900}{8.314 \times T(K)}\right) \quad (10)$$

and its half-life is given by:

$$t_{\frac{1}{2}}(s) = \frac{\ln\frac{1}{2}}{-k_d} \quad (11)$$

Therefore, at 80 °C and considering toluene as solvent, $t_{1/2}$(AIBN) is 1.4 h, this way a reaction time of 4 h means that roughly 7/8 of the AIBN would have been decomposed.

Table 10 shows the effect of different particle sizes on the average molecular weight of thiol-ene polymerization in miniemulsion at 80 °C using 1 mol% of AIBN (in relation to $Bu(SH)_2$) as initiator. As it is shown in Table 10, number-average molecular weight seems to reach a peak value as average particle size approaches 190 nm when thiol:ene ratio is 1:1 (M3). Non-stoichiometric experiments (M11, M12) were performed in order to observe the effect in molecular weight and if the molecular weight would respond to the change in the particle size similarly to its behaviour in stoichiometric reactions (M1, M3, M10).

Table 10. Number and weight average molecular weights of polymer samples synthesized in miniemulsion at 80°C for 4 h using AIBN at 1 mol% and different concentrations of surfactants to obtain different particle sizes (M1, M3, M10). Plus, samples synthesized with 20% excess of dithiol (M11, M12).

Entry	Surf.	[Surf.] ($mmol \cdot cm^{-3}$)	Dp (nm)	thiol/ene	M_N (kDa)	M_W (kDa)
M1	Lut. AT 80	8	196 ± 1	1:1	11.13	38.26
M3	SDS	8	188 ± 3	1:1	15.46	41.78
M10	SDS	16	138 ± 1	1:1	5.19	17.60
M11	SDS	8	158 ± 1	1.2:1	2.79	5.84
M12	SDS	16	142 ± 3	1.2:1	2.40	4.65

When thiol-to-ene ratio was increased to 1.2:1, M11 and M12, molecular weight dropped considerably in comparison to the stoichiometric polymerization, M3 and M10.

Comparison between bulk and miniemulsion polymerization results indicates radical compartmentalization effect occurs in thiol-ene polymerization in miniemulsion; however not as prominent as it happens in traditional free-radical polymerization in miniemulsion. Radical compartmentalization occurs when a single radical is confined to the droplet and thus bimolecular termination is supressed. On the other hand, a significant increase in the droplet size might make bimolecular termination more likely to occur due to the higher content of radicals inside the droplet. In traditional miniemulsion systems radical compartmentalization leads to faster polymerization rates and higher molecular weights (LANDFESTER, 2003 COSTA *et al.*, 2013). On the other hand, thiol-ene polymerization in miniemulsion not only depends on average number of radicals per particle but mainly of the stoichiometry. Therefore, there is a radical compartmentalization effect as long as the stoichiometry in the polymerization locus is not compromised.

Miniemulsion polymerization is a heterophase technique, which means that the components are partitioned between organic and aqueous phases, especially those compounds that possess a significant solubility in the both phases, which is the case of the 1,4-butanedithiol. This partition between the two phases may change local stoichiometry inside the droplet, the polymerization locus, which may be accounted for the observed results because thiol-ene polymerization is intrinsically reliant on the stoichiometry (CRAMER *et al.*, 2003).

The observed effect can be explained by the great difference in interfacial area inflicted by the change in droplet/particle diameter. Thiyl radicals are mostly produced inside the droplet because AIBN is an organo-soluble initiator. However, $Bu(SH)_2$ has a significant solubility in water (1.32 $mg \cdot mL^{-1}$), close to the solubility of MMA in water, and therefore $Bu(SH)_2$, and consequently thiyl radicals, are able to leave the droplet to the water phase. An increase in interfacial area means that more radicals are capable of leaving the droplet to the water phase and consequently the composition inside the droplet is changed. Thiol-ene step-growth polymerization is strictly dependent on the functional group ratio, non-stoichiometric reactions are known to significantly reduce functional group conversion in thiol-ene photopolymerization (CRAMER; BOWMAN, 2001; CRAMER *et al.*, 2003) and therefore the

molecular weight is also reduced as observed when comparing reactions M3 to M11 and M10 to M12.

The influence of the type and the amount of initiator were evaluated. Table 11 displays number average and weight average molecular weight results of miniemulsion and bulk polymerizations where AIBN (organo-soluble) and KPS (water-soluble) were used as initiators in different concentrations (0.5, 1, 1.5, 2 mol%). Miniemulsion and bulk experiments underwent polymerization for 4 h at 80°C.

Table 11. Number average and weight average molecular weight of miniemulsion and bulk polymerizations with different type (AIBN and KPS) and amount (0.5, 1, 1.5, 2 mol%) of initiator in relation to dithiol and carried out at 80°C for 4 h. Lut. AT80 at 8 mmol·cm^{-3} was used as surfactant.

Entry	AIBN (mol%)	KPS (mol%)	Dp (nm)	M_N (kDa)	M_W (kDa)
M13	0.5	-	224 ± 2	5.76	13.54
M1	1	-	196 ± 1	11.13	38.29
M14	1.5	-	218 ± 2	7.67	21.48
M15	2	-	207± 1	9.74	26.20
B5	0.5	-	-	6.46	16.15
B6	1	-	-	8.26	21.39
B7	1.5	-	-	8.83	20.31
B8	2	-	-	7.72	15.67
M16	-	0.5	192 ± 2	9.18	24.88
M4	-	1	195 ± 1	7.31	22.37
M17	-	1.5	170 ± 1	6.58	17.04
M18	-	2	177± 1	6.25	14.88

It can be seen in Table 11 that increasing the concentration of AIBN from 0.5 to 1% M_N increases for both miniemulsion (M13 and M1 respectively) and bulk (B5 and B6 respectively) polymerizations, however when AIBN concentration is further increased molecular weight starts to fall off. As for KPS, it was observed a decline in molecular weight with the increase in initiator concentration just as happens in traditional free radical polymerization (ODIAN, 2009). Figures 19, 20 and 21 show the molecular weight distributions of the samples from Table 11. Figure 19 corresponds to miniemulsion polymerizations containing 0.5; 1; 1.5 and 2% of AIBN; Figure 20 corresponds to bulk polymerizations containing 0.5; 1; 1.5; and 2% of AIBN; and Figure 21 corresponds to miniemulsion polymerizations containing 0.5; 1; 1.5; and 2% of KPS.

Figure 19. Molecular weight distribution in terms of normalized signal vs. retention time of miniemulsion polymerization experiments (80°C, 4h) containing AIBN at 0.5 (M13), 1 (M1), 1.5 (M14) and 2 mol% (M15) in relation to dithiol.

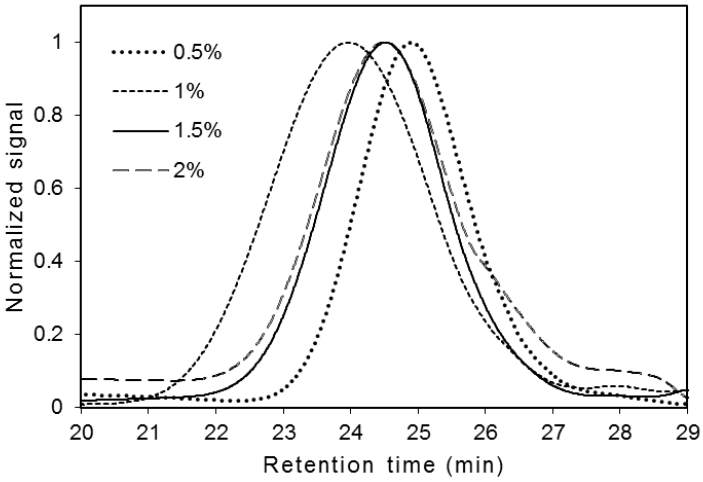

The influence of initiator concentration in molecular weight is very little explored in thiol-ene polymerization, probably because, in most cases, a polymeric network is obtained and in this case, molecular weight cannot be measured. Even initiator concentration effects on kinetics are not well explored; most of the works (CRAMER *et al.*, 2003; NORTHROP; COFFEY, 2012) focus on thiols and enes with different functionalities and thiol–to-ene ratios. However, a paper (COLE; JANKOUSKY; BOWMAN, 2013) evaluates the influence of initiator concentration in the kinetics of redox initiated thiol-ene bulk polymerization, but only functional groups conversion was evalueated.

Figure 20. Molecular weight distribution in terms of normalized signal vs. retention time of bulk polymerization experiments (80°C, 4 h) containing AIBN at 0.5 (B5), 1 (B6), 1.5 (B7) and 2 mol% (B8) in relation to dithiol.

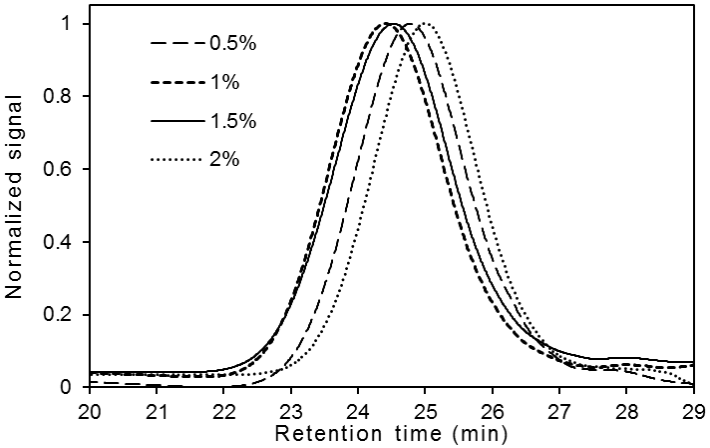

Figures 19, 20 and 21 show the difference in the molecular weight distribution according to the amount and type of the initiator. In traditional free radical polymerization, molecular weight is directly dependent of the amount of initiator, the higher the concentration the lower the molecular weight; and this behaviour is observed independent on the type of the initiator, water or organo-soluble. However, in thiol-ene polymerization a different behaviour is observed. AIBN provided the best molecular weight result at the concentration of 1 mol%, concentrations of 0.5, 1.5 and 2 mol% resulted in lower molecular weight for both miniemulsion and bulk polymerization. In its turn, KPS behaved exactly the way is considered common in free radical polymerizations, the lower the concentration the higher the molecular weight. The precise explanation for the observed results might be obtained through further kinetic experiments.

Figure 21. Molecular weight distribution in terms of normalized signal vs. retention time of miniemulsion polymerization experiments (80°C, 4 h) containing KPS at 0.5 (M16), 1 (M4), 1.5 (M17) and 2 mol% (M18) in relation to dithiol.

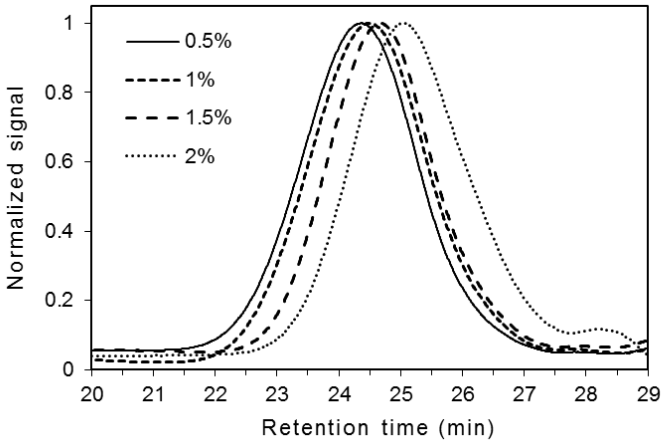

5.3.3 Thermal properties and crystallinity

Polymeric samples were submitted to thermal analysis through differential scanning calorimetry and results are displayed in Figure 22. The melting temperature of polymers resultant from either miniemulsion or bulk polymerization are presented in Table 12. The synthesized poly(thioether-ester)s presented a double-melting behaviour observed in semicrystalline polymers (HIRAKAWA; HIRAMATSU, 1980; YU *et al.*, 1983; YASUNIWA *et al.*, 2004). The lower temperature peak is due to the partial melting and recrystallization of the imperfect crystallite, whilst the higher temperature peak corresponds to the melting of the better-organised crystallite (YU *et al.*, 1983). It was observed a slight variation in the temperature of melt according to molecular weight of miniemulsion samples, i.e. samples with lower molecular weight had their melting peak shifted to the left and therefore indicating a melting temperature a few degrees lower (see Figure 22).

Figure 22. Differential scanning calorimetry curve showing melting temperatures of the polymers resultant from both miniemulsion polymerization: (a) M7 (Lut. AT 80, 60°C), (b) M8 (Lut. AT80, 70°C), (c) M1 (Lut. AT80, 80°C), (d) M9 (Lut. AT80, 90°C), (e) M3 (SDS, 80°C); and bulk polymerization: (f) B6 (80°C). Initiator: AIBN 1 mol%.

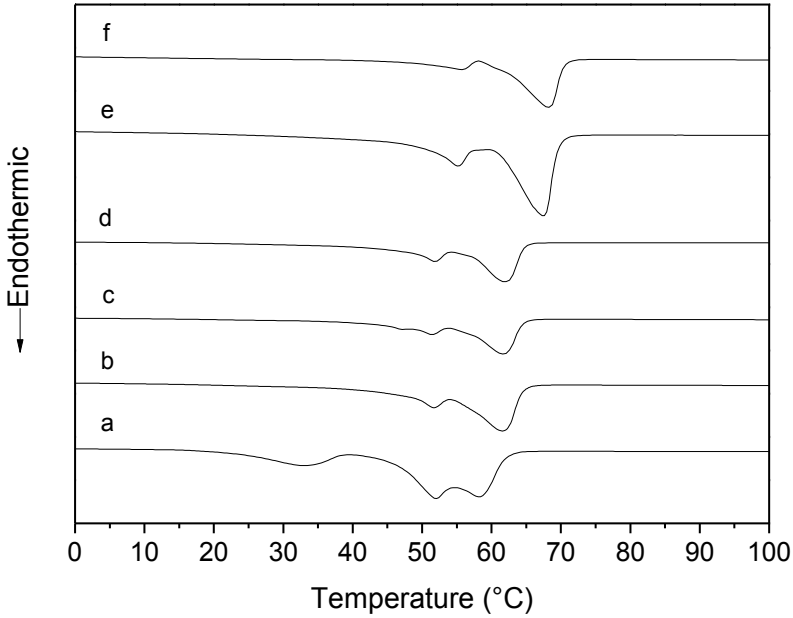

It was not possible to observe the glass transition temperature (T_G) through DSC, even though some samples were cooled down to -70°C; and this is due to their crystallinity. It may be possible, however, to determine the T_G through relaxation methods such as dynamic mechanical and dielectric spectroscopies as reported (FOCARETE *et al.*, 2001) by other authors who worked with highly crystalline polymers. The crystallinity observed in these poly(thioether-ester)s is an effect of intra- and intermolecular interactions between functional groups, and a highly linear structure. It is important to notice that it was not possible to determine the degree of crystallinity through DSC due to the lack of data about the polymer such as the enthalpy of a fully crystalline reference or an exothermic recrystallization event. The method used by calculating the degree of crystallinity through Eq. 9 based on the peaks from XRD gives a fair approach, even though it is

difficult to draw an amorphous halo unambiguously. Poly (DGU-Bu$(SH)_2$) samples presented crystallinity degrees between 20 and 50%.

Figure 23. X-ray diffraction spectra of the polymers resultant from both miniemulsion at different temperatures: (a) M7 (60°C), (b) M8 (70°C), (c) M1 (80°C), (d) M9 (90°C), (e) M3***** (80°C); and bulk polymerization: (f) B6***** (80°C). Initiator: AIBN 1 mol%. All samples were analysed as powder except (*****) samples that were analysed as thin films.

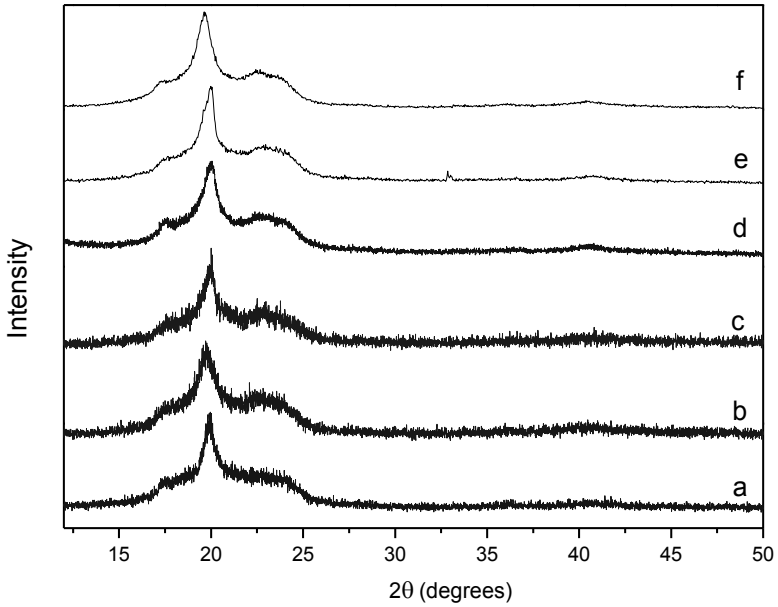

Table 12. Melting temperature, degree of crystallinity and the respective molecular weights of poly (DGU-Bu$(SH)_2$) samples. All samples were analysed as powder except (*) samples that were analysed as thin films.

Entry	T_m (°C)	X_C (%)	Mn (kDa)	M_W (kDa)
B6	68	22*	8.26	21.39
M7	58	43	2.18	4.64
M8	62	45	10.9	34.66
M1	62	36	11.1	38.18
M9	62	50	9.7	26.77
M3	68	32*	15.5	41.85

Jasinski *et al.* (2014a) also reported the synthesis of poly(thioether-ester) with a high degree of crystallinity (55%) through thiol-ene polymerization in miniemulsion. They observed the semicrystalline behaviour revealed by an exothermic recrystallization peak at 6°C and an endothermic melting peak at 18°C.

Polymers comprising a high degree of crystallinity are interesting because it plays a large role on the thermal, mechanical, and other important properties of polymers. The extent of crystallinity developed in a polymer sample is a consequence of both thermodynamic and kinetic factors (ODIAN, 2009).

5.3.4 The effect of co-stabilizers and their possible use as liquid core

Crodamol GTCC and hexadecane were tested as co-stabilizers. They were added in a concentration of 10% (w.% in relation to the monomers) to miniemulsion whose formulations contained 12 $mmol \cdot cm^{-3}$ of Lutensol AT50. Figure 25 shows the particle size distribution for the latex containing 10% of either HD or Crodamol. The addition of either co-stabilizers yielded lower average particle size and narrower size distribution in comparison to M2 (Table 6) by preventing the Ostwald ripening. However, PSD results from previous miniemulsion experiments also indicates that depending on surfactant type and concentration there is no need for co-stabilizers because DGU is sufficiently hydrophobic to provide some diffusional stability.

Co-stabilizer concentrations were further increased to 50% in an attempt to produce nanocapsules. The amount of water was increased in order to maintain the weight ratio between organic and aqueous phases. Samples containing 50% of co-stabilizer, M19 and M20, presented an increase of roughly 15 nm in the average particle size though size distribution dispersion was preserved. Table 13 summarizes the results obtained in the co-stabilizer evaluation.

Table 13. Lattices prepared with hexadecane (HD) and Crodamol GTCC (Crod.) used as co-stabilizers at 10 and 50% (w%) relative to the monomers (the amount of water was increased in 10 and 50% to maintain the same water/organic phase w./w. ratio). Lut. AT50 was used at 11 mmol·cm^{-3} (M5, M6) and 8 mmol·cm^{-3} (M19, M20).

Entry	HD	Crod.	Dp_0 (nm)	PDI_0	Dp_f (nm)	PDI_f
M5	10%	-	210 ± 2	0.22 ± 0.02	199 ± 2	0.19 ± 0.02
M19	50%	-	232 ± 2	0.22 ± 0.01	215 ± 1	0.20 ± 0.01
M6	-	10%	212 ± 2	0.20 ± 0.02	199 ± 1	0.20 ± 0.01
M20	-	50%	221 ± 1	0.21 ± 0.01	215 ± 3	0.22 ± 0.01

Figure 24. TEM images of miniemulsions from Table 13 containing; (a) 10% (M5) and (b) 50% (M19) of HD; and (c) 10% (M6) and (d) 50% (M20) of Crodamol. Scale bar: 1µm.

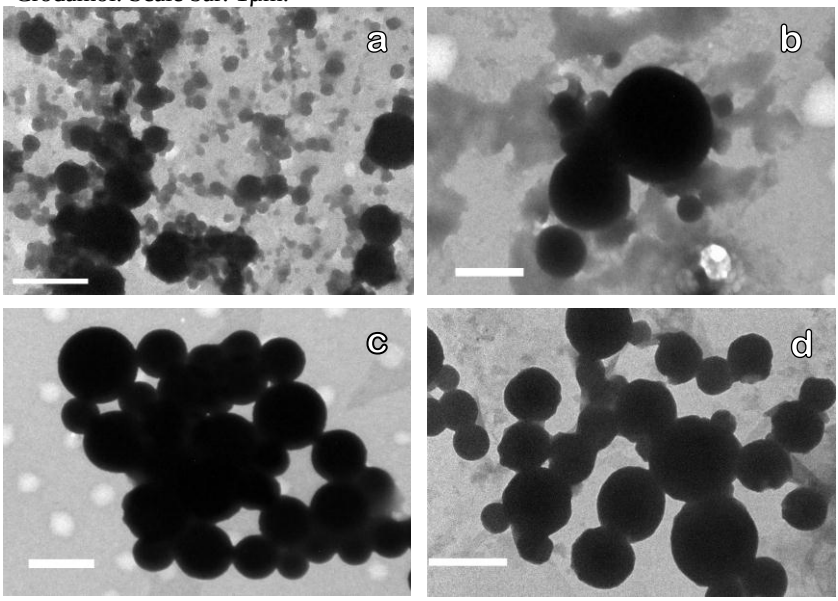

Figure 24 shows micrographs from sub-micrometric particles containing: (a) 10% of HD (M5), (b) 50% of HD (M19), (c) 10% of Crodamol (M6), and (d) 50% of Crodamol (M20). As already mentioned herein, the melting temperature of the synthesized linear polysulfide makes TEM analyses only possible to perform at low current. Figures 24b and 24d do not display any phase separation between the polymer

and the co-stabilizer. Therefore, it can not be stated that morphology of these samples are core-shell or any other type of morphology for that matter. The morphology of the samples containing 50% of co-stabilizer must be further investigated through different analytical techniques such as DSC.

Figure 25 displays the PSD for the nanoparticles synthesized using different type and concentration of co-stabilizers. M5 and M6 present only a slight difference regarding the distribution and both contain a small population of macro-particles, the same behaviour is observed for M19 and M20.

Figure 25. PSD for the nanoparticles synthesized using co-stabilizers: : (a) 10% of HD (M5), (b) 50% of HD (M19), (c) 10% of Crodamol (M6), and (d) 50% of Crodamol (M20).

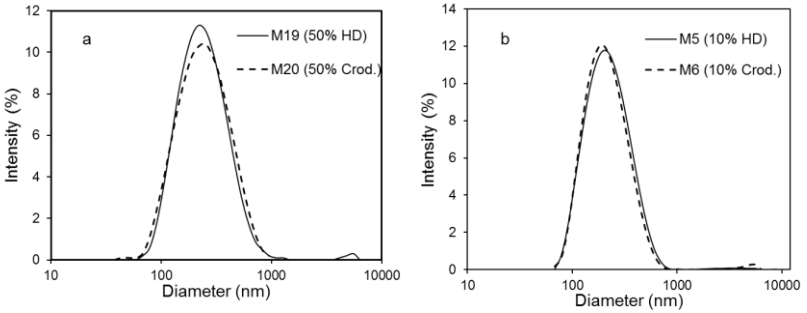

Differential scanning calorimetry (Figure 26) and transmission electron microscopy (Figure 24) were used also to investigate whether sub-micrometric capsules were formed or not.

Differential scanning calorimetry thermal analysis have shown (Figure 26a) a clear phase separation between the hexadecane and the polymeric phase; i.e. separated melting peaks for the hexadecane at 18°C (further confirmed independently through DSC) and for the polymer at 66°C. However, morphology is not quite clear since no phase segregation can be observed in Figure 24b. Morphology could be, for example, nanocapsules with hexadecane as liquid core and polymer as shell or hexadecane could be divided in several small liquid cores dispersed in the polymeric matrix.

Figure 26. Differential scanning calorimetry of latex samples containing 50 w.% of co-stabilizer in relation to both monomers: (a) HD (M19) and (b) Crod. (M20) from Table 9. Plus, DSC of pure hexadecane and Crodamol are also shown for comparison.

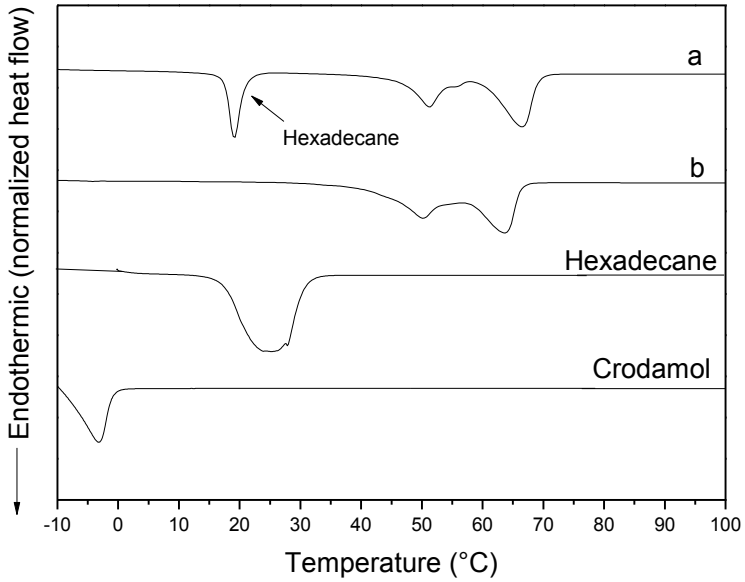

Melting temperature of Crodamol is around - 3 °C (measured through DSC, Figure 26). However, it has been verified through DSC (Figure 26b) that there is not any peak for the melting of Crodamol for miniemulsion polymerization when using Crodamol as co-stabilizer (M20, Table 13) at the same concentration (50 w.%) as hexadecane. The apparent melting temperature of the sample containing Crodamol (Figure 26b (M20)) has decreased from 66 to 63 °C. In addition, the partition of the double T_m peaks is not as clear as in the pure polymeric sample. Furthermore, the enthalpy of melting (ΔH_m) of the polymer sample synthesized with Crod. as co-stabilizer is 23 $J \cdot g^{-1}$; whilst a polymer synthesized similarly but without co-stabilizer has ΔH_m = 42 $J \cdot g^{-1}$. This means that the addition of 50 w.% of Crodamol (in relation to the monomers) to the formulation reduced crystalline domains by half approximately. Therefore, DSC results indicate that phase separation did not occur and Crodamol is most likely solubilized in the polymeric matrix. due to the formation of the homogeneous mixture polymer-Crodamol. Some other analytical techniques can be useful to further

investigate the internal structure of nanoparticles such as TEM of microtomed samples and solid state NMR (STUBBS; SUNDBERG, 2005). In addition, tension interface measurements between polymer/water phase, polymer/HD, polymer/Crod., HD/water phase, and Crod./water phase would help to figure out how phases behave in the nanostructure.

5.3.5 Thiol-ene polymerization kinetics in miniemulsion

Thiol-ene polymerization kinetics in miniemulsion of DGU and $Bu(SH)_2$ was investigated using either AIBN or KPS as initiators. Both initiators were tested in the same concentrations of 1 mol% in relation to the dithiol monomer in experiments carried out at 80°C. Gravimetric conversions of $Bu(SH)_2$ higher than 85% were obtained within 15 minutes of reaction. Moreover, dried latex samples were submitted to FTIR analyses with the intention of quantifying the double bonds of the residual diene monomer. However, samples taken after 15 minutes of reaction did not display any measurable double bond peak in FTIR spectra.

FTIR spectra of dried latexes taken at 0 min. and 20 min. of polymerization are presented in Figure 27 for the polymerization using AIBN and in Figure 28 for polymerization using KPS. Both experiments were carried out at 80°C with 1 mol% of either AIBN or KPS and thiol:ene 1:1.

Figure 27. FTIR spectra of dried latex samples taken at 0 min. and 20 min. of polymerization. Experiment was carried out at 80°C with 1 mol% of AIBN and thiol:ene 1:1. The comparison evidenced rapid consumption of double bonds **(**1640 cm^{-1}) and the formation of sulphide bonds (720 cm^{-1}).

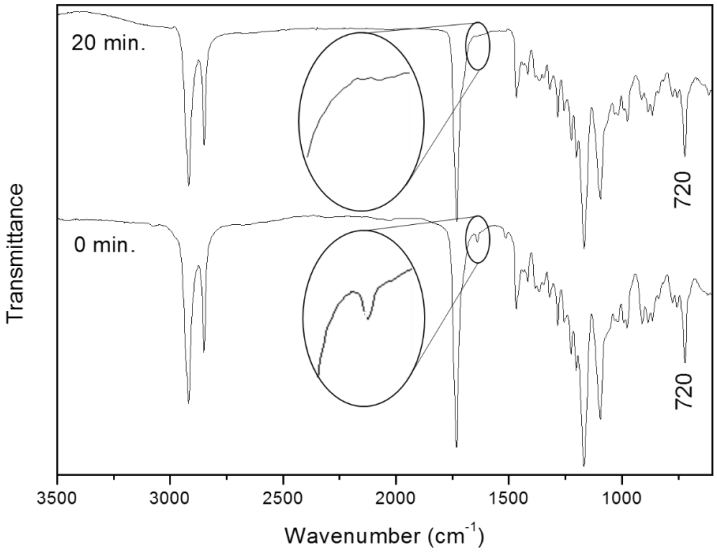

It can be noticed in Figure 27 that peaks at 3076 cm^{-1} and 910 cm^{-1}, that correspond respectively to =C—H stretch in the unsaturated hydrocarbon chain and CH_2 out-of-plane wag from $CH=CH_2$ in vinyl compounds, no longer are discernible in Figure 27 when compared to Figure 13. A very small peak at 1640 cm^{-1} (C=C stretch) can be seen in Figure 27 in the curve correspondent to the sample taken at the beginning of the polymerization (0 min.), however for the sample taken at 20 min. no peak can be seen at 1640 cm^{-1}. Samples were not washed prior to the FTIR analyses, which means that the peaks correspondent to double bonds are most likely due to the presence of residual DGU. Furthermore, it can be noticed the presence of sulphide bonds (S—C) at 720 cm^{-1} in the sample resultant from the addition of the thiyl radicals across the double bond.

A similar behaviour can be observed in Figure 28 correspondent to the thiol-ene polymerization in miniemulsion with KPS. However, KPS provided a slower kinetics and therefore at the beginning of the polymerization (0 min.) a strong peak at 910 cm^{-1} (indicated in Figure 28 by a black arrow) can still be noticed, and corresponding to =C—H

stretch in the unsaturated hydrocarbon chain of DGU. A peak at 1640 cm^{-1} (C=C stretch) can be also seen in Figure 28 in the curve correspondent to the sample taken at the beginning of the polymerization (0 min.). However, for the sample taken at 20 min. no peak can be seen at 1640 cm^{-1} and the strong peak at 910 cm^{-1} cannot be seen. In addition, it can be noticed (20 min.) the presence of sulphide bonds (S—C) at 720 cm^{-1} in the sample resultant from the addition of the thiyl radicals across the double bond.

Figure 28. FTIR spectra of dried lattices samples taken at 0 min. and 20 min. of polymerization. Experiment was carried out at 80°C with 1 mol% of KPS and thiol:ene 1:1. The comparison evidenced rapid consumption of double bonds **(**1640 cm^{-1} and 910 cm^{-1}) and the formation of sulphide bonds (720 cm^{-1})

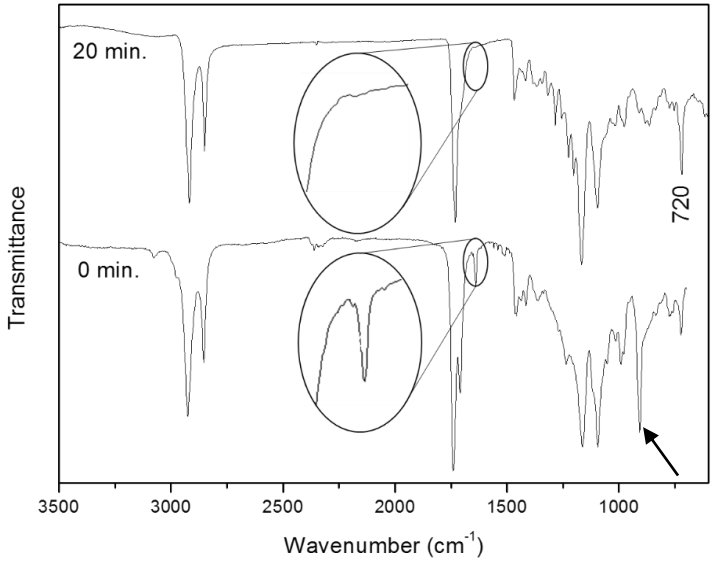

Figure 29 shows the normalized number and weight average molecular weights progress with the polymerization time in thiol-ene miniemulsion polymerization at 80°C using 1 mol% of AIBN (in relation to dithiol) and 8 mmol cm^{-3} of SDS. The increase of molecular weight with reaction time is a characteristic of step-growth polymerizations. It is important to notice that even though FTIR (Figure 27) does not indicate any measurable peak of double bonds after 20 minutes, molecular weight still increases until 200 minutes of reaction. This is probably because there are sufficient double bonds associated to

oligomers to keep polymer growth but not many DGU single molecules, if any; and thus double bond signal is insignificant toward other functional groups present in the macromolecule.

Figure 29. Normalized number and weight average molecular weights progress with reaction time in thiol-ene miniemulsion polymerization at 80°C using 1 mol% of AIBN and 8 mmol cm^{-3} of SDS. Dp = 164 ± 1 nm. M_N = 5.7 kDa. M_W = 13.6 kDa.

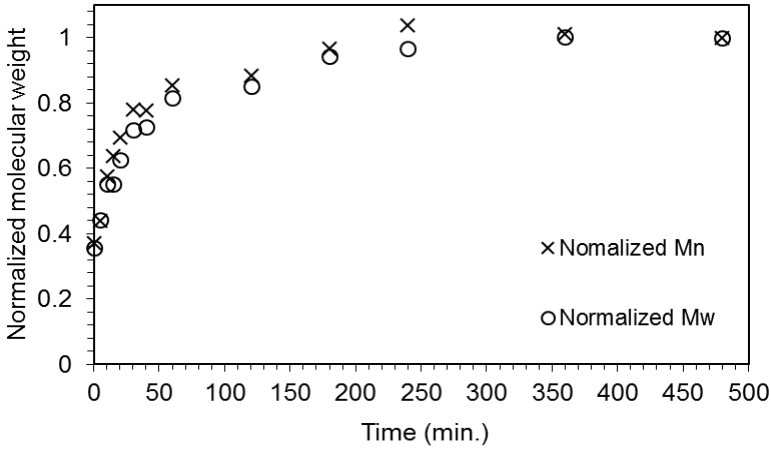

Figure 30. Normalized number and weight average molecular weights progress with reaction time in thiol-ene miniemulsion polymerization at 80°C using 1 mol% of KPS and 8 mmol cm^{-3} of SDS. Dp = 166 ± 1 nm. M_N = 3.1 kDa. M_W = 6.3 kDa.

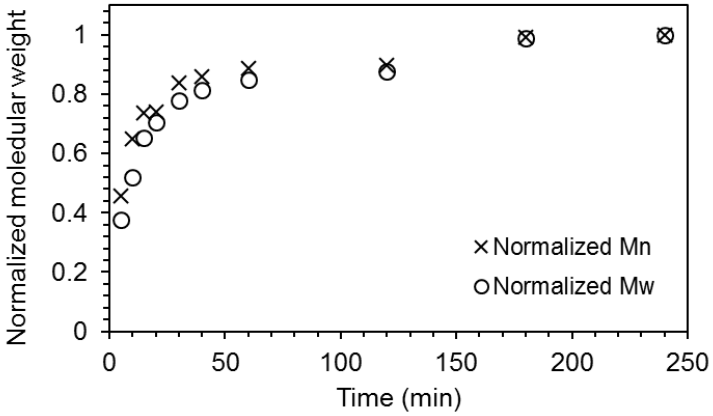

Figure 30 shows the normalized number and weight average molecular weights progress with the polymerization time in thiol-ene miniemulsion polymerization at 80°C using 1 mol% of KPS (in relation to dithiol) and 8 mmol cm^{-3} of SDS. Kinetics using KPS shows a behaviour similar to the molecular weight kinetics using AIBN as initiator displayed in Figure 28. Even though FTIR (Figure 28) does not indicate any measurable peak of double bonds after 20 minutes, molecular weight still increases until 200 minutes of reaction. Probably FTIR technique is not sensitive enough to pick up residual double bond peaks in macromolecules such as oligomers and polymers.

It is not clear the reason why KPS provides a much lower, half approximately, molecular weight than AIBN. KPS, being a water-soluble ionic compound, only forms radicals in aqueous phase and this might be favourable to thiyl-thiyl termination (Figure 6) to form disulphide in the water even before thiyl radicals could enter the droplets. On the other hand, AIBN, being an organo-soluble initiator, favours droplet nucleation (LANDFESTER, 2003).

5.4 FINAL CONSIDERATIONS

Herein, thiol-ene polymerization was utilized to synthesize poly(thioether-ester) nanoparticles through miniemulsion polymerization using a fully renewable monomer (DGU) indirectly derived from vegetable oil and sugar. Different parameters were tested: reaction temperature, reaction time, initiator concentration, and surfactant type and concentration, and the addition of co-stabilizer. Lattices did not present great difference regarding stability or particle diameter when co-stabilizer were added to the formulation, noticeable increase in particle size was observed only when co-stabilizers were used at high weight percentage (50%). In general, by increasing the temperature higher molecular weight was obtained probably due to functional group conversion since thiol-ene follows step-growth mechanism. In addition, AIBN (organo-soluble initiator) was found to present an ideal concentration among the tested concentrations to improve molecular weight, while when KPS (water soluble initiator) is used a decrease in initiator concentration enhances molecular weight. Moreover, AIBN provided polymeric samples with higher molecular weight than KPS. .Particle morphology was observed by TEM. Particle size was $\leq$ 200 nm and particle size dispersion $\approx$ 0.2. The best results regarding molecular weight (M_N up to 11 kDa) were obtained through miniemulsion polymerization at 80°C using AIBN at 1% (mol% in

relation to dithiol) Furthermore, DSC and XRD analyses showed that the synthesized polymer is semi-crystalline with a degree of crystallinity of at least 20% and temperature of melting around 60°C. Finally, nanoparticles with a co-stabilizer liquid phase, possibly liquid core, were obtained and phase separation was observed through DSC. In future works the kinetics of thiol-ene polymerization in miniemulsion should be investigated to evaluate phenomena such as radical compartmentalization and the development of molecular weight with reaction time. Also thiol-ene miniemulsion polymerization of DGU could be used to synthesize nanocapsules of active compounds. Lastly, nanoparticles derived from renewable resources synthesized herein possess hydrolysable bonds in the main polymeric chain and therefore the (bio) degradation of the poly(DGU-Bu$(SH)_2$) could be investigated.

CHAPTER VI

6 FINAL CONSIDERATIONS

6.1 CONCLUSION

In this work, it was reported the synthesis of a renewable α,ω-diene diester monomer, dianhydro-D-glucityl diundec-10-enoate (DGU), produced from 10-undecenoic acid (derived from castor oil) and isosorbide (derived from starch). DGU was copolymerized with 1,4-butanedithiol ($Bu(SH)_2$) through thiol-ene polymerization both in bulk and miniemulsion to yield linear semi-crystalline poly(thioether-ester)s. Different parameters were evaluated such as reaction temperature, initiator concentration, and surfactant type and concentration.

The synthesis of novel monomers from bio-feedstock was evidenced to be a powerful tool to produce differentiated polymers with prospective for diverse applications. Brazil, as one of the world's biggest producers of vegetable oil, possesses a great potential to develop sustainable chemistry based products using vegetable oils as raw materials.

DGU was successfully copolymerized with $Bu(SH)_2$ via thiol-ene polymerization both in bulk and in miniemulsion. Polymer obtained by miniemulsion polymerization resulted in a higher molecular weight when compared to bulk polymerization. Thus, there is evidence of the occurrence of radical compartmentalization. Poly(thioether-ester) nanoparticles were obtained through miniemulsion polymerization and morphology was evaluated by TEM. Microscopy analyses have shown spherical nanoparticles. DLS has shown that according to surfactant type and concentration particles from 130 up to 250 nm can be obtained. However, components are partitioned between organic and aqueous phases, especially those compounds that possess a significant solubility in the both phases, which is the case of the 1,4-butanedithiol. This partition between the two phases may change local stoichiometry inside the droplet. As thiol-ene polymerization is strictly dependent of stoichiometry, this might have been the reason for the decrease in molecular weights values when particle size was reduced. Non-stoichiometric attempts containing a 20% excess of dithiol further confirmed that thiol-ene polymerization is reliant on stoichiometry.

In general, increasing the temperature of the polymerization there is an increase in molecular weight. thiol-ene polymerization is a step-growth polymerization that proceeds as free radical reactions and

therefore it needs undergo initiation. In step-growth polymerizations, molecular weight depends on functional group conversion, with the increase in temperature the initiator decomposes at a faster rate and thus functional groups are allowed to react faster and the degree of polymerization is enhanced because more thiyl radicals are being generated. 80°C was the temperature condition that provided the best molecular weight results for both miniemulsion and bulk polymerization.

In traditional free radical polymerization, molecular weight is directly dependent of the amount of initiator, the higher the concentration the lower the molecular weight; and this behaviour is observed independent on the type of the initiator, water or organo-soluble. However, in thiol-ene polymerization a different behaviour for AIBN was observed, among the concentrations tested, the intermediary concentration of 1 mol% presented the best molecular weight result. On the other hand, KPS provided its highest molecular result with the lowest concentration of 0.5 mol%. Furthermore, DSC and XRD analyses have shown that the synthesized polymer was semi-crystalline with a degree of crystallinity of at least 20% and T_m around 60°C. In addition, depending on the co-stabilizer type, hexadecane of Crodamol, and amount, phase segregation inside the polymer particles was observed through DSC. Finally, thiol-ene polymerization kinetics in miniemulsion has shown that even though FTIR does not indicate any measurable peak of double bonds after 20 minutes, molecular weight still increases until 200 minutes of reaction. It is not clear the reason why KPS provides a much lower, half approximately, molecular weight than AIBN. KPS, being a water-soluble ionic compound, only forms radicals in aqueous phase and this might be favourable to thiyl-thiyl termination to form disulphide in the water even before thiyl radicals could enter the droplets. On the other hand, AIBN, being an organo-soluble initiator, favours droplet nucleation.

6.2 FURTHER WORK

1. To synthesize other types of diene monomers.
2. To evaluate other types of thiols comprising different functional groups to perform thiol-ene polymerization in miniemulsion.
3. To test DGU as crosslinking agent for MMA and styrene
4. To investigate the actual morphology of nanoparticles containing high amount of hexadecane and Crodamol®. Some

other microscopy techniques, such as SEM and AFM, can be utilized to gain additional information to supplement TEM and DSC results.

5. To synthesize nanoparticles via thiol-ene polymerization in miniemulsion with different ene or thiol surface functional groups.
6. Further investigation of kinetics by evaluating functional group conversion through NMR. To investigate why AIBN and KPS, different types of initiator, behave differently in thiol-ene polymerization.
7. To test the biocompatibility of the synthesized nanoparticles by evaluating *in vitro* cytotoxicity in fibroblast cells and hemocompatibility of poly(thioether-ester) nanoparticles.
8. Many works in the literature state that thiol-ene polymerization is not inhibited by oxygen. However, it should be further investigated until what extent this statement is valid.
9. To evaluate poly(DGU-Bu$(SH)_2$) degradation. Since it is a polymer with ester groups in the main chain, it is susceptible to hydrolysis.
10. Improvement of the evaluation of crystallinity since it might affect the susceptibility to hydrolysis, i.e. affects polymer degradation. To obtain a fully crystalline polymer sample to use as reference in DSC analyses.

7 REFERENCES

ACOSTA ORTIZ, R.; MARTINEZ, A. Y. R.; GARCÍA VALDEZ, A. E.; BERLANGA DUARTE, M. L. Preparation of a crosslinked sucrose polymer by thiol-ene photopolymerization using dithiothreitol as comonomer. **Carbohydrate Polymers**, v. 82, n. 3, p. 822–828, 2010.

AIMETTI, A. A.; MACHEN, A. J.; ANSETH, K. S. Poly(ethylene glycol) hydrogels formed by thiol-ene photopolymerization for enzyme-responsive protein delivery. **Biomaterials**, v. 30, n. 30, p. 6048–6054, 2009.

AMATO, D. V.; AMATO, D. N.; FLYNT, a. S.; PATTON, D. L. Functional, sub-100 nm polymer nanoparticles via thiol–ene miniemulsion photopolymerization. **Polymer Chemistry**, 2015.

ANTONIETTI, M.; LANDFESTER, K. Polyreactions in miniemulsions. **Progress in Polymer Science**, v. 27, n. 4, p. 689–757, 2002.

ASUA, J. M. Miniemulsion polymerization. **Progress in Polymer Science**, v. 27, n. 7, p. 1283–1346, 2002.

AUVERGNE, R.; DESROCHES, M.; CLERC, S.; CARLOTTI, S.; CAILLOL, S.; BOUTEVIN, B. New biobased epoxy hardeners: Thiol-ene addition on oligobutadiene. **Reactive and Functional Polymers**, v. 72, n. 6, p. 393–401, 2012.

BAIER, G.; WINZEN, S.; MESSERSCHMIDT, C.; FRANK, D.; FICHTER, M.; GEHRING, S.; MAILÄNDER, V.; LANDFESTER, K. Heparin-Based Nanocapsules as Potential Drug Delivery Systems. **Macromolecular Bioscience**, p. 765–776, 2015.

BARRÈRE, M.; LANDFESTER, K. Polyester synthesis in aqueous miniemulsion. **Polymer**, v. 44, n. 10, p. 2833–2841, 2003.

BECHTHOLD, N.; TIARKS, F.; WILLERT, K.; LANDFESTER, K.; ANTONIETTI, M. Miniemulsion polymerization: applications and new materials. **Macromolecular Symposia**, v. 555, p. 549–555, 2000.

BEHZADI, S.; SERPOOSHAN, V.; SAKHTIANCHI, R.; MÜLLER, B.; LANDFESTER, K.; CRESPY, D.; MAHMOUDI, M. Protein corona change the drug release profile of nanocarriers: The "overlooked" factor at the nanobio interface. **Colloids and Surfaces B: Biointerfaces**, v. 123, p. 143–149.

BELGACEM, M. N.; GANDINI, A. Materials from Vegetable Oils: Major Sources, Properties and Applications. In: Belgacem, M. N.; Gandini, A. **Monomers, Polymers and Composites from Renewable Resources**. 1st Ed. Oxford: Elsevier, 2008. p. 39-66.

BERGER, F.; DELHALLE, J.; MEKHALIF, Z. Undec-10-ene-1-thiol multifunctional molecular layer as a junction between metallic zinc and polymer coatings on steel. **Electrochimica Acta**, v. 54, n. 26, p. 6464–6471, 2009.

BERNARDY, N.; ROMIO, A. P.; BARCELOS, E. I.; DAL PIZZOL, C.; DORA, C. L.; LEMOS-SENNA, E.; ARAUJO, P. H. H.; SAYER, C. Nanoencapsulation of quercetin via miniemulsion polymerization. **Journal of Biomedical Nanotechnology**, v. 6, n. 2, p. 181–186, 2010.

BESSE, V.; AUVERGNE, R.; CARLOTTI, S.; BOUTEVIN, G.; OTAZAGHINE, B.; CAILLOL, S.; PASCAULT, J. P.; BOUTEVIN, B. Synthesis of isosorbide based polyurethanes: An isocyanate free method. **Reactive and Functional Polymers**, v. 73, n. 3, p. 588–594, 2013.

BLACK, M.; RAWLINS, J. W. Thiol-ene UV-curable coatings using vegetable oil macromonomers. **European Polymer Journal**, v. 45, n. 5, p. 1433–1441, 2009.

BRANDRUP, J.; IMMERGUT, E. H.; GRULKE, E. A.; ABE, A.; BLOCH, D. R. **Polymer Handbook**. 4th. ed. New York: John Wiley & Sons, Inc., 1999. 1 v.

ÇAKMAKÇI, E.; MÜLAZIM, Y.; KAHRAMAN, M. V.; APOHAN, N. K. Preparation and characterisation of boron containing thiol-ene photocured hybrid coatings. **Progress in Organic Coatings**, v. 75, n. 1-2, p. 28–32, 2012.

CARDOSO, P. B.; ARAÚJO, P. H. H.; SAYER, C. Encapsulation of jojoba and andiroba oils by miniemulsion polymerization. Effect on molar mass distribution. **Macromolecular Symposia**, v. 324, n. 1, p. 114–123, 2013.

CARDOSO, P. B.; MUSYANOVYCH, A.; LANDFESTER, K.; SAYER, C.; DE ARAÚJO, P. H. H.; MEIER, M. A R. ADMET reactions in miniemulsion. **Journal of Polymer Science, Part A: Polymer Chemistry**, v. 52, n. 9, p. 1300–1305, 2014.

CARIOSCIA, J. A.; LU, H.; STANBURY, J. W.; BOWMAN, C. N. Thiol-ene oligomers as dental restorative materials. **Dental Materials**, v. 21, n. 12, p. 1137–1143, 2005.

CARLBORG, C. F.; VASTESSON, A.; LIU, Y.; VAN DER WIJNGAART, W.; JOHANSSON, M.; HARALDSSON, T. Functional off-stoichiometry thiol-ene-epoxy thermosets featuring temporally controlled curing stages via an UV/UV dual cure process. **Journal of Polymer Science, Part A: Polymer Chemistry**, v. 52, n. 18, p. 2604–2615, 2014.

CARLSON, D. D.; KNIGHT, A. R. Reactions of Thiyl Radicals. XI. Further Investigations of Thiol–Disulfide Photolyses in the Liquid Phase. **Canadian Journal of Chemistry**, 1973.

CHALMERS, J. M.; MEIER, R. J. (ed.). Polymer Morphology and Structure. In: **Molecular Characterisation and Analysis of Polymers**. 1st. ed. Elsevier Ltd., 2008. p. 776.

CHEN, Y.; YAN, G.; WANG, X.; QIAN, H.; YI, J.; HUANG, L.; LIU, P. Bio-functionalization of micro-arc oxidized magnesium alloys via thiol-ene photochemistry. **Surface and Coatings Technology**, v. 269, p. 191–199, 2015.

CHIARADIA, V.; VALÉRIO, A.; FEUSER, P. E.; OLIVEIRA, D. De; ARAÚJO, P. H. H.; SAYER, C. Incorporation of superparamagnetic nanoparticles into poly(urea-urethane) nanoparticles by step growth interfacial polymerization in miniemulsion. **Colloids and Surfaces A: Physicochemical and Engineering Aspects**, 2015.

CLARK, J. H. Chemistry goes green. **Nature Chemistry**, v. 1, n. 1, p. 12–13, 2009.

CLAUDINO, M. **Thiol – ene coupling of renewable monomers : at the forefront of bio-based polymeric materials.** 2011. 63 p. Licentiate Thesis (degree of licentiate of Technology) - Kungliga Tekniska Högskolan, Stockholm, 2011.

COLE, M.; JANKOUSKY, K.; BOWMAN, C. Redox initiation of bulk thiol–ene polymerizations. **Polymer chemistry**, v. 4, n. 4, p. 1167–1175, 2013.

COSTA, C.; TIMMERMANN, S. A. S.; PINTO, J. C.; ARAÚJO, P. H. H.; SAYER, C. Compartmentalization Effects on Miniemulsion Polymerization with Oil-Soluble Initiator. **Macromolecular Reaction Engineering**, n. 7, p. 221-231, 2013.

CRAMER, N. B.; BOWMAN, C. N. Kinetics of thiol-ene and thiol-acrylate photopolymerizations with real-time Fourier transform infrared. **Journal of Polymer Science, Part A: Polymer Chemistry**, v. 39, n. 19, p. 3311–3319, 2001.

CRAMER, N. B.; DAVIES, T.; O'BRIEN, A. K.; BOWMAN, C. N. Mechanism and modeling of a thiol-ene photopolymerization. **Macromolecules**, v. 36, n. 12, p. 4631–4636, 2003.

ROMERA, C.; CARDOSO, P. B.; MEIER, M. a. R.; SAYER, C.; ARAÚJO, P. H. H. Acyclic triene metathesis (ATMET) miniemulsion polymerization of linseed oil produces polymer nanoparticles with comparable molecular weight to that of bulk reactions. **European Journal of Lipid Science and Technology**, v. 117, n. 2, p. 235–241, 2015.

DELOITTE. Opportunities for the chemical industry An analysis of the market potential and competitiveness of North-West Europe Preface – The biotechnology (r)evolution or the greening of the chemical value chain. n. September, 2014.

DURHAM, O. Z.; SHIPP, D. a. Suspension thiol-ene photopolymerization: Effect of stabilizing agents on particle size and stability. **Polymer**, v. 55, n. 7, p. 1674–1680, 2014.

EIA - U.S. ENERGY INFORMATION ADMINISTRATION. **PETROLEUM AND OTHER LIQUIDS. Spot prices.** Disponível em: <http://www.eia.gov/dnav/pet/pet_pri_spt_s1_d.htm>. Acesso em: 27 jul. 2015.

ESEN, H.; KÜSEFOĞLU, S.; WOOL, R. Photolytic and free-radical polymerization of monomethyl maleate esters of epoxidized plant oil triglycerides. **Journal of Applied Polymer Science**, v. 103, n. 1, p. 626–633, 2007.

ESPINOSA, L. M.; MEIER, M. A. R. Plant oils: The perfect renewable resource for polymer science?! **European Polymer Journal**, v. 47, n. 5, p. 837–852, 2011.

FEIDENHANS'L, N. a.; LAFLEUR, J. P.; JENSEN, T. G.; KUTTER, J. P. Surface functionalized thiol-ene waveguides for fluorescence biosensing in microfluidic devices. **Electrophoresis**, v. 35, n. 2-3, p. 282–288, 2014.

FENOUILLOT, F.; ROUSSEAU, a.; COLOMINES, G.; SAINT-LOUP, R.; PASCAULT, J. P. Polymers from renewable 1,4:3,6-dianhydrohexitols (isosorbide, isomannide and isoidide): A review. **Progress in Polymer Science**, v. 35, n. 5, p. 578–622, 2010.

FEUSER, P. E.; BUBNIAK, L. D. S.; SILVA, M. C. D. S.; VIEGAS, A. D. C.; FERNANDES, A. C.; RICCI-JUNIOR, E.; NELE, M.; TEDESCO, A. C.; SAYER, C.; ARAÚJO, P. H. H. De. Encapsulation of magnetic nanoparticles in poly(methyl methacrylate) by miniemulsion and evaluation of hyperthemia in U87MG cells. **European Polymer Journal**, v. 68, p. 355–365, 2015.

FIRDAUS, M.; MONTERO DE ESPINOSA, L.; MEIER, M. a R. Terpene-based renewable monomers and polymers via thiol-ene additions. **Macromolecules**, v. 44, n. 18, p. 7253–7262, 2011.

FLÈCHE, G.; HUCHETTE, M. Preparation, Properties and Chemistry. **Starch/Stärke**, v. 174, n. 1, p. 26–30, 1986.

FOCARETE, M. L.; SCANDOLA, M.; KUMAR, A.; GROSS, R. a. Physical Characterisation of Poly (ω - pentadecalactone) Synthesized by Lipase-Catalyzed Ring-Opening Polymerization. **Journal of Polymer Science Part B: Polymer Physics**, v. 39, p. 1721–1729, 2001.

FOKOU, P. A.; MEIER, M. A. R. Use of a renewable and degradable monomer to study the temperature- dependent olefin isomerization during ADMET polymerizations. **Journal of the American Chemical Society**, v. 131, n. 5, p. 1664–1665, 2009.

GALBIS, J. A. A; GARCÍA-MARTÍN, M. G. Sugar as Monomers. In: Belgacem, M. N.; Gandini, A. **Monomers, Polymers and Composites from Renewable Resources**. 1st Ed. Oxford: Elsevier, 2008. p. 90–114.

GÜNAY, K. A.; THEATO, P.; KLOK, H. A. Standing on the shoulders of hermann staudinger: Post-polymerization modification from past to present. **Journal of Polymer Science, Part A: Polymer Chemistry**, v. 51, n. 1, p. 1–28, 2013.

GÜNAY, K. A.; THEATO, P.; KLOK, H.-A. History of Post-Polymerization Modification. In: THEATO, P.; KLOK, H.-A. **Functional Polymers by Post-Polymerization Modification**. 1st Ed. Weinheim: Wiley-VCH Verlag GmbH & Co. KGaA, 2011. p. 1–44.

HACHET, E.; SERENI, N.; PIGNOT-PAINTRAND, I.; RAVAINE, V.; SZARPAK-JANKOWSKA, A.; AUZÉLY-VELTY, R. Thiol-ene clickable hyaluronans: From macro-to nanogels. **Journal of Colloid and Interface Science**, v. 419, p. 52–55, 2014.

HIRAKAWA, S.; HIRAMATSU, N. Melting Behavior of Poly(ethylene terephthalate) Crystallized and Annealed under Elevated Pressure. **Polymer Journal**, v. 12, n. 2, p. 105–111, 1980.

HOLMBERG, K.; JÖNSSON, B.; KRONBERG, B.; LINDMAN, B. **Surfactants and polymers in aqueous solution**. 2nd. ed. Chichester: John Wiley & Sons Ltd, 2002, 562p.

HOYLE, C. E.; BOWMAN, C. N. Thiol-ene click chemistry. **Angewandte Chemie**, v. 49, n. 9, p. 1540–1573, 2010.

HOYLE, C. E.; LEE, T. Y.; ROPER, T. Thiol-enes: Chemistry of the past with promise for the future. **Journal of Polymer Science, Part A: Polymer Chemistry**, v. 42, n. 21, p. 5301–5338, 2004.

IONESCU, M.; RADOJČIĆ, D.; WAN, X.; PETROVIĆ, Z. S.; UPSHAW, T. a. Functionalized vegetable oils as precursors for polymers by thiol-ene reaction. **European Polymer Journal**, v. 67, p. 439–448, 2015.

JASINSKI, F.; LOBRY, E.; TARABLSI, B.; CHEMTOB, A.; NOUEN, D. Le; CRIQUI, A. Light-Mediated Thiol − Ene Polymerization in Miniemulsion: A Fast Route to Semicrystalline Polysulfide Nanoparticles. **ACS Macro Letters**, v. 3, p. 958–962, 2014.

JIMÉNEZ-RODRIGUEZ, C.; EASTHAM, G. R.; COLE-HAMILTON, D. J. Dicarboxylic acid esters from the carbonylation of unsaturated esters under mild conditions. **Inorganic Chemistry Communications**, v. 8, n. 10, p. 878–881, 2005.

KHARASCH, M. S.; READ, J.; MAYO, F. R. **Chemistry and Industry**, v. 57, p. 752, 1938.

KI, C. S.; LIN, T.-Y.; KORC, M.; LIN, C.-C. Thiol-ene hydrogels as desmoplasia-mimetic matrices for modeling pancreatic cancer cell growth, invasion, and drug resistance. **Biomaterials**, v. 35, n. 36, p. 9668–9677, 2014.

KNIGHT, A. R. Photochemistry of Thiol. In: PATAI, S. (Ed.). |**The Chemistry of Thiol Group.**. Bristol: John Wiley & Sons, 1974. p. 481–956.

KOHRI, M.; KOBAYASHI, A.; FUKUSHIMA, H.; KOJIMA, T.; TANIGUCHI, T.; SAITO, K.; NAKAHIRA, T. Enzymatic miniemulsion polymerization of styrene with a polymerizable surfactant. **Polymer Chemistry**, v. 3, n. 4, p. 900, 2012.

KOLB, N.; MEIER, M. a R. Grafting onto a renewable unsaturated polyester via thiol-ene chemistry and cross-metathesis. **European Polymer Journal**, v. 49, n. 4, p. 843–852, 2013.

KREYE, O.; TÓTH, T.; MEIER, M. a R. Copolymers derived from rapeseed derivatives via ADMET and thiol-ene addition. **European Polymer Journal**, v. 47, n. 9, p. 1804–1816, 2011.

KREYE, O.; TÜRÜNÇ, O.; SEHLINGER, A.; RACKWITZ, J.; MEIER, M. a R. Structurally diverse polyamides obtained from monomers derived via the Ugi multicomponent reaction. **Chemistry - A European Journal**, v. 18, n. 18, p. 5767–5776, 2012.

KUHLMANN, M.; REIMANN, O.; HACKENBERGER, C. P. R.; GROLL, J. Cysteine-Functional Polymers via Thiol-ene Conjugation. **Macromolecular Rapid Communications**, v. 36, n. 5, p. 472–476, 2015.

LANDFESTER, K. Miniemulsions for Nanoparticle Synthesis. **Topics in Current Chemistry**, v. 227, p. 75–123, 2003.

LANDFESTER, K. Miniemulsion polymerization and the structure of polymer and hybrid nanoparticles. **Angewandte Chemie - International Edition**, v. 48, n. 25, p. 4488–4508, 2009.

LEJA, K.; LEWANDOWICZ, G. Polymer biodegradation and biodegradable polymers - A review. **Polish Journal of Environmental Studies**, v. 19, n. 2, p. 255–266, 2010.

LERCH, S. **Uptake mechanism, intracellular trafficking and endo-lysosomal ph monitoring of polystyrene nanoparticles**. 2012. Dissertation (Doktor rerum naturalium) - Max Planck Graduate Center mit der Johannes Gutenberg-Universität Mainz Angefertigt am Max-Planck-Institut für Polymerforschung, 2012.

LI, F.; HANSON, M. .; LAROCK, R. . Soybean oil–divinylbenzene thermosetting polymers: synthesis, structure, properties and their relationships. **Polymer**, v. 42, n. 4, p. 1567–1579, 2001.

LI, F.; LAROCK, R. C. New Soybean Oil – Styrene – Divinylbenzene Thermosetting Copolymers . II . Dynamic Mechanical Properties. **Journal of Applied Polymer** Science, v. 80, p. 658–670, 2001.

LI, F.; LAROCK, R. C. Novel polymeric materials from biological oils. **Journal of Polymers and the Environment**, v. 10, n. 1-2, p. 59–67, 2002a.

LI, F.; LAROCK, R. C. New soybean oil-Styrene-Divinylbenzene thermosetting copolymers?IV. Good damping properties. **Polymers for Advanced Technologies**, v. 13, n. 6, p. 436–449, 2002b.

LI, Q.; ZHOU, H.; HOYLE, C. E. The effect of thiol and ene structures on thiol-ene networks: Photopolymerization, physical, mechanical and optical properties. **Polymer**, v. 50, n. 10, p. 2237–2245, 2009.

LIN, C.-C.; KI, C. S.; SHIH, H. Thiol-norbornene photoclick hydrogels for tissue engineering applications. **Journal of Applied Polymer Science**, v. 132, n. 8, p. 1-11, 2015.

LOBRY, E.; JASINSKI, F.; PENCONI, M.; CHEMTOB, A.; CROUTXÉ-BARGHORN, C.; OLIVEROS, E.; BRAUN, A. M.; CRIQUI, A. Continuous-flow synthesis of polymer nanoparticles in a microreactor via miniemulsion photopolymerization. **RSC Advances**, v. 4, n. 82, p. 43756–43759, 2014.

LU, H.; CARIOSCIA, J. a.; STANSBURY, J. W.; BOWMAN, C. N. Investigations of step-growth thiol-ene polymerizations for novel dental restoratives. **Dental Materials**, v. 21, n. 12, p. 1129–1136, 2005.

LU, Y.; LAROCK, R. C. Novel polymeric materials from vegetable oils and vinyl monomers: Preparation, properties, and applications. **Chemistry and Sustainability, Energy & Materials**, v. 2, n. 2, p. 136–147, 2009.

LU, Y.; LAROCK, R. C. Novel biobased plastics, rubbers, composites, coatings and adhesives from agricultural oils and by-products. **ACS Symposium Series**, v. 1043, p. 87–102, 2010.

LUCAS, N.; BIENAIME, C.; BELLOY, C.; QUENEUDEC, M.; SILVESTRE, F.; NAVA-SAUCEDO, J. E. Polymer biodegradation: Mechanisms and estimation techniques - A review. **Chemosphere**, v. 73, n. 4, p. 429–442, 2008.

MARTIN, D.; JOURDAIN, J. L.; LE BRAS, G. Kinetics and mechanism for the reactions of H atoms with CH3SH and C2H5SH. **International Journal of Chemical Kinetics**, v. 20, n. 11, p. 897–907, 1988.

MARVEL, C. S.; CHAMBERS, R. R. Polyalkylene Sulfides from Diolefins and Dimercaptans. **Journal of the America Chemical Society**, v. 70, n. 4, p. 993–998, 1948.

MEIER, M. a R.; METZGER, J. O.; SCHUBERT, U. S. Plant oil renewable resources as green alternatives in polymer science. **Chemical Society reviews**, v. 36, n. 11, p. 1788–1802, 2007.

MEIORIN, C.; ARANGUREN, M. I.; MOSIEWICKI, M. a. Vegetable oil/styrene thermoset copolymers with shape memory behavior and damping capacity. **Polymer International**, v. 61, n. 5, p. 735–742, 2012.

MEISSNER, M.; THOMPSON, H. W. The Photolysis of Mercaptans. **Transactions of the Faraday Society**, v. 34, p. 1238–1239, 1938.

MERKEL, T.; HECHT, L. L.; SCHOTH, A.; WAGNER, C.; MUÑOZ-ESPÍ, R.; LANDFESTER, K.; SCHUCHMANN, H. P. Continuous Preparation of Polymer/Inorganic Composite Nanoparticles via Miniemulsion Polymerization. In: Kind, M.; Peukert, W.; Rehage, H.; Schuchmann, H. P. **Colloid Process Engineering**. 1st. ed. Springer International Publishing, 2015. p. 345–370.

MESSERSCHMIDT, S. K. E.; MUSYANOVYCH, A.; ALTVATER, M.; SCHEURICH, P.; PFIZENMAIER, K.; LANDFESTER, K.; KONTERMANN, R. E. Targeted lipid-coated nanoparticles: Delivery of tumor necrosis factor-functionalized particles to tumor cells. **Journal of Controlled Release**, v. 137, n. 1, p. 69–77, 2009.

MORGAN, C. R.; MAGNOTTA, F.; KETLEY, a. D. Thiol/ene photocurable polymers. **Journal of Polymer Science: Polymer Chemistry Edition**, v. 15, n. 3, p. 627–645, 1977.

MUELLER, R. J. Biological degradation of synthetic polyesters-Enzymes as potential catalysts for polyester recycling. **Process Biochemistry**, v. 41, n. 10, p. 2124–2128, 2006.

MÜLLER, R. J.; KLEEBERG, I.; DECKWER, W. D. Biodegradation of polyesters containing aromatic constituents. **Journal of Biotechnology**, v. 86, n. 2, p. 87–95, 2001.

MUTLU, H. **Sustainable, efficient approaches to renewable platform chemicals and polymers**. 2012. Thesis (Doktors der Naturwissenschaften). Karlsruher Institut für Technologie (KIT) - Universitätsbereich, Germany, 2012.

NAIR, L. S.; LAURENCIN, C. T. Biodegradable polymers as biomaterials. **Progress in Polymer Science**, v. 32, n. 8-9, p. 762–798, 2007.

NORTHROP, B. H.; COFFEY, R. N. Thiol-ene click chemistry: Computational and kinetic analysis of the influence of alkene functionality. **Journal of the American Chemical Society**, v. 134, n. 33, p. 13804–13817, 2012.

O'BRIEN, A. K.; CRAMER, N. B.; BOWMAN, C. N. Oxygen inhibition in thiol-acrylate photopolymerizations. **Journal of Polymer Science, Part A: Polymer Chemistry**, v. 44, n. 6, p. 2007–2014, 2006.

ODIAN, G. **Principles of polymerization**. 4th. ed. Hoboken, New Jersey: John Wiley & Sons, 2009. 839 p.

OKADA, M. Chemical syntheses of biodegradable polymers. **Progress in Polymer Science**, v. 27, n. 1, p. 87–133, 2002.

OKADA, M.; TACHIKAWA, K.; AOI, K. Biodegradable polymers based on renewable resources. II. Synthesis and biodegradability of

polyesters containing furan rings. **Journal of Polymer Science Part A: Polymer Chemistry**, v. 35, n. 13, p. 2729–2737, 1997.

OKADA, M.; TACHIKAWA, K.; AOI, K. Biodegradable Polymers Based on Renewable Resources . III . Copolyesters Composed of 1 , 4 : 3 , 6-Dianhydro- D -glucitol , 1 , 1-Bis (5-carboxy-2-furyl) ethane and Aliphatic Dicarboxylic Acid Units. **Journal of Applied Polymer Science**, v. 81 p. 2721–2734, 2000.

OKADA, M.; TSUNODA, K.; TACHIKAWA, K.; AOI, K. Biodegradable Polymers Based on Renewable Resources . IV . Enzymatic Degradation of Polyesters Composed of 1 , 4 : 3 . 6-Dianhydro- D -glucitol and Aliphatic Dicarboxylic Acid Moieties. **Journal of Applied Polymer Science**, 77 p. 338–346, 2000.

OVETKOVIĆ, I.; MILIĆ, J.; IONESCU, M.; PETROVIĆ, Z. S. Preparation of 9-hydroxynonanoic acid methyl ester by ozonolysis of vegetable oils and its polycondensation. **Hemijska Industrija**, v. 62, n. 6, p. 319–328, 2008.

POLLONI, A. E. **SÍNTESE DE MATERIAIS POLIMÉRICOS ASSISTIDA POR ULTRASSOM.** 2014. 89 p. Dissertação (Mestrado em Engenharia Química) - Programa de Pós-Graduação em Engenharia Química, Centro Tecnológico, Universidade Federal de Santa Catarina, Florianópolis, 2014.

POSNER, T. Beiträge zur Kenntniss der ungesättigten Verbindungen. Über die Addition von Mercaptanen an ungesättigte Kohlenwasserstoffe. **Berichte der deutschen chemischen Gesellschaft**, v. 38, n. 1, p. 646–657, 1905.

PUGH, R. I.; PRINGLE, P. G.; DRENT, E. Tandem isomerisation–carbonylation catalysis: highly active palladium(II) catalysts for the selective methoxycarbonylation of internal alkenes to linear esters. **Chemical Communications**, v. 1, n. 16, p. 1476–1477, 2001.

QI, G.; JONES, C. W.; SCHORK, F. J. Enzyme-initiated miniemulsion polymerization. **Biomacromolecules**, v. 7, n. 11, p. 2927–2930, 2006.

QUINZLER, D.; MECKING, S. Renewable resource-based poly(dodecyloate) by carbonylation polymerization. **Chemical communications**, n. 36, p. 5400–5402, 2009.

QUINZLER, D.; MECKING, S. Linear semicrystalline polyesters from fatty acids by complete feedstock molecule utilization. **Angewandte Chemie**, v. 49, n. 25, p. 4306–4308, 2010.

REDDY, S. K.; ANSETH, K. S.; BOWMAN, C. N. Modeling of network degradation in mixed step-chain growth polymerizations. **Polymer**, v. 46, n. 12, p. 4212–4222, 2005.

ROBERTS, J. J.; BRYANT, S. J. Comparison of photopolymerizable thiol-ene PEG and acrylate-based PEG hydrogels for cartilage development. **Biomaterials**, v. 34, n. 38, p. 9969–9979, 2013.

ROMIO, A. P.; BERNARDY, N.; LEMOS SENNA, E.; ARAÚJO, P. H. H.; SAYER, C. Polymeric nanocapsules via miniemulsion polymerization using redox initiation. **Materials Science and Engineering C**, v. 29, n. 2, p. 514–518, 2009a.

ROMIO, A. P.; RODRIGUES, H. H.; PERES, A.; DA CAS VIEGAS, A.; KOBITSKAYA, E.; ZIENER, U.; LANDFESTER, K.; SAYER, C.; ARAÚJO, P. H. H. Encapsulation of magnetic nickel nanoparticles via inverse miniemulsion polymerization. **Journal of Applied Polymer Science**, v. 129, n. 3, p. 1426–1433, 2013.

ROMIO, A. P.; SAYER, C.; ARAÚJO, P. H. H.; AL-HAYDARI, M.; WU, L.; DA ROCHA, S. R. P. Nanocapsules by miniemulsion polymerization with biodegradable surfactant and hydrophobe. **Macromolecular Chemistry and Physics**, v. 210, n. 9, p. 747–751, 2009b.

ROPER, T. M.; GUYMON, C. a.; JÖNSSON, E. S.; HOYLE, C. E. Influence of the alkene structure on the mechanism and kinetics of thiol-alkene photopolymerizations with real-time infrared spectroscopy. **Journal of Polymer Science, Part A: Polymer Chemistry**, v. 42, n. 24, p. 6283–6298, 2004.

ROSE, M.; PALKOVITS, R. Isosorbide as a renewable platform chemical for versatile applications-quo vadis? **Chemistry & Sustainability, Energy & Materials**, v. 5, n. 1, p. 167–176, 2012.

RYBAK, A.; FOKOU, P. a.; MEIER, M. a R. Metathesis as a versatile tool in oleochemistry. **European Journal of Lipid Science and Technology**, v. 110, n. 9, p. 797–804, 2008.

RYBAK, A.; MEIER, M. a R. Acyclic diene metathesis with a monomer from renewable resources: Control of molecular weight and one-step preparation of block copolymers. **Chemistry & Sustainability, Energy & Materials**, v. 1, n. 6, p. 542–547, 2008.

RYDHOLM, a E.; HELD, N. L.; BOWMAN, C. N.; ANSETH, K. S. Gel permeation chromatography characterisation of the chain length distributions in thiol-acrylate photopolymer networks. **Macromolecules**, v. 39, n. 23, p. 7882–7888, 2006a.

RYDHOLM, A. E.; ANSETH, K. S.; BOWMAN, C. N. Effects of neighboring sulfides and pH on ester hydrolysis in thiol-acrylate photopolymers. **Acta Biomaterialia**, v. 3, n. 4, p. 449–455, 2007.

RYDHOLM, A. E.; BOWMAN, C. N.; ANSETH, K. S. Degradable thiol-acrylate photopolymers: Polymerization and degradation behavior of an in situ forming biomaterial. **Biomaterials**, v. 26, n. 22, p. 4495–4506, 2005.

RYDHOLM, A. E.; REDDY, S. K.; ANSETH, K. S.; BOWMAN, C. N. Controlling network structure in degradable thiol-acrylate biomaterials to tune mass loss behavior. **Biomacromolecules**, v. 7, n. 10, p. 2827–2836, 2006b.

RYDHOLM, A. E.; REDDY, S. K.; ANSETH, K. S.; BOWMAN, C. N. Development and characterisation of degradable thiol-allyl ether photopolymers. **Polymer**, v. 48, n. 15, p. 4589–4600, 2007.

SADLER, J. M.; TOULAN, F. R.; NGUYEN, A. P. T.; KAYEA, R. V.; ZIAEE, S.; PALMESE, G. R.; LA SCALA, J. J. Isosorbide as the

structural component of bio-based unsaturated polyesters for use as thermosetting resins. **Carbohydrate Polymers**, v. 100, p. 97–106, 2014.

SANGERMANO, M.; COLUCCI, G.; FRAGALE, M.; RIZZA, G. Hybrid organic-inorganic coatings based on thiol-ene systems. **Reactive and Functional Polymers**, v. 69, n. 9, p. 719–723, 2009.

SCHORK, F. J.; LUO, Y.; SMULDERS, W.; RUSSUM, J. P.; BUTTÉ, A.; FONTENOT, K. Miniemulsion polymerization. **Advances in Polymer Science**, v. 175, p. 129–255, 2005.

SENIHA GÜNER, F.; YAĞCI, Y.; TUNCER ERCIYES, a. Polymers from triglyceride oils. **Progress in Polymer Science**, v. 31, n. 7, p. 633–670, 2006.

SHALABY, S. W.; SHAH, K. R. Chemical Modifications of Natural Polymers and Their Technological Relevance. In: Shalaby, S. W.; McCormick, C. L.; Butler, B. G. **Water-Soluble Polymers: Synthesis, Solution Properties, and Applications.** Washington: ACS Symposium 467, American Chemical Society, 1991, p. 74–80, 1991.

STAUDT, T.; MACHADO, T. O.; VOGEL, N.; WEISS, C. K.; ARAUJO, P. H. H.; SAYER, C.; LANDFESTER, K. Magnetic polymer/nickel hybrid nanoparticles via miniemulsion polymerization. **Macromolecular Chemistry and Physics**, v. 214, n. 19, p. 2213–2222, 2013.

STEER, R. P.; KNIGHT, a. R. Reactions of thiyl radicals. VI. Photolysis of ethanethiol. **Canadian Journal of Chemistry**, v. 47, n. 8, p. 1335–1345, 1969.

STENZEL, M. H. Bioconjugation using thiols: Old chemistry rediscovered to connect polymers with nature's building blocks. **ACS Macro Letters**, v. 2, n. 1, p. 14–18, 2013.

ŠTORHA, A.; MUN, E. a.; KHUTORYANSKIY, V. V. Synthesis of thiolated and acrylated nanoparticles using thiol-ene click chemistry: towards novel mucoadhesive materials for drug delivery. **RSC Advances**, v. 3, n. 30, p. 12275, 2013.

STUBBS, J. M.; SUNDBERG, D. C. A round robin study for the characterisation of latex particle morphology - Multiple analytical techniques to probe specific structural features. **Polymer**, v. 46, p. 1125–1138, 2005.

TIAN, H.; TANG, Z.; ZHUANG, X.; CHEN, X.; JING, X. Biodegradable synthetic polymers: Preparation, functionalization and biomedical application. **Progress in Polymer Science**, v. 37, n. 2, p. 237–280, 2012.

TRZASKOWSKI, J.; QUINZLER, D.; BÄHRLE, C.; MECKING, S. Aliphatic long-chain C20 polyesters from olefin metathesis. **Macromolecular Rapid Communications**, v. 32, n. 17, p. 1352–1356, 2011.

TURLEY, D. B. The Chemical Value of Biomass. In: Clark, J. H., Deswarte, F. **Introduction to Chemicals from Biomass**. Chichester: John Wiley & Sons Ltd, 2008. p. 21–46.

TÜRÜNÇ, O.; FIRDAUS, M.; KLEIN, G.; MEIER, M. a. R. Fatty acid derived renewable polyamides via thiol–ene additions. **Green Chemistry**, v. 14, n. 9, p. 2577, 2012.

TÜRÜNÇ, O.; MEIER, M. a R. Fatty acid derived monomers and related polymers via thiol-ene (Click) additions. **Macromolecular Rapid Communications**, v. 31, n. 20, p. 1822–1826, 2010.

TÜRÜNÇ, O.; MEIER, M. A R. The thiol-ene (click) reaction for the synthesis of plant oil derived polymers. **European Journal of Lipid Science and Technology**, v. 115, n. 1, p. 41–54, 2013.

UGELSTAD, J., EL-AASSER, M. S. and VANDERHOFF, J. W. J. Emulsion polymerization: Initiation of polymerization in monomer droplets. **Journal of Polymer Science: Polymer Letters Edition**, v. 11, no. 8, p. 503-513, 1973.

USDA – United States Department of Agriculture. Oilseeds: World Market and Trade. Foreign Agricultural Service Circular Series FOP, 2015.

VALÉRIO, A.; ARAÚJO, P. H. H.; SAYER, C. Preparation of Poly (Urethane-urea) Nanoparticles Containing Açaí Oil by Miniemulsion Polymerization. **Polímeros**, v. 23, n. 4, p. 451–455, 2013.

VALÉRIO, A.; DA ROCHA, S. R. P.; ARAÚJO, P. H. H.; SAYER, C. Degradable polyurethane nanoparticles containing vegetable oils. **European Journal of Lipid Science and Technology**, v. 116, n. 1, p. 24–30, 2014.

VAN DEN BERG, O.; DISPINAR, T.; HOMMEZ, B.; DU PREZ, F. E. Renewable sulfur-containing thermoplastics via AB-type thiol-ene polyaddition. **European Polymer Journal**, v. 49, n. 4, p. 804–812, 2013.

VANDENBERGH, J.; PEETERS, M.; KRETSCHMER, T.; WAGNER, P.; JUNKERS, T. Cross-linked degradable poly(β-thioester) networks via amine-catalyzed thiol-ene click polymerization. **Polymer**, v. 55, n. 16, p. 3525–3532, 2014.

VERHÉ, R. Industrial Products from Lipids and Proteins. In: Stevens, C. V.; Verhé, R. (Ed.). **. Renewable Bioresources: Scope and Modification for Non-Food Applications**. 1st. ed. Chichester, UK: John Wiley & Sons, Ltd, 2004. p. 208–250.

VILELA, C.; SILVESTRE, A. J. D.; MEIER, M. a R. Plant Oil-Based Long-Chain C-26 Monomers and Their Polymers. **Macromolecular Chemistry and Physics**, v. 213, n. 21, p. 2220–2227, 2012.

WANG, K.; LU, J.; YIN, R.; CHEN, L.; DU, S.; JIANG, Y.; YU, Q. Preparation and properties of cyclic acetal based biodegradable gel by thiol-ene photopolymerization. **Materials Science and Engineering C**, v. 33, n. 3, p. 1261–1266, 2013.

WITT, U.; EINIG, T.; YAMAMOTO, M.; KLEEBERG, I.; DECKWER, W. D.; MÜLLER, R. J. Biodegradation of aliphatic-aromatic copolyesters: Evaluation of the final biodegradability and ecotoxicological impact of degradation intermediates. **Chemosphere**, v. 44, n. 2, p. 289–299, 2001.

WU, J. F.; FERNANDO, S.; WEERASINGHE, D.; CHEN, Z.; WEBSTER, D. C. Synthesis of soybean oil-based thiol oligomers. **Chemistry & Sustainability, Energy & Materials**, v. 4, n. 8, p. 1135–1142, 2011.

WU, W.-X.; QU, L.; LIU, B.-Y.; ZHANG, W.-W.; WANG, N.; YU, X.-Q. Lipase-catalyzed synthesis of acid-degradable poly(β-thioether ester) and poly(β-thioether ester-co-lactone) copolymers. **Polymer**, v. 59, p. 187–193, 2015.

XIA, Y.; LAROCK, R. C. Castor oil-based thermosets with varied crosslink densities prepared by ring-opening metathesis polymerization (ROMP). **Polymer**, v. 51, n. 12, p. 2508–2514, 2010.

YANG, K.; HUANG, X.; ZHU, M.; XIE, L.; TANAKA, T.; JIANG, P. Combining RAFT polymerization and thiol-ene click reaction for core-shell structured polymer@BaTiO3 nanodielectrics with high dielectric constant, low dielectric loss, and high energy storage capability. **ACS Applied Materials and Interfaces**, v. 6, n. 3, p. 1812–1822, 2014.

YASUNIWA, M.; TSUBAKIHARA, S.; SUGIMOTO, Y.; NAKAFUKU, C. Thermal analysis of the double-melting behavior of poly(L-lactic acid). **Journal of Polymer Science, Part B: Polymer Physics**, v. 42, n. 1, p. 25–32, 2004.

YOKOE, M.; AOI, K.; OKADA, M. Biodegradable polymers based on renewable resources. IX. Synthesis and degradation behavior of polycarbonates based on 1,4:3,6-dianhydrohexitols and tartaric acid Derivatives with pendant functional groups. **Journal of Polymer Science, Part A: Polymer Chemistry**, v. 43, n. 17, p. 3909–3919, 2005.

YOKOE, M.; KEIGO, a. O. I.; OKADA, M. Biodegradable polymers based on renewable resources. VII. Novel random and alternating copolycarbonates from 1,4:3,6-dianhydrohexitols and aliphatic diols. **Journal of Polymer Science, Part A: Polymer Chemistry**, v. 41, n. 15, p. 2312–2321, 2003.

YOON, W. J.; OH, K. S.; KOO, J. M.; KIM, J. R.; LEE, K. J.; IM, S. S. Advanced polymerization and properties of biobased high Tg polyester of isosorbide and 1,4-cyclohexanedicarboxylic acid through in situ acetylation. **Macromolecules**, v. 46, n. 8, p. 2930–2940, 2013.

YOSHIMURA, T.; SHIMASAKI, T.; TERAMOTO, N.; SHIBATA, M. Bio-based polymer networks by thiol–ene photopolymerizations of allyl-etherified eugenol derivatives. **European Polymer Journal**, v. 67, p. 397–408, 2015.

YU, T.; BU, H.; HU, J.; ZHANG, W.; GU, Q. The double melting peaks of poly (ethylene terephthalate). **Polymer communications**, p. 83-91, 1983.

ZOU, J.; HEW, C. C.; THEMISTOU, E.; LI, Y.; CHEN, C. K.; ALEXANDRIDIS, P.; CHENG, C. Clicking well-defined biodegradable nanoparticles and nanocapsules by UV-induced thiol-ene cross-linking in transparent miniemulsions. **Advanced Materials**, v. 23, n. 37, p. 4274–4277, 2011.